

**Performance of sandy soil mixed with calcium-
magnesium composite as attenuation layer for
geogenic contaminants**

2020

Lincoln Waweru Gathuka

Abstract

One strategy currently being explored in the development of a technically simple, economical, and practical countermeasure when reusing excavated soils and rocks that contain geogenic heavy metals as fill materials in an embankment, is the installation of a compacted layer of a base material of sandy soil mixed with stabilizing agent underlain the contaminated pile. A key issue related to its design is the selection of a suitable base material and agent to achieve the desired permeability, attenuation, and pH buffering function, considering the commercial availability, ease of use, suitability for several heavy metals, compliance with regulations, and so on. This study proposes the use of a sandy soil (natural soil) mixed with calcium-magnesium (Ca-Mg) composite as the attenuation layer. Geoenvironmental reliability of this composite was investigated considering its arsenic (As) attenuation, pH buffering, and water retention characteristics, as a function of the different particle sizes of this agent and acid (H_2SO_4) concentrations.

From batch-type tests it was found out that natural soil has a capacity to increase pH and to reduce metal concentrations from solution. This function plays an important role because the attenuation layer can be heterogeneous in attenuation performance and maybe cracked due to earthquakes and static deformation with time, during long-term services. Freundlich parameter, K – a good index for quantifying the contaminant attenuation property of a solid material – was estimated to be $11 \text{ cm}^3/\text{g}$. By introducing the Ca-Mg composite into the soil matrix, the attenuation function and capability to buffer pH of the natural soil became more effective, but in the order of decreasing particle size (i.e. coarse < fine < powder). Highest As retention by the solid materials was noted in the soil-powder agent composite, where K reached $535 \text{ cm}^3/\text{g}$ which is about 50-times higher compared to that of the natural soil. The soil-agent composite was capable of raising pH to alkaline conditions and retain more As with more acid input which might be due to more negative-surface charge and/or precipitation reactions. However, when the pH of the soil-agent composite suspension decreases below the precipitation pH (about $\text{pH}=5$), reduction in the amounts of As retained by the soil-agent composite is expected.

Using column tests it was found out that the composite could lower concentrations of As-applied to values below the acceptable limit; for many flow volumes and different pH conditions. Removal ratio (R_r) was generally $>95\%$, and As concentrations were under the allowable limit of 0.01 mg/L . This suggests that by lining possible acid-generating materials on top of the attenuation layer constructed using this composite, we can expect it to reduce As in leachate to negligible amounts for a long period/volumes of flow. Also, although this agent offers a higher pH buffering property, this feature decreased over time with continuous permeation due to the leaching of carbonates from the agent with more volumes of flow. Presence of Ca and Mg carbonates (from agent) in the soil increases the extent of precipitation mechanism, and precipitation of calcium arsenate is expected, which is less mobile and toxic, and stable over a wide pH range.

By adding powder agent to the soils, the air-entry value (ψ_a) and residual saturation (S_{rf}) were increased, and the highest S_{rf} is expected for the granite soil-powder agent composite; but not verified due to the small range of applied air pressures. Considering silica sand (of $\psi_a=0.9 \text{ kPa}$), adding 5%

powder agent increases ψ_a to 1.5 kPa. Also, although the coarse agent reduced ψ_a of the soil due to its particle size, the soil-coarse agent composite still exhibited a higher S_{rf} . Taking granite soil-coarse agent composite (of $\psi_a=0.7$ kPa) as an example, S_{rf} reached 63%, which is much higher than that of the natural soil. This shows that Ca-Mg composite does not only enhance the attenuation function of soil, but also can improve the water retention properties of sands, especially for a well-graded soil. Poorly graded sandy soils like silica sand may not be suitable base material, for they drastically become impermeable (hydraulic conductivity, $k=1\times 10^{-14}$ m/s) from small changes in negative pressures. When permeability is too low, infiltrate water cannot pass through the layer, and saturation degree (S_r) in the embankment will increase, which risks the stability of the embankment.

In conclusion, although powder agent offers better improvement to the attenuation, pH buffering, and water retention properties of a natural soil, coarse agent which is cheaper to produce and offers better material handling, can be applied as a material for the attenuation layer. Less, but long-term reactivity expected when using this particle size of agent.

Acknowledgements

First and foremost, I acknowledge a great debt of gratitude to my supervisor and mentor, Professor Takeshi Katsumi, for all the guidance, support and invaluable opportunities he has provided to me throughout my master's and Ph.D. studies. It has been a great honor for me to be his student. I deeply appreciate all his time out of his extremely tight schedule and insightful advice offered from his immense knowledge to improve and maximize my research work. If it were not for him, I would probably have not learned the true depth and weight of this research, nor would I have been able to take necessary steps that shaped this dissertation.

I would also like to express my sincere gratitude to Associate Professor Atsushi Takai, who has greatly inspired me with his excellent example both on academic and personal levels. I am especially grateful for his attentive supervision and wise counsel shared from his rich background. Due to his constant support, my Ph.D. experience has always been very comfortable and motivational.

My gratitude extends to Professor Toru Inui, Professor Giancarlo Flores, and Professor Masaki Takaoka, who have shared their intellectual knowledge with me and helped strengthen my research outcome.

In regards to my daily research activities having been productive and stimulating, it is in large part thanks to my lab mates, including Mr. Tomohiro Kato and Ms. Ando L. Rabenarimanitra, for their intelligence and excellent teamwork.

I also acknowledge the crucial role Ms. Miho Yasumoto played in arranging our lab environment and coordinating related trips and events, which helped my research activities be conducted as smoothly as possible.

I gratefully acknowledge the Japanese government (MEXT) scholarship has made my Ph.D. work possible.

Lastly, I cannot thank my family enough for their love and faith in me. Jane Wagaki, Morris Wagaki, Vivian N. Gathuka, and all the other family members, especially Samuel Gathuka Waweru, my father and my role model, who originally incited me since my childhood to set and pursue my high academic goals. And Aki Ishihara, my best friend, and loving life partner, for her endless trust in my potential, her encouraging words and constant efforts in ensuring my well-being.

This dissertation was not possible to complete without support by countless people, and I hereby promise to repay my debt of gratitude to all through striving further in research and contributing its outcome to the welfare of mankind and the global environment.

Table of contents

Abstract	i
Acknowledgements	iii
List of tables and figures	vii
List of tables	vii
List of figures	vii
Chapter 1 Introduction	1
1.1 General remarks	1
1.2 Organisation of the dissertation	3
References for Chapter 1	4
Chapter 2 Literature review	7
2.1 Management of excavated surplus soil containing geogenic contamination	7
2.1.1 Sustainable reuse of excavated surplus soil	7
2.1.2 Handling of excavated soils that contain geogenic contaminants	8
2.1.2.1 Soils and rocks containing geogenic heavy metals	8
2.1.2.2 Leaching behaviour of excavated soils containing geogenic contaminants	12
2.1.2.3 Current status on the reuse of geogenic contaminated soils	13
2.2 Attenuation layer method	14
2.3 Calcium-magnesium composite as a stabilizing agent	17
References for Chapter 2	20
Chapter 3 Enhanced attenuation function of a natural soil	27
3.1 General remarks	27
3.2 Materials and methods	27
3.2.1 Materials	27
3.2.2 Batch-type experiment	30
3.2.2.1 Arsenic attenuation	30
3.2.2.2 Determination of buffer capacity using acid titration experiment	31
3.2.2.3 Determining relationship of pH and buffer capacity on arsenic attenuation	32
3.3 Results and discussions	32
3.3.1 Effect of different particle sizes of agent	32
3.3.2 Effect of curing period	34
3.3.3 Effect of solution pH	36
3.3.4 pH changes	38
3.3.5 Relation of pH and buffer capacity on arsenic attenuation	39
3.4 Conclusions for Chapter 3	40
References for Chapter 3	41
Chapter 4 Attenuation performance with time	43
4.1 General remarks	43
4.2 Materials and methods	43

4.2.1 Materials	43
4.2.2 Column test under saturated flow conditions	43
4.2.3 Analytical solution for a one-dimensional contaminant transport	45
4.3 Results and discussions	46
4.3.1 Attenuation performance with time based on column test	46
4.3.2 Analytical solution for arsenic transport in the soil columns.....	51
4.3.3 Expected arsenic attenuation mechanism	53
4.4 Conclusions for Chapter 4	54
References for Chapter 4.....	55
Chapter 5 Water retention properties	57
5.1 General remarks	57
5.2 Materials and methods.....	57
5.2.1 Materials	57
5.2.2 Water retention tests	58
5.2.3 Fitting water retention parameters with van Genuchten model.....	60
5.3 Results and discussions	61
5.3.1 Water retention property.....	61
5.3.2 Permeability function of sands mixed with different agent sizes.....	63
5.4 Conclusions for Chapter 5	65
References for Chapter 5.....	65
Chapter 6 Practical implications.....	67
6.1 General remarks	67
6.2 Analytical solution of arsenic transport in attenuation layer	67
References for Chapter 6.....	70
Chapter 7 Conclusions and future research.....	71
7.1 Conclusions	71
7.2 Future research.....	73

List of tables and figures

List of tables

- Table 1.1: Regulatory guidelines for the excavated soils and rocks containing geogenic heavy metals.
- Table 1.2: Comparison of different countermeasures applied when utilizing geogenic contaminated materials.
- Table 2.1: Japanese classification standard for excavated soils and their recommended applications.
- Table 2.2: Examples of projects that generated soils and rocks containing geogenic contaminants.
- Table 2.3: Arsenic sources and concentrations in earth materials.
- Table 2.4: Crust abundance of several geogenic heavy metals.
- Table 2.5: Several large-scale construction projects ongoing in Japan.
- Table 2.6: Effectiveness of Ca-Mg composite to attenuate several contaminants.
- Table 3.1: Physicochemical characterization of the natural soil.
- Table 3.2: Properties of the calcium-magnesium composite.
- Table 3.3: Conditions for the batch-type experiment.
- Table 3.4: Isotherm parameters for different composites cured for 0, 7, and 28 days.
- Table 3.5: Isotherm parameters for different composites contacting solutions of pH of 2, 4, and 6.
- Table 4.1: Experimental conditions of the column test.
- Table 4.2: Contaminant transport parameters applied in the analytical model.
- Table 5.1: Basic properties of soils.
- Table 5.2: Summary of experimental approach.
- Table 5.3: Soil hydraulic parameters.
- Table 6.1: Contaminant transport parameters of different composites.

List of figures

- Figure 1.1: Schematic of the attenuation layer method.
- Figure 1.2: Structure and content of the dissertation.
- Figure 2.1: Spatial distribution of some geogenic heavy metals in the northern Honshu area, Japan (Ujiiie-Mikoshiha et al., 2006).
- Figure 2.2: Map showing (a) the spatial distribution of arsenic in the Kanto region and (b) the planned route for the Tokyo Outer Ring Road. Geochemical map extracted from Ohta et al. (2011).
- Figure 2.3: General decision flow for the proper reuse and/or management of geogenic contaminated soils and rocks (modified from MLIT (2010)).
- Figure 2.4: Embankment with attenuation layer underlain contaminated geomaterials.
- Figure 2.5: Representation of the construction process of the attenuation layer. Photo retrieved Feb 1, 2020, from <https://cpds.kentsu.co.jp/technology/detail?id=40>
- Figure 2.6: Hydraulic conductivity of a compacted composite of decomposed granite soil and stabilizing agent based on falling head, flexible-wall permeameter test, distilled water as permeant (Mo et al., 2015b).
- Figure 2.7: Enhanced sorption of a base material by adding Ca-Mg composite of powder type (Mo et al., 2015a).
- Figure 2.8: Permeability characteristics under continuous permeation (Mo, 2019).
- Figure 2.9: Arsenic amounts at column exit with continuous permeation using a 1 mg/L As solution under different flow rates (Mo, 2019).
- Figure 2.10: Comparison of pH buffering capacity of different stabilizing agents (Ito et al., 2014).
- Figure 3.1: Characteristics of the sieved soil in (a) particle size distribution and (b) compaction property.

Figure 3.2: Particle size distribution of the fine and coarse Ca-Mg composite.

Figure 3.3: Photo of a compacted soil sample prepared for the curing step.

Figure 3.4: Pictorial representation of typical steps for batch-type test showing 1) preparation of arsenic solutions, 2) adding soil samples to solution, 3) shaking step, 4) centrifugation step, 5) analysis of arsenic amounts using atomic absorption spectrophotometer and 6) analysis of water-soluble ion amounts using inductively coupled spectrophotometer.

Figure 3.5: Freundlich isotherms for 0-day cured samples after contacting As solutions of pH 6 for 24 h.

Figure 3.6: Representative linear isotherm to calculate the K_d values for 0-day cured samples at low concentration ranges under pH 6 conditions.

Figure 3.7: Relationship between K_d and SSA of agent.

Figure 3.8: Representative linear isotherms for calculating the K_d values for the different composites.

Figure 3.9: Relationship of K_d value and curing time when low concentration range is considered.

Figure 3.10: Changes in K_d of natural soil under different pH conditions.

Figure 3.11: Changes in K_d of soil-agent composites under different pH conditions.

Figure 3.12: pH changes and the leaching profiles of water-soluble metal ions for four composites of sandy soil and different agent sizes.

Figure 3.13: pH buffering curves of composites of soil and different agent sizes.

Figure 3.14: Relation of pH and buffer capacity on arsenic attenuation by composites.

Figure 4.1: Column test in a) schematic details of the flexible wall permeameter and b) appearance of the test setup.

Figure 4.2: Breakthrough curves of natural soil when permeated with arsenic solutions of different pH.

Figure 4.3: pH changes with flow volumes of solution of different pH in natural soil.

Figure 4.4: Relationship between Ca^{2+} , Mg^{2+} and pH changes by natural soil.

Figure 4.5: Relationship between Ca^{2+} , Mg^{2+} and arsenic attenuated by natural soil.

Figure 4.6: Arsenic breakthrough curves for composites permeated with arsenic solutions of pH 6.

Figure 4.7: Arsenic breakthrough curves for composites permeated with arsenic solutions of low pH of 2.

Figure 4.8: pH changes with flow volumes of contaminated solution of (a) pH 6 and (b) low pH of 2 in columns of different composites.

Figure 4.9: Relationship between Ca^{2+} , Mg^{2+} and pH changes for composites permeated with solutions of pH 6.

Figure 4.10: Relationship between Ca^{2+} , Mg^{2+} and As attenuated by composites permeated with solutions of pH 6.

Figure 4.11: Profile of arsenic concentration at column exit for a natural soil (top), soil-fine agent composite (middle), and soil-coarse agent composite (bottom).

Figure 4.12: Eh-pH-As characteristics of composites of soil and different sizes of agent when permeated with solution of low pH of 2 (above) and pH 6 (bottom).

Figure 5.1: Particle-size distribution curves of base materials and coarse Ca-Mg composite.

Figure 5.2: Schematic setup of the low suction device (Tempe cell) for measuring the water retention property.

Figure 5.3: Schematic setup of the soil column method.

Figure 5.4: Typical soil-water characteristic curve (Fredlund et al., 1994).

Figure 5.5: Effect of different Ca-Mg composite sizes on the water retention property of a well-graded sandy soil.

Figure 5.6: Effect of different agent sizes on the water retention property of a poorly-graded sandy soil.

Figure 5.7: Water retention properties of sands mixed with Ca-Mg composite of coarse type (Case 3 and 6).

Figure 5.8: Permeability functions of (a) decomposed granite soil and (b) silica sand mixed with different agent sizes.

Figure 5.9: Water permeability characteristics of composites with changes in the degree of saturation.

Figure 6.1: Conceptual model for the simplified field condition.

Figure 6.2: Profiles of arsenic concentration exiting the attenuation layer with volumes of flow.

Figure 6.3: Breakthrough curve for an initial arsenic concentration of 100 $\mu\text{g/L}$ in a 30 cm-thick attenuation layer.

Figure 6.4: Breakthrough time for solute under one set of performance criteria for a composite of a sandy soil and agent of coarse type.

Chapter 1 Introduction

1.1 General remarks

Over the past decades, many stakeholders have become aware that soils and rocks containing geogenic heavy metals, like arsenic (As), boron (B), flourine (F), lead (Pb), and so on, are often excavated from the massive projects for road, rail, and other infrastructure-related developments in many countries, including Japan (MLIT, 2014; Tabelin et al., 2018). Although there are significant benefits of reusing of excavated surplus soil such as life prolongation of final disposal sites, the reduction of CO₂ emissions, business cost-saving, and so on (Magnusson et al., 2015; Yamana et al., 2019), their reuse for geotechnical purposes is much discouraged in Japan due to public consciousness and the conservative environmental laws and/or regulations against all kinds of contaminants. Their proper management and/or effective utilization are big geotechnical and geoenvironmental challenges due to (1) the significantly large volumes excavated (MLIT, 2014), (2) difficulty in predicting the quality and quantity of leachate due to the chemical and physical heterogeneities of the solid materials (Naka, 2014), and (3) the highly non-linear coupling of geochemical and physical processes (Amos et al., 2015).

Katsumi et al. (2019) pointed out that in most cases such materials exhibit leaching amounts of 2 to 3-times higher than the acceptable limits (refer to Table 1.1) regulated under the Soil Contamination Countermeasures Law (SCCL), although in some situations slightly higher concentrations than the limit are reported. Therefore, to realize the compatibility between the reuse of excavated geological materials that contain geogenic heavy metals and contaminant control, moderate regulations and their interpretations are necessary. Also, a practical and secure way of reusing such geogenic contaminated materials needs to be defined in such a manner, as to be flexible enough for many site applications, while ensuring an acceptable level of protection for the environment and public health.

One strategy currently being explored in the development of a technically simple, cheap, and practical countermeasure for the geogenic contaminated soils and rocks, when utilized as fill materials of an embankment, is the installation of (1) a compacted attenuation layer underlain the pile of contaminated geomaterials, as shown in Figure 1.1, using a base material of sandy soil mixed with stabilizing agent. In this way, contamination of the surrounding environment should be prevented by the attenuation and pH buffering capabilities of the permeable layer (Nozaki et al., 2013a). And (2) a cover

Table 1.1: Regulatory guidelines for the excavated soils and rocks containing geogenic heavy metals.

Heavy metal	Regulatory limits	
	Composition value (mg/kg)	Leaching concentrations (mg/L)
As	150	0.01
Pb	150	0.01
F	4000	0.8
B	4000	1.0
Cd	150	0.01
Se	150	0.01
Hg	15	0.0005
Cr(VI)	250	0.05

Source: Katsumi et al. (2019).

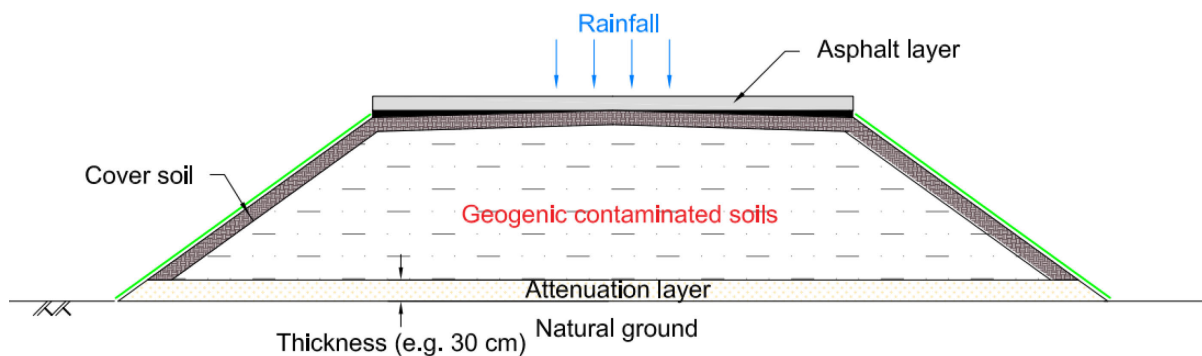


Figure 1.1: Schematic of the attenuation layer method.

system to intercept the air flux and percolation of rainwater into the underlying pile. By limiting the amount of air entering the embankment, oxidation reactions can be slowed. Likewise, by reducing the flow of water into the pile, the quantity of contaminated drainage can be reduced (Yanful et al., 1993; Tangviroon et al., 2017). Unlike the layered system using geomembranes, this new approach has various merits due to its low construction cost, better mechanical stability, and constructability with sufficient compaction as indicated in Table 1.2. However, the countermeasure until now is not implemented in many sites, due to insufficient information to verify its capability and reliability. There is a clear need to gain public acceptance, convince legislators, and establish the endurance of this cost-effective method. One key concern that needs to be addressed is related to the design/construction of the attenuation layer, which is, how to select suitable constituent materials to achieve the desired hydraulic performance, attenuation, and pH buffering functions, considering their availability, ease of use/handling, suitability for several contaminants, compliance with regulations, and so on.

Table 1.2: Comparison of different countermeasures applied when utilizing geogenic contaminated materials.

Approach	Remediation technology	Remarks
Isolation	Liners	<ul style="list-style-type: none"> • Use seepage control systems to intercept the air flux and percolation of rainfall into contaminated pile. • Widely applied because of its high capability. • Possible slippage at the geomembrane-soil interface (Fleming et al., 2006). • Damage due to direct contact with coarse gravel (Fox et al., 2014). • Expensive (e.g. highly-skilled techniques, leachate treatment facilities are required): 6,400 yen/m³ (Nozaki et al., 2013a).
Immobilization	Solidification/stabilization	<ul style="list-style-type: none"> • Blending contaminated soil with cement-based or organic additives, and so on, to immobilize contaminants in the soil. • Pre-evaluation using field samples is required (Nozaki et al., 2013a). • Expensive (e.g. yard required for mixing soils with agent, leachate treatment facilities are required): 10,500 yen/m³ (Nozaki et al., 2013a). • Long-term performance under actual field conditions is not fully verified.
Toxicity and/or mobility reduction	Attenuation layer method	<ul style="list-style-type: none"> • Installation of permeable soil layer with a capacity to attenuate heavy metals from the overlain contaminated pile. • Can be installed on flat, uneven, or sloped ground (Tatsuhara et al., 2015) • Better mechanical stability between soil and layer (Katsumi et al., 2019). • Better constructability without potential damage (Tatsuhara et al., 2015). • Low cost: 3,000 yen/m³ (Nozaki et al., 2013a). • Long-term performance under actual field conditions is not fully verified.

As a material for the attenuation layer, calcium-magnesium (Ca-Mg) composite which is produced by blending special additives with calcinations of natural minerals – with similar chemical property as dolomite ($\text{CaMg}(\text{CO}_3)_2$) – has various merits due to its high attenuation capacity (Kikuchi et al., 2012; Mo et al., 2015b), suitability for several contaminants (Bobeia et al., 2012; Kikuchi et al., 2012), high capabilities to increase pH (Ito et al., 2014), stability of immobilized compounds (Itaya et al., 2013), and so on.

Although Mo et al. (2015b) studied the effectiveness of a natural soil amended with the powder Ca-Mg composite (which is one of the three available particle sizes of this agent), the applicability of the composite under low pH of 2 to 4, which can naturally occur in such contaminated geological materials due to a high S/Ca mole ratio in the solid material (Inui et al., 2013; Paikaray, 2015) has not yet been verified. Also, the applicability of the coarse agent (2-9.5 mm) which is cheaper to produce, offers better material handling, can be homogeneously distributed in the base material (soil), and is expected to offer less, but long-term reactivity has not yet been studied.

Also, in most cases, stakeholders put emphasis on the hydraulic conductivity (Nozaki et al., 2013b; Mo et al., 2015a) and attenuation capacity (Tabelin et al., 2013; Tabelin et al., 2014; Mo et al., 2015b) when selecting suitable materials as the attenuation layer. However, the seepage conditions in this layer are not often considered and can significantly influence its functions (Ghasemzadeh, 2008; Francisca et al., 2012). Soil water retention characteristic is one of the important soil hydraulic properties in the simulation of seepage conditions, and therefore needs to be better understood.

Main objective of this study was to evaluate the geoenvironmental reliability of natural soil (sandy soil) mixed with the coarse agent. To achieve this goal, (1) batch-type tests were carried to obtain basic information regarding the performance of composites of the soil and different particle sizes of this agent from the viewpoints of As attenuation, and the relationship of pH and buffer capacity on As attenuation. (2) Performance of the composite over time was investigated using column test under saturated conditions, which can more closely simulate the in-situ water in contact with the solid materials and allows for the measurement of the time-lapse release of contaminants. (3) Water retention characteristics were investigated using the Tempe cell and soil column, to acquire detailed quantitative information pertaining to the effect of using different base materials and particle sizes of the agent.

1.2 Organisation of the dissertation

This dissertation is composed of 7 chapters as shown in Figure 1.2. An overview of the purpose of the research is presented in Chapter 1. The conceptual framework and organizing principles on the proper and sustainable reuse of surplus soil that contain geogenic heavy metals as construction materials are presented in Chapter 2. This chapter contains a summary discussion of surplus soil reuse, geogenic contamination, and the concept of attenuation layer method is introduced. The objective of Chapter 1 is to establish the technical basis and justification for the premise that this countermeasure has potential to reduce the mass flux of geogenic heavy metals released from the contaminated geomaterials in an embankment, sufficiently to meet regulatory requirements.

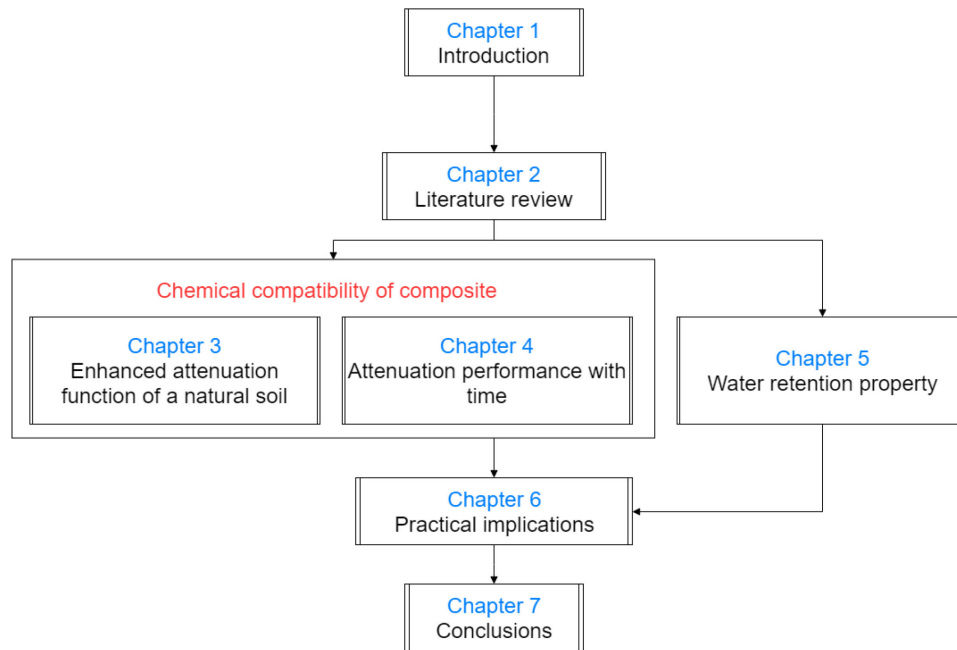


Figure 1.2: Structure and content of the dissertation.

Chapter 3 through 6 present the technical evaluation of the composites of a natural soil (sandy soil) and different particle sizes of the agent as the attenuation layer. The objective of Chapter 3 is to obtain basic information about the performance of the materials from the viewpoints of As attenuation, and the relationship of pH and buffer capacity on As attenuation. The objective of Chapter 4 is to obtain information regarding their performance with time/ continuous interaction with leachate. The objective of Chapter 5 is to evaluate the water retention characteristics of composites with different base material and particle sizes of this agent, so as to acquire detailed quantitative information pertaining to their effect on the hydraulic properties of the attenuation layer. The objective of Chapter 6 is to demonstrate the reliability of using this composite as the attenuation layer. Chapter 7 presents the main findings from this study and suggestions for further research on this topic.

References for Chapter 1

- Amos, R. T., Blowes, D. W., Bailey, B. L., Segeo, D. C., Smith, L., and Ritchie, A. I. M. 2015. Waste-rock hydrogeology and geochemistry. *Applied Geochemistry*, 57: 140-156.
- Bobeja, J., Kikuchi, S., Kuninishi, K., Yamashita, S., Katsumi, T., and Inui, T. 2012. Performance of immobilization materials against lead and arsenic contaminated soils. *Proceedings of the 10th National Symposium on Ground Improvement*, Kyoto, Japan.
- Fleming, I. R., Sharma, J. S., and Jogi, M. B. 2006. Shear strength of geomembrane-soil interface under unsaturated conditions. *Geotextiles and Geomembranes*, 24(5): 274-284.
- Fox, P. J., Thielmann, S. S., Stern, A. N., and Athanassopoulos, C. 2014. Interface shear damage to a HDPE geomembrane. I: Gravelly compacted clay liner. *Journal of Geotechnical and*

- Geoenvironmental Engineering*, 140(8): 04014039.
- Francisca, F., Carro Pérez, M., Glatstein, D., and Montoro, M. 2012. Contaminant transport and fluid flow in soils. In Szigethy (Ed.), *Horizons in Earth Science Research*, 97-131: Nova Science Publishers, Inc.
- Ghasemzadeh, H. 2008. Heat and contaminant transport in unsaturated soil. *International Journal of Civil Engineering*, 6(2): 90-107.
- Inui, T., Katsumi, T., Takai, A., and Kamon, M. 2013. Factors affecting heavy metal leaching in excavated rocks with natural contamination. In Manassero et al. (Eds.), *Coupled Phenomena in Environmental Geotechnics*, 587-592: CRC Press.
- Itaya, Y., Kikuchi, S., Yoshimatsu, T., and Kuninishi, K. 2013. Clarification of insolubilization mechanism of heavy metals using magnesium/calcium composite material. *Proceedings of the 19th Conference on Groundwater and Soil Contamination and its Countermeasures*, Japan. (In Japanese).
- Ito, K., Kuninishi, K., Itaya, Y., and Suzuki, M. 2014. Distribution and stability of heavy metals sorbed on Ca/Mg compound material. *Proceedings of the 20th Conference on Groundwater and Soil Contamination and its Countermeasures*, Japan. (In Japanese).
- Katsumi, T., Inui, T., Yasutaka, T., and Takai, A. 2019. Towards sustainable soil management — reuse of excavated soils with natural contamination —. *Proceedings of the 8th International Congress on Environmental Geotechnics Volume 1*, Hangzhou, China.
- Kikuchi, S., Kuninishi, K., and Itaya, Y. 2012. Basic discussion on the applicability of Ca/Mg composite material in sorption layer method. *67th Annual Conference of the Japan Society of Civil Engineers*, Japan. (In Japanese).
- Magnusson, S., Lundberg, K., Svedberg, B., and Knutsson, S. 2015. Sustainable management of excavated soil and rock in urban areas - A literature review. *Journal of Cleaner Production*, 93: 18-25.
- MLIT 2014. Investigation results of construction by-products in 2012. Retrieved from <http://www.mlit.go.jp/sogoseisaku/region/recycle/fukusanbutsu/jittaichousa/index01.htm>. (In Japanese).
- Mo, J., Inui, T., Katsumi, T., Kuninishi, K., and Shintaro, H. 2015a. Effectiveness of immobilizing agent used as a sorption layer against natural contamination. *Japanese Geotechnical Society Special Publication*, 1(4): 19-24.
- Mo, J., Inui, T., Katsumi, T., Takai, A., Kuninishi, K., and Hayashi, S. 2015b. Performance of sorption layer using Ca/Mg immobilizing agent against natural contamination. *10th Asian Regional Conference of IAEG*, Kyoto, Japan.
- Naka, A. (2014). *Hydraulic performance and chemical compatibility of mineral barriers to mitigate natural contamination from excavated rocks*. Kyoto University, Retrieved from

<http://hdl.handle.net/2433/188879>

- Nozaki, F., Shimizu, Y., and Ito, K. 2013a. Discussion on construction method of heavy metals adsorption layer. *Proceedings of the 19th Symposium on Soil and Groundwater Contamination and Remediation*. (In Japanese).
- Nozaki, T., Matsuyama, Y., Sugiyama, A., Moriya, M., Komukai, Y., and Nagase, T. 2013b. Fundamental study of soil materials for absorbent construction method using MgO material. *Proceedings of the 19th Symposium on Soil and Groundwater Contamination and Remediation*. (In Japanese).
- Paikaray, S. 2015. Arsenic geochemistry of acid mine drainage. *Mine Water and the Environment*, 34(2): 181-196.
- Tabelin, C. B., Igarashi, T., Arima, T., Sato, D., Tatsuhara, T., and Tamoto, S. 2014. Characterization and evaluation of arsenic and boron adsorption onto natural geologic materials, and their application in the disposal of excavated altered rock. *Geoderma*, 213: 163-172.
- Tabelin, C. B., Igarashi, T., Villacorte-Tabelin, M., Park, I., Opiso, E. M., Ito, M., and Hiroyoshi, N. 2018. Arsenic, selenium, boron, lead, cadmium, copper, and zinc in naturally contaminated rocks: A review of their sources, modes of enrichment, mechanisms of release, and mitigation strategies. *Science of the Total Environment*, 645: 1522-1553.
- Tabelin, C. B., Igarashi, T., Yoneda, T., and Tamamura, S. 2013. Utilization of natural and artificial adsorbents in the mitigation of arsenic leached from hydrothermally altered rock. *Engineering Geology*, 156: 58-67.
- Tangviroon, P., Hayashi, R., and Igarashi, T. 2017. Effects of additional layer(s) on the mobility of arsenic from hydrothermally altered rock in laboratory column experiments. *Water Air and Soil Pollution*, 228(5): 191.
- Tatsuhara, T., Jikihara, S., Tatsumi, T., and Igarashi, T. 2015. Effects of the layout of adsorption layer on immobilizing arsenic leached from excavated rocks. *Japanese Geotechnical Journal*, 10(4): 635-640. (In Japanese).
- Yamana, M., Tomizawa, Y., Fujiwara, T., Mizuta, K., Mizuno, K., Inui, T., Katsumi, T., and Kamon, M. 2019. Management of the soils discharged from shield tunnel excavation. *Proceedings of the 8th International Congress on Environmental Geotechnics Volume 1*, Singapore.
- Yanful, E. K., Bell, A. V., and Woyshner, M. R. 1993. Design of a composite soil cover for an experimental waste rock pile near Newcastle, New Brunswick, Canada. *Canadian Geotechnical Journal*, 30(4): 578-587.

Chapter 2 Literature review

2.1 Management of excavated surplus soil containing geogenic contamination

2.1.1 Sustainable reuse of excavated surplus soil

Massive projects are being undertaken in many parts of the world for road, rail, and other infrastructure-related developments, including more recently the renovation of urbanized areas with underground facilities such as buildings and subways. In many situations, these developments have resulted in considerably huge volumes of excavated geological materials produced (Haid and Hammer, 2009; MLIT, 2014; Meistro et al., 2019; Walsh et al., 2019). For example, excavation in the mountainous terrains of Katzenberg, Germany for a 9.4-km long rail line, excavated an estimated 2.3 million m³ of rocks and debris (Haid and Hammer, 2009). In Italy, the 53-km Terzo Valico rail line project mainly consisted of underground excavations and earthworks which amounted to nearly 14 million m³ (Meistro et al., 2019). From a report by the Japanese Ministry of Land, Infrastructure, and Transport (MLIT), about 140 million m³ of soils were generated nationwide in 2012 (MLIT, 2014) and much more is expected from the many relatively large-scale projects that are ongoing, for example, in the Tokyo metropolitan area in the run-up to the 2020 Tokyo Olympics and Paralympics.

Over the past decades, many efforts have been made to change from the traditional surplus soil handling approaches, based on transporting them to waste dumps, to a more environmentally friendly sustainable approach which maximises on their reuse (Katsumi and Inui, 2013; Magnusson et al., 2015). This could finally lead to less need for quarry aggregates and landfill avoidance thereby prolonging the life spans of final disposal sites. Many examples on the reuse of surplus soil can be found in literature (Chittoori et al., 2012; Eras et al., 2013; Walsh et al., 2019; Yamana et al., 2019), in any case, their reuse in the project itself and/or close to the vicinity has significant merits to the environment due to (1) the reduction in carbon footprint, for example, Eras et al. (2013) estimated the reuse of about 700,000 m³ of excavated geological materials in an industrial construction project as saving about 4000 tonnes of CO₂ from transportation fuels. And (2) reduced project costs and traffic congestions following from reduced hauling distances (Walsh et al., 2019; Yamana et al., 2019).

Possibilities of reuse for surplus soil may vary depending on their soil type, permeability, settling behaviour, and strength characteristics, which are some of the most important geotechnical aspects considered (Katsumi et al., 2004; Arulrajah et al., 2012). In Japan, after segregating the excavated geological materials based on the soil type, water content, and their resistance, as indicated in Table 2.1, such materials can be reused in various earthworks (Katsumi et al., 2004). Good quality soils, such as sand or gravel, have been reused as road base and/or fill materials for shallow geostructures. In some situations, by adding chemical or mineral-based additives, soils characterized by poor geotechnical features can be changed into valuable construction materials (Cheng and Huang, 2018; Yamana et al., 2019). For example, to properly and effectively reuse about 950,000 m³ of excavated soils (construction sludge) – generated from the Hanshin Expressway shield tunnel construction project – with low cone penetration strength ($q_c=30$ to 50 kN/m²), about 60 kg/m³ gypsum-based additive was mixed with these

Table 2.1: Japanese classification standard for excavated soils and their recommended applications.

Classification of soil	Parameters		Embankment	Subgrade	Backfill in structures
	Strength ^a , q_c (kN/m ²)	Water content, w (%)			
1 st class soil (e.g. sand and gravel)	-	-	○	○	○
2 nd class soil (e.g. sandy soil)	>800	-	○	○	○
3 rd class soil (e.g. clayey soil)	>400	<40 ^b	○	△	△
4 th class soil (e.g. clayey soil ^c)	>200	40-80	△	△	△
Sludge	<200	>80	X	X	X

Source: Katsumi et al. (2004).

^a Cone penetration strength, q_c , determined according to JIS A 1228 “Cone index test method for compacted soil”.

^b Except for volcanic cohesive soils.

^c Clayey soil in the 3rd class is exempted.

Note: Symbol ○ indicates that soil can be used as it is, △ indicates that some stabilization methods are needed prior to soil use, and X indicates that soil in many cases is disposed of.

soils, for them to achieve sufficient mechanical properties as a reclamation material ($q_c > 400$ kN/m², pH of 6 to 9) (Yamana et al., 2019).

2.1.2 Handling of excavated soils that contain geogenic contaminants

2.1.2.1 Soils and rocks containing geogenic heavy metals

Over recent years, many cases about different kinds of geogenic heavy metals in the excavated soils and rocks were reported globally, for example in the USA (Gonzalez et al., 2005), Italy (Cremisini and Armiento, 2016), China (Li et al., 2007; Yu et al., 2010), Hong Kong (Li et al., 2017b; Cui et al., 2018), and Japan (Takahashi et al., 2011; Li et al., 2018; Tabelin et al., 2018). In Japan, for example, significantly huge volumes of geogenic contaminated materials in the hundreds of thousands of cubic meters were produced from various construction works, some of which are listed in Table 2.2 (MLIT, 2014). As indicated in Table 2.3, these heavy metals, commonly arsenic (As), lead (Pb), boron (B), fluorine (F), and selenium (Se), can be found in sulphide (e.g. pyrite and arsenopyrite), clay (e.g. kaolinite and illite), and/or carbonaceous minerals (e.g. calcite and siderite) as their main and/or sub-components, due to chemical and mineralogical changes of host rock by geothermal fluids (Pirajno, 2009). Also, in low-temperature (<150 °C) sedimentary geothermal environments, under reducing conditions, the contaminants might accumulate in marine sediments (Tanaka, 1988; Li et al., 2013).

Table 2.2: Examples of projects that generated soils and rocks containing geogenic contaminants.

Tunnel construction works	Heavy metal	Excavated volume (m ³)
Nakagoshi tunnel, Hokkaido	As	800,000
Odatekita-Kosaka tunnel, Akita	As, Se, F	900,000
Nakagoshi tunnel, Hokkaido	As	800,000
Hakkoda tunnel, Aomori	As, Pb, Cd, Se	540,000
Subway Tozai line, Sendai	As, Pb, Cd, Se, F	400,000

Source: MLIT (2010).

Table 2.3: Arsenic sources and concentrations in earth materials.

Arsenic minerals	Chemical formula	Source
Native arsenic	As	Hydrothermal veins.
Niccolite	NiAs	Vein deposits and norites.
Realgar	AsS	Vein deposits, often associated with orpiment, clays, and limestones, also deposits from hot springs.
Orpiment	As ₂ S ₃	Hydrothermal veins, hot springs, volcanic sublimation products.
Cobaltite	CoAsS	High temperature deposits, metamorphic rocks.
Arsenopyrite	FeAsS	The most abundant As mineral, dominantly in mineral veins.
Tennantite	(Cu,Fe) ₁₂ As ₄ S ₁₃	Hydrothermal veins.
Enargite	Cu ₃ AsS ₄	Hydrothermal veins.
Arsenolite	As ₂ O ₃	Secondary mineral formed by oxidation of arsenopyrite native arsenic and other As minerals.
Clauderite	As ₂ O ₃	Secondary mineral formed by oxidation of realgararsenopyrite and other As minerals.
Scorodite	FeAsO ₄ ·2H ₂ O	Secondary mineral.
Anabergite	(Ni,Co) ₃ (AsO ₄) ₂ ·8H ₂ O	Secondary mineral.
Hoernesite	Mg ₃ (AsO ₄) ₂ ·8H ₂ O	Secondary mineral, smelter wastes.
Haematolite	(Mn,Mg) ₄ Al(AsO ₄)(OH) ₈	Secondary mineral.
Conichalcite	CaCu(AsO ₄)(OH)	Secondary mineral.
Pharmacosiderite	Fe ₃ (AsO ₄) ₂ (OH) ₃ ·5H ₂ O	Oxidation product of arsenopyrite and other As minerals.
Materials	Concentration, As (mg/kg)	Process
Igneous material		Cooling and solidification of magma or lava.
Basalt	<1-113	
Ultrabasics	<1-16	
Granites	<1-15	
Sedimentary material		Formed by the deposition of material (organic and/or minerals) at the earth's surface and within bodies of water.
Shales and clays	<1-500	
Sandstones	<1-120	
Limestones	<1-20	
Phosphorites	3-100	

Source: Panagiotaras and Nikolopoulos (2015).

Because of active volcanic activities and geographical proximity of Japan to the circum-Pacific belt, many areas in Japan are reported to have exceptionally high contents of geogenic heavy metals than the global cited average, for example, as indicated in Table 2.4 the average content of As in the islands of Japan is 6.5-7.1 mg/kg which is about 3-times higher than the global crust average (1.8 mg/kg).

Table 2.4: Crust abundance of several geogenic heavy metals.

	Cd	Cr(VI)	Hg	Se	Pb	As	F	B
Global crust average (mg/kg)	0.2	100	0.08	0.05	13	1.8	625	10
Crust average of continent (mg/kg)	0.098	185	0.08	0.05	8	1	625	10
Crust average of Japan (mg/kg)	-	84	-	-	16.9	6.5-7.1	-	-
Japan river sediment average (mg/kg)	0.158	65.2	0.054	-	23.1	9.32	-	-

Source: MLIT (2010).

From a geochemical mapping of northern Honshu in Northeast Japan by Ujiie-Mikoshiba et al. (2006), high concentrations of several heavy metals (e.g. As and Sb) were recognised as shown in Figure 2.1, and can be related to the active geothermal areas near volcanoes and ore deposits. These high amounts reflect not only the increased abundance of primary metal-rich sulphide minerals that are susceptible to oxidation in the surface environment but also secondary minerals (e.g. scorodite) formed as reaction products of the original ore minerals, which have varying solubility in oxidising conditions in groundwaters and/or surface waters.

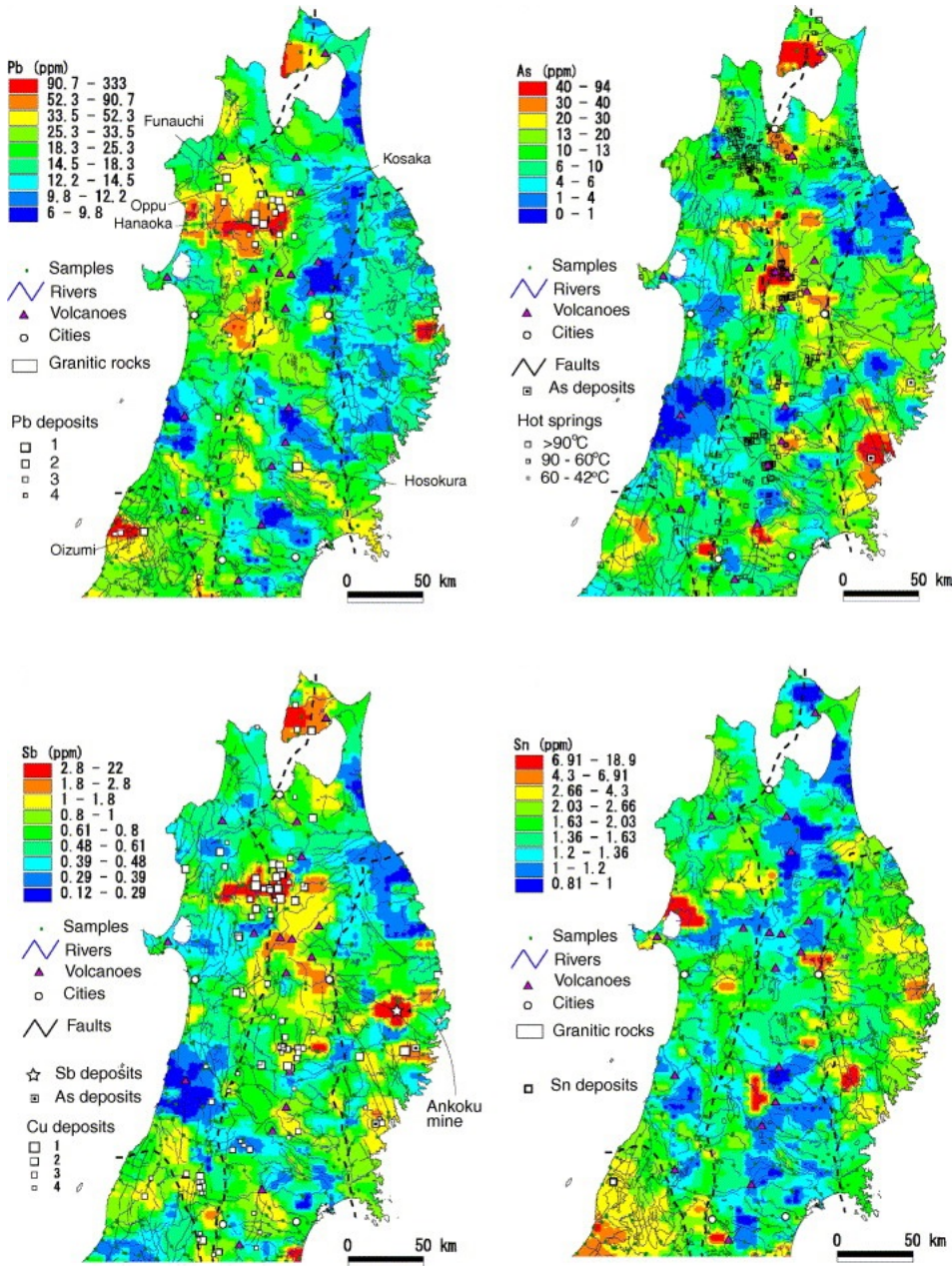


Figure 2.1: Spatial distribution of some geogenic heavy metals in the northern Honshu area, Japan (Ujiie-Mikoshiba et al., 2006).

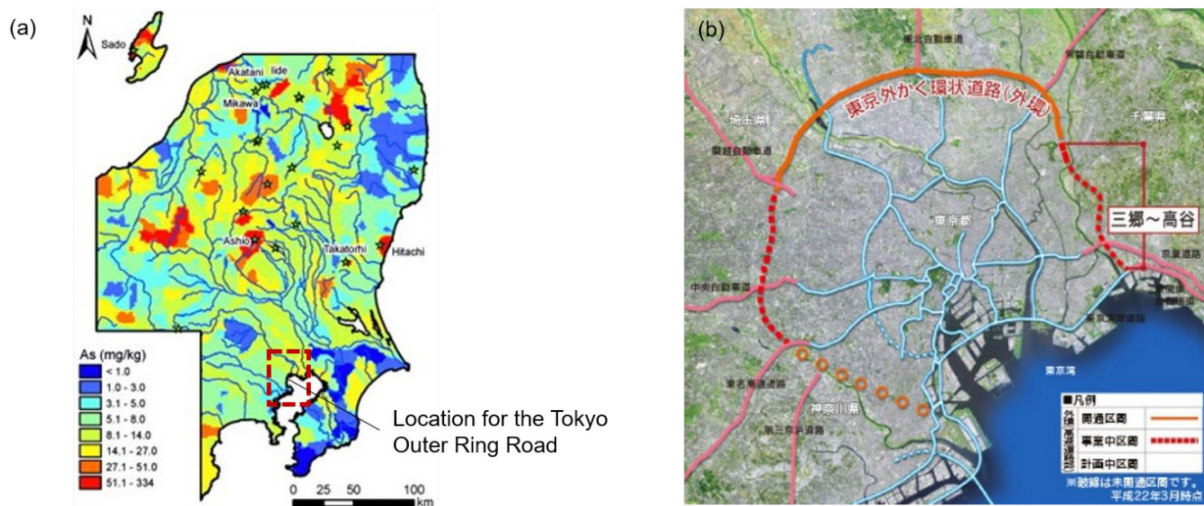


Figure 2.2: Map showing (a) the spatial distribution of arsenic in the Kanto region and (b) the planned route for the Tokyo Outer Ring Road. Geochemical map extracted from Ohta et al. (2011).

Many massive projects ongoing in Japan, for example, the Tokyo Outer Ring Road, shown in Figure 2.2, and others like the Chuo Shinkansen (Maglev) project, listed in Table 2.5, are expected to produce significantly huge volumes of geogenic contaminated soils and rocks (Li et al., 2017a; Katsumi, 2018). It is generally recognised that one of the most important environmental risks associated with the reuse of such contaminated geological materials is the potential release and subsequent migration of different kinds of contaminants from the materials into the environment, for example, As (Tamoto et al., 2015; Li et al., 2017a; Tabelin et al., 2017), B (Tabelin et al., 2012a; Tabelin et al., 2018), Pb (Tabelin and Igarashi, 2009; Yokobori et al., 2015), Se (Igarashi et al., 2013), and so on.

To verify that the environmental impact of such geological materials is negligible or within the acceptable values, their geoenvironmental parameters, for example, pH, geochemical composition, leaching concentrations, and the transport of the contaminants in the subsurface, have become important issues to consider for proper reuse and/or management, as shown in Figure 2.3, but, in recent years, emphasis is on their metal leaching property. Many stakeholders have recognised that, although they are marginally contaminated, in many cases, they exhibit leaching amounts above the acceptable levels, especially As (Tabelin et al., 2012d; Igarashi et al., 2013; Inui et al., 2013). Katsumi et al. (2019) found out that in many situations, they exhibit leaching amounts of 2-3 times higher than the acceptable limits regulated under the Soil Contamination Countermeasures Law (SCCL), but in some cases, slightly higher values are reported.

Table 2.5: Several large-scale construction projects ongoing in Japan.

Project	Route	Completion scheduled	Total length	Tunnel
Chuo Shinkansen (Maglev)	Shinagawa-Nagoya	2027	285.6 km	86% (246.6 km)
Hokkaido Shinkansen	Hakodate-Sapporo	2031	211.5 km	76% (160.2 km)
Hokuriku Shinkansen	Kanazawa-Tsuruga	2023	113 km	13 tunnels (19.7 km)
Tokyo Outer Ring Road	Toumei JCT-Oizumi JCT		16 km	Entire route

Source: Katsumi (2018).

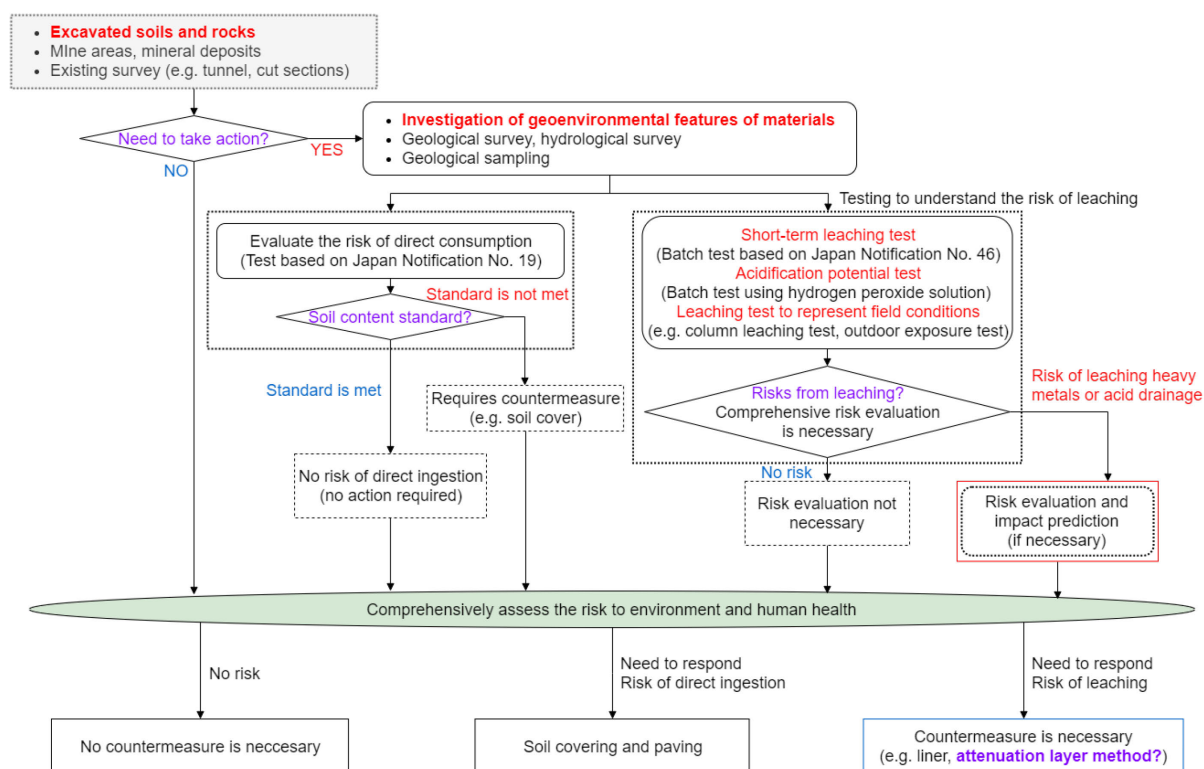


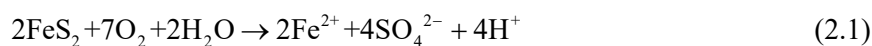
Figure 2.3: General decision flow for the proper reuse and/or management of geogenic contaminated soils and rocks (modified from MLIT (2010)).

2.1.2.2 Leaching behaviour of excavated soils containing geogenic contaminants

Arsenic is one of the most commonly reported heavy metals found in the excavated-geogenic contaminated soils and rocks (refer to Table 2.2). According to Panagiotaras and Nikolopoulos (2015), the element can be found in various kinds of minerals, but the most common are arsenopyrite (FeAsS), orpiment (As_2S_3), realgar (As_2S_2), and pyrite (FeS_2) – where it is commonly found as a solid solution.

Most sulphide minerals are very stable and insoluble in water if they are left undisturbed under reducing conditions in the subsurface (Smedley and Kinniburgh, 2002). However, in surface environments, mobilization of the heavy metals is triggered, and typically is governed by several complex processes which most probably are (1) the combined effects of oxidation of sulfide minerals, dissolution of soluble minerals (Tabelin et al., 2012b), (2) neutralization by calcite and/or other acid-neutralizing alkali minerals (Tabelin et al., 2012c), and (3) ad/desorption reactions of the elements onto minerals found in the materials.

Inherent in the oxidation of FeS_2 by aerated water is the formation of sulfate ion (SO_4^{2-}), ferrous iron (Fe^{2+}) and hydrogen ion (H^+), which can be represented by a simplified reaction (2.1). The presence of *acidithiobacillus ferrooxidans* bacteria, which naturally exists in the ground, can enhance the oxidation of pyrite and the dissolved Fe^{2+} in aerated water, especially under low pH conditions (2.2). At a $\text{pH} < 4$, ferric ion (Fe^{3+}) can be precipitated out as ferric hydroxide ($\text{Fe}(\text{OH})_3$), which releases more acid in the environment (2.3), and/or can remain soluble and directly oxidize more FeS_2 , liberating more acid



(more H^+) into the surroundings, unless neutralized by calcite and/or other alkaline minerals (Inui et al., 2013; Paikaray, 2015).

In surface environments, atmospheric precipitation may wash the contaminants into surrounding soils, sediments, surface waters, and groundwaters, which could harm aquatic wildlife and possibly threaten human health. According to Ravenscroft et al. (2011), long exposure of As to the public can result in a wide variety of clinical effects, ranging from skin lesions to cancer, and death.

2.1.2.3 Current status on the reuse of geogenic contaminated soils

Conflict between the ever-increasing need to reuse surplus soil and the conservative environmental laws/regulations to prevent contamination has become apparent since 2003, after the establishment of the SCCL by the Japanese Ministry of Environment (MOE). Over recent years, it has become a serious issue to handle such materials which would be reused for the other purposes of construction (Katsumi et al., 2019). Some challenges involved in managing the geogenic contaminated soils and rocks commonly include (1) the significantly large volumes produced (MLIT, 2014), (2) difficulty in predicting the quality and quantity of leachate due to chemical and physical heterogeneities in the solid materials (Naka, 2014) and, (3) the highly non-linear coupling of geochemical and physical processes (Amos et al., 2015).

Consequently, such materials are commonly dumped in disposal sites that have been installed with a geomembrane liner or compacted clay layer, or a combination of both (Lange et al., 2010; Tabelin et al., 2018). This material transfer will not only rapidly fill up the limited disposal sites, but also might cause severe damage to the environment and people (Ocak, 2009; Zhan et al., 2018). For example, due to the rapid filling of waste dumps to the extreme height and a lack of consideration for proper drainage systems, a catastrophic failure of a soil disposal site in South-eastern China occurred (Zhan et al., 2018). To prevent such severe problems and/or accidents, not only proper management of the soil disposal sites, but also the sustainable reuse for surplus soils that contain geogenic heavy metals is necessary.

Moderate regulations and their interpretations are necessary to realize the compatibility between surplus soil reuse and contaminant control, especially when geogenic contamination is of concern. This is because, in many situations, such materials exhibit leaching amounts of only 2-3 times higher (or just slightly higher in some cases) than the regulatory limits (Katsumi et al., 2019), which is unlike the soils enriched with contaminants from anthropogenic sources (Francisca et al., 2012). Some progress is noted following discussions particularly between the environment regulatory governments and authorities which handle the construction and development of infrastructure; since 2017, the SCCL was revised to follow the manner described by MLIT to realize the reuse of such materials under proper management

(Katsumi et al., 2019). A practical but secure way of reusing such marginally contaminated soils also needs to be defined in such a way as to be flexible enough for many site applications, while ensuring an acceptable level of protection for the environment and public health (Birle et al., 2010; Katsumi et al., 2019). Prevention of the leaching and transport of contaminants mainly requires the protection of sulphide minerals from air, water, and bacteria, for example by denser compaction, installation of earthen covers, mixing with stabilizing agents, and/or containment with geomembranes.

2.2 Attenuation layer method

Although the installation of layered systems like geomembranes as a countermeasure is convenient for a safer design, the method might be considered excessive for geogenic contaminated soils. First, a high upfront cost; Nozaki et al. (2013) estimated the cost of applying this countermeasure to be about 6,000 yen/m³. This high cost is in part due to the need for constructing drainage and water treatment facilities, highly-skilled techniques, thoroughly standardized installation conditions, and a time-consuming construction process. From an economic perspective, this countermeasure is irrational, especially because of (1) the significantly large volumes of material that are produced and need to be reused, and (2) leaching concentrations which commonly are slightly above the regulatory limits. Second, in some situations, the cover soil slips on the geomembrane, mostly due to design not taking into account the saturated soil conditions; the soil might take with it the geomembrane, making it to tear (Fleming et al., 2006; Rowe and Yu, 2019). Slippage failure will tend to increase infiltration and a large volume of leachate being generated. Third, puncture damage of geomembranes can occur during the short-term period, for example, during construction, and/or over the long-term services, for example, perforation of the geomembrane by a heavy loaded sharp stone (Fox et al., 2014). This limits the degree of compaction to be applied to the soils and soil type to be reused in an embankment. Also, punctures will increase leakages, and eventually contamination of the surrounding environment (Katsumi et al., 2001).

One strategy currently being explored in the development of a cost-effective countermeasure when reusing the geogenic contaminated soils as fill materials in an embankment is, as shown in Figure 2.4 the installation of (1) a compacted attenuation layer underlain the contaminated pile, using a base material of sandy soil mixed with a stabilizing agent. Tatsuhara et al. (2015) found out that by constructing the attenuation layer undermost in an embankment, heavy metals released from the contaminated pile can be effectively attenuated for longer periods as leachate flows through the layer. And (2) a cover system to intercept oxygen flux and percolation of rainwater into the underlying pile. By limiting the amount of air entering the embankment, the oxidation reaction can be slowed. Likewise, by reducing the flow of water into the pile, the quantity of contaminated drainage can be reduced (Yanful et al., 1993; Tangviroon et al., 2017).

There are several advantages to using the attenuation layer method. To mention just a few, first, it requires relatively low investments to execute; Nozaki et al. (2013a) estimated that by applying this countermeasure about 3,500 yen can be saved for each cubic meter of soil reused (>50% cost reduction) when compared to layered systems using geomembranes. Note that these estimates do not consider site-specific details and maintenance. This countermeasure is cheap, in part, because of less need to construct

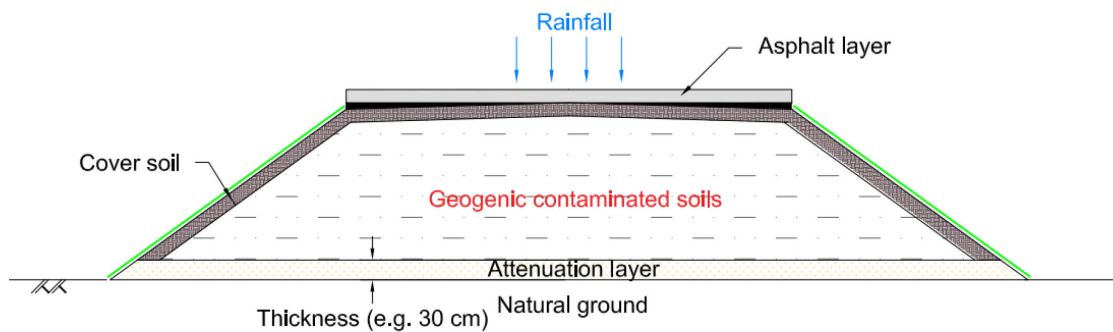


Figure 2.4: Embankment with attenuation layer underlain contaminated geomaterials.

additional facilities, such as drainage and water treatment facilities, and construction is relatively easy and fast to execute.

Second, as shown in Figure 2.5, the construction of the attenuation layer commonly involves the mixing of a natural soil (sandy soil) and a stabilizing agent, followed by the laying of the composite with proper compaction either on a flat, uneven, or sloped ground (Tatsuhara et al., 2015). Such flexibility in construction is necessary for the method to be applicable for many sites.

Third, it allows for denser compaction of contaminated material. This will reduce the infiltration rate which is important as it affects the leachate residence time (t_c) – duration the leachate is in contact with the solid material – thereby affecting the extent of geochemical processes that mobilize the heavy metals (Katsumi, 2015). Another merit of dense compaction is that it allows for the reuse of significantly large volumes of soils, which is necessary considering the huge amounts of contaminated soils and rocks excavated and need to be reused.

However, the implementation of this method has not yet been fully realized, due to mainly the lack of adequate information to verify its capability and reliability. There is a clear need to gain public acceptance, convince legislators, and establish the endurance of this countermeasure. One key concern is how to select a suitable base material and agent to achieve the desired hydraulic performance, contaminant attenuation, and pH buffering function, with considerations to the price, availability, ease of use/handling, safety to workers, suitability for several contaminants, and compliance with regulations.

Contaminant attenuation as defined by Yong and Mulligan (2003) refers to the reduction of toxicity and concentration during contaminant plume in soils and is an important issue to consider when contaminants are involved. Batch-type experiments where contaminated solutions are brought into contact with solid materials for a specified time, and column tests which can more closely simulate the



Figure 2.5: Representation of the construction process of the attenuation layer. Photo retrieved Feb 1, 2020, from <https://cpds.kentsu.co.jp/technology/detail?id=40>

in-situ water in contact with the solid materials, and also allows for the measurement of the time-lapse release of contaminants (Tabelin et al., 2014; Tatsuhara et al., 2015) are widely applied to evaluate the attenuation capacity of materials deemed suitable for use as the attenuation layer.

In most cases, it is reported that the materials can attenuate soluble and/or potentially soluble contaminants by converting them into sparingly soluble minerals, for example, earthen materials such as volcanic ash soil (Tabelin et al., 2014) and decomposed granite soil (Mo et al., 2015b), and stabilizing agents such as magnesium oxide (Nozaki et al., 2013b), zeolite (Naka et al., 2012), dolomite (Naruse et al., 2014), calcium-magnesium composite (Mo et al., 2015b). However, in most cases, it was concluded that the pH should be adjusted between pH 6 and 8 to achieve optimum performance (Tabelin et al., 2014). Moreover, in some situations, the attenuation capacity of a material might be limited by the type and/or the speciation of the heavy metal (Minja and Ebina, 2002). In reality, different kinds of contaminants might be simultaneously released (Tabelin et al., 2017) and depending on the content of pyrite relative to calcite, leachate might be acidic – in the case of a high S/Ca mole ratio in soil –, neutral, and/or alkaline – in the case the soil has a high content of calcite and/or other alkaline minerals (Inui et al., 2013; Paikaray, 2015). These issues need to be considered when choosing suitable materials as the attenuation layer, especially agent, which has a significant role to play in the attenuation of contaminants.

One of the recommendations by Nozaki et al (2013b) is to mix a base material of sandy soil with 100 kg/m³ agent, and laying the composite with proper compaction (Dc 95%) to achieve a 50 cm-thick attenuation layer with a hydraulic conductivity (*k*) lower than 1×10⁻⁵ m/s. The principal objectives of the design are to attain sufficient leachate residence time for a better attenuation function and, also, to provide for proper drainage of water inside the embankment, which is important to reduce pore pressures that tend to reduce the stability of an embankment. As shown in Figure 2.6, Mo et al. (2015b) found out that decomposed granite soil (of under 2-mm) has a *k* value of 5×10⁻⁷ m/s, which is within the permeable range. Even when 3% (or 30 g/kg-soil) or 5% (or 50 g/kg-soil) agent was mixed with the soil, slight changes in *k* were observed, but still, the composite was permeable (*k*=3.7×10⁻⁷ to 1.2×10⁻⁶ m/s).

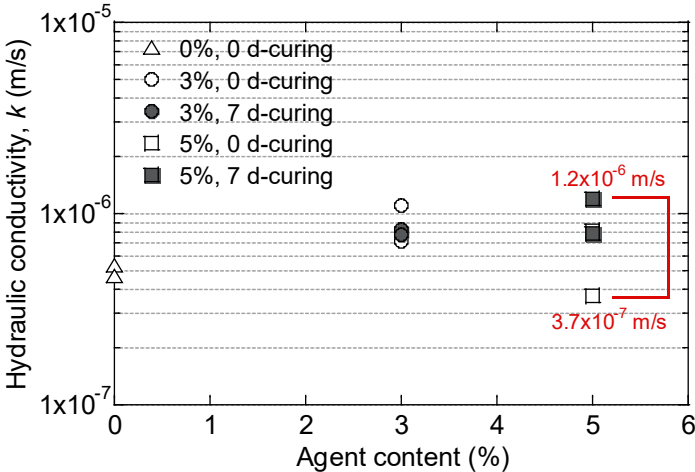


Figure 2.6: Hydraulic conductivity of a compacted composite of decomposed granite soil and stabilizing agent based on falling head, flexible-wall permeameter test, distilled water as permeant (Mo et al., 2015b).

2.3 Calcium-magnesium composite as a stabilizing agent

Over recent years, calcium-magnesium (Ca-Mg) composite which is produced by blending special additives with calcinations of natural minerals – with similar chemical property as dolomite ($\text{CaMg}(\text{CO}_3)_2$) – is considered as a material for the attenuation layer. Several studies show that by calcining such natural minerals ($\text{CaMg}(\text{CO}_3)_2$), their attenuation capacity can be enhanced due to (1) the increased surface area available for mass transfer and (2) higher amounts of sorptive compounds such as calcium carbonate (CaCO_3) and magnesium oxide (MgO) (Naruse et al., 2014; Salameh et al., 2015; Calugaru et al., 2016). Also, it was reported that such minerals are capable of attenuating Cd (Kocaoba, 2007), Pb (Pehlivan et al., 2009), As (Ayoub and Mehawej, 2007; Salameh et al., 2010; Salameh et al., 2015), F (Sasaki et al., 2013), B (Kuriwada et al., 2012), and other heavy metals that are commonly found in the geogenic contaminated soils and rocks.

Over recent years, the effectiveness of this agent of powder type of under 0.075 mm (which is one of the three available particle sizes of this material) has been studied (Kikuchi et al., 2012; Itaya et al., 2013; Mo et al., 2015b). Kikuchi et al. (2012) investigated the leaching concentrations from a composite of simulated contaminated soil and the powder agent. Although this approach is different from the attenuation layer method – natural clean soil is mixed with an agent – the results summarized in Table 2.6 demonstrate that by mixing about 50 kg/m^3 agent with the contaminated soil, the leaching amounts of several kinds of heavy metals can be decreased to levels below the acceptable limits. Concentrations of As, F, and B could be further decreased to much lower amounts when $>100 \text{ kg/m}^3$ agent was added. This shows that during design/construction of the attenuation layer, the agent content is one of the key parameters to consider.

Mo et al. (2015a) found out that the attenuation function of a natural soil can be improved when amended with this agent. As shown in Figure 2.7, the As attenuation function of the base material was improved with increasing agent content, which is similar to the findings by Kikuchi et al. (2012). For a composite with 5% (50 g/kg-soil) agent content, the As removal efficiency was $>95\%$, which is about a 40% improvement in removal efficiency. Also, although the authors found out that the unconfined compressive strength of the soil can be also improved by curing this composite, it was noted that the curing process might not offer any obvious changes to the attenuation capacity of this composite.

Table 2.6: Effectiveness of Ca-Mg composite to attenuate several contaminants.

Target contaminant	Amount of immobilizing agent added (kg/m^3)				Environmental standard (mg/L)	Leachate pH
	0	50	100	200		
	Leaching concentrations (mg/L)					
As(III)	0.42	0.01	0.005	0.003	0.01	9.1-9.7
Pb	0.26	0.01	0.009	0.009	0.01	8.9-9.9
F	1.2	0.8	0.6	0.4	0.8	8.9-9.9
Cr(VI)	1.61	0.02	0.02	0.01	0.05	9.1-9.7
B	1.6	1.0	0.5	-	1.0	9.4-9.7

Source: Kikuchi et al. (2012).

Note: Aging period for soils mixed with this agent was 1 day.

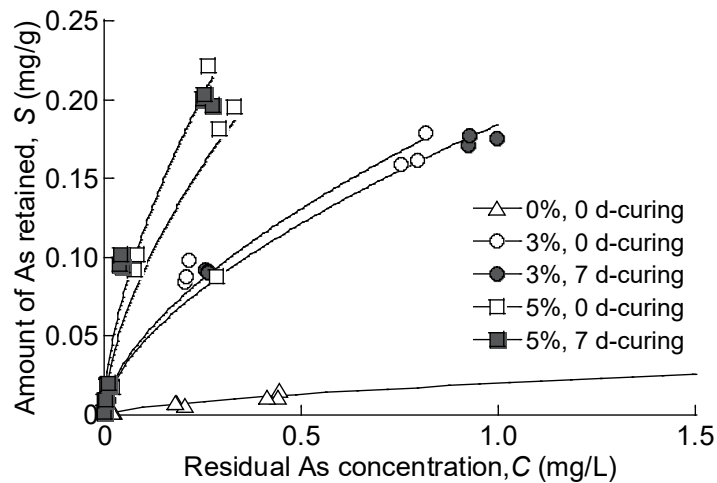


Figure 2.7: Enhanced sorption of a base material by adding Ca-Mg composite of powder type (Mo et al., 2015a) .

Hydraulic performance of attenuation layer is crucial because it affects flow conditions (flow rate, residence time, etc.) of the leachate inside the layer, which is a key issue for the attenuation process. Unlike some low-permeability waste containment barriers, there are no specific regulations on the criteria of the hydraulic conductivity for the attenuation layer, although some researchers suggest $k < 1 \times 10^{-5}$ m/s (Nozaki et al., 2013). Mo (2019) found out that this agent does not significantly change the hydraulic conductivity values of sandy soil. Furthermore, the author found out that the hydraulic conductivity of this soil-agent composite can be maintained over time between $k = 1 \times 10^{-6}$ m/s and 1×10^{-7} m/s. If the water permeability characteristics of this composite is expressed by the leachate residence time ($t_c = L\phi/ki$, where L is the thickness of the attenuation layer, ϕ is the porosity of the layer, and i is hydraulic gradient), for a typical 30 cm-thick layer, and assuming $\phi = 0.3$, t_c is expected to be more than 25 h and is preferred for it provides better attenuation performance as shown in Figure 2.9.

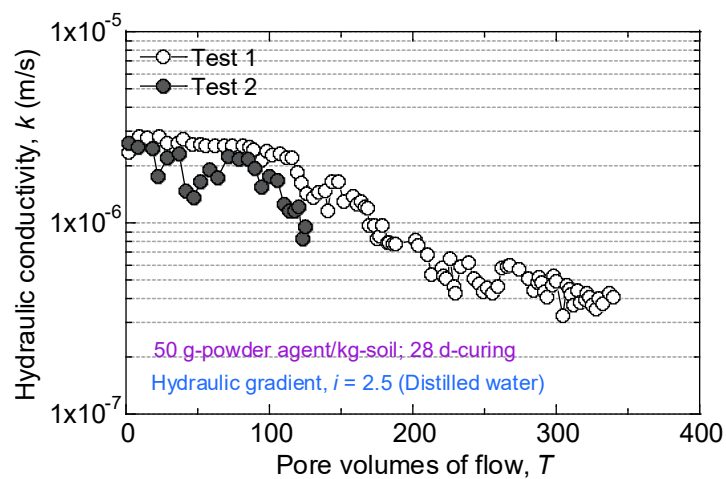


Figure 2.8: Permeability characteristics under continuous permeation (Mo, 2019).

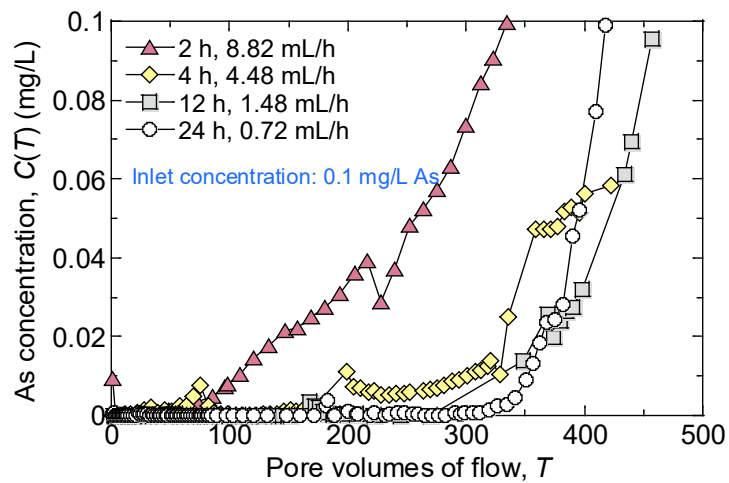


Figure 2.9: Arsenic amounts at column exit with continuous permeation using a 1 mg/L As solution under different flow rates (Mo, 2019).

Ito et al. (2014) found out that this material has a high capability to increase pH to above pH 10 – strongly alkaline conditions – when brought into contact with solutions with different concentrations of acid (HCl), which is due to the high carbonates content. For an acid input of 0 mmol H⁺/kg-soil to 45 mmol H⁺/kg-soil, this material had better pH buffering capabilities when compared to calcite (CaCO₃), although it was found to be slightly less reactive compared to MgO, as illustrated in Figure 2.10. Also, Seo et al. (2015) confirmed that the presence of co-existing anions (SO₄²⁻, Cl⁻, and NO₃⁻) and different pH conditions of 2 to 10 did not affect the high attenuation capacity of this material. It can be therefore concluded that this material can be used as a constituent of the attenuation layer, due to the high capabilities to increase pH and decrease concentrations of several kinds of heavy metals in leachate.

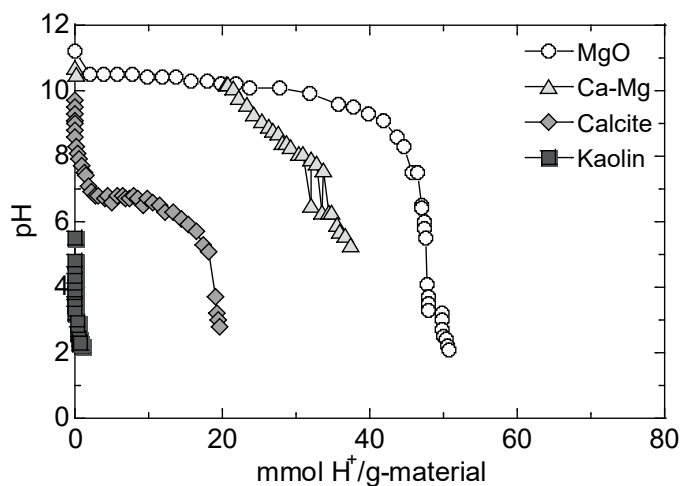
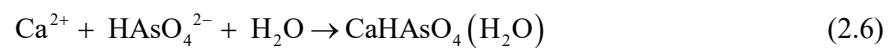
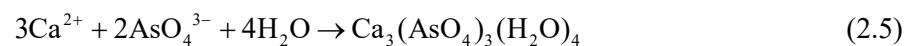
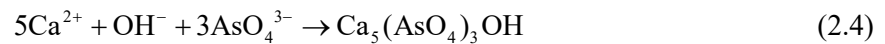


Figure 2.10: Comparison of pH buffering capacity of different stabilizing agents (Ito et al., 2014).

In an effort to clarify the As sorption mechanism of Ca-Mg composite, Itaya et al. (2013) carried out X-ray diffraction (XRD), X-ray fluorescence (XRF), scanning electron microscopy and energy dispersive spectroscopy (SEM-EDS) analysis on the residue after batch-type experiments. According to the authors, due to the addition of this material, pH will increase and H_3AsO_3 will start to transfer into H_2AsO_3^- . As(III) will be oxidized to As(V). Precipitation of calcium arsenate – less mobile compounds that are stable over a wide pH range (Bothe and Brown, 1999) – will be generated according to the following chemical reactions:



As a material for the attenuation layer, this Ca-Mg composite is found to have various merits due to its high attenuation capacity, suitability for several contaminants, high capabilities to increase pH, stability, and so on. However, the applicability of the composite of natural soil and this agent under low pH of 2 to 4, which can naturally occur in such contaminated geological materials due to a high S/Ca mole ratio in the solid material (Inui et al., 2013; Paikaray, 2015) has not yet been verified. Also, the applicability of the coarse (2-9.5 mm) agent that is cheaper to produce (e.g. due to fewer production processes), offers better material handling, can be homogeneously distributed in the host soil and expected to offer less, but long-term reactivity, has not yet been studied.

References for Chapter 2

- Amos, R. T., Blowes, D. W., Bailey, B. L., Sego, D. C., Smith, L., and Ritchie, A. I. M. 2015. Waste-rock hydrogeology and geochemistry. *Applied Geochemistry*, 57: 140-156.
- Arulrajah, A., Ali, M. M. Y., Piratheepan, J., and Bo, M. W. 2012. Geotechnical properties of waste excavation rock in pavement subbase applications. *Journal of Materials in Civil Engineering*, 24(7): 924-932.
- Ayoub, G. M. and Mehawej, M. 2007. Adsorption of arsenate on untreated dolomite powder. *J Hazard Mater*, 148(1-2): 259-266.
- Bothe, J. V. and Brown, P. W. 1999. The stabilities of calcium arsenates at 23 +/- 1 degrees C. *Journal of Hazardous Materials*, 69(2): 197-207.
- Calugaru, I. L., Neculita, C. M., Genty, T., Bussière, B., and Potvin, R. 2016. Performance of thermally activated dolomite for the treatment of Ni and Zn in contaminated neutral drainage. *Journal of Hazardous Materials*, 310: 48-55.

- Cheng, Y. and Huang, X. 2018. Effect of mineral additives on the behavior of an expansive soil for use in highway subgrade soils. *Applied Sciences*, 9(1): 30.
- Chittoori, B., Puppala, A., Reddy, R., and Marshall, D. 2012. Sustainable reutilization of excavated trench material. In *GeoCongress 2012*, 4280-4289.
- Cremisini, C. and Armiento, G. 2016. High geochemical background of potentially harmful elements. The “geochemical risk” and “natural contamination” of soils and water: awareness and policy approach in Europe with a focus on Italy.
- Cui, J.-l., Zhao, Y.-p., Li, J.-s., Beiyuan, J.-z., Tsang, D. C. W., Poon, C.-s., Chan, T.-s., Wang, W.-x., and Li, X.-d. 2018. Speciation, mobilization, and bioaccessibility of arsenic in geogenic soil profile from Hong Kong. *Environmental Pollution*, 232: 375-384.
- Eras, J. J. C., Gutierrez, A. S., Capote, D. H., Hens, L., and Vandecasteele, C. 2013. Improving the environmental performance of an earthwork project using cleaner production strategies. *Journal of Cleaner Production*, 47: 368-376.
- Fleming, I. R., Sharma, J. S., and Jogi, M. B. 2006. Shear strength of geomembrane-soil interface under unsaturated conditions. *Geotextiles and Geomembranes*, 24(5): 274-284.
- Fox, P. J., Thielmann, S. S., Stern, A. N., and Athanassopoulos, C. 2014. Interface shear damage to a HDPE geomembrane. I: Gravelly compacted clay liner. *Journal of Geotechnical and Geoenvironmental Engineering*, 140(8): 04014039.
- Gonzalez, A. R., Ndung'u, K., and Flegal, A. R. 2005. Natural occurrence of hexavalent chromium in the aromas red sands aquifer, California. *Environmental Science & Technology*, 39(15): 5505-5511.
- Haid, H.-G. and Hammer, H. 2009. Katzenberg tunnel - environmental and approval constraints on the recycling of tunnel spoil material. *Geomechanik und Tunnelbau*, 2(5): 643-651.
- Igarashi, T., Sasaki, R., and Tabelin, C. B. 2013. Chemical forms of arsenic and selenium leached from mudstones. *Procedia Earth and Planetary Science*, 6: 105-113.
- Inui, T., Katsumi, T., Takai, A., and Kamon, M. 2013. Factors affecting heavy metal leaching in excavated rocks with natural contamination. In Manassero et al. (Eds.), *Coupled Phenomena in Environmental Geotechnics*, 587-592: CRC Press.
- Itaya, Y., Kikuchi, S., Yoshimatsu, T., and Kuninishi, K. 2013. Clarification of insolubilization mechanism of heavy metals using magnesium/calcium composite material. *Proceedings of the 19th Conference on Groundwater and Soil Contamination and its Countermeasures*, Japan. (In Japanese).
- Ito, K., Kuninishi, K., Itaya, Y., and Suzuki, M. 2014. Distribution and stability of heavy metals sorbed on Ca/Mg compound material. *Proceedings of the 20th Conference on Groundwater and Soil Contamination and its Countermeasures*, Japan. (In Japanese).
- Katsumi, T. 2015. Soil excavation and reclamation in civil engineering: Environmental aspects. *Soil Science and Plant Nutrition*, 61(sup1): 22-29.

- Katsumi, T. 2018. Towards sustainable soil management: Case studies of the reuse of tsunami deposits and excavated soils with natural contamination *Workshop of Sustainable Remediation*. Tokyo, Japan.
- Katsumi, T., Benson, C. H., Foose, G. J., and Kamon, M. 2001. Performance-based design of landfill liners. *Engineering Geology*, 60(1-4): 139-148.
- Katsumi, T. and Inui, T. 2013. Recycling materials in geotechnical applications. *Third International Conference on Sustainable Construction Materials and Technologies*, Kyoto, Japan.
- Katsumi, T., Inui, T., Yasutaka, T., and Takai, A. 2019. Towards sustainable soil management — reuse of excavated soils with natural contamination —. *Proceedings of the 8th International Congress on Environmental Geotechnics Volume 1*, Hangzhou, China.
- Katsumi, T., Kamon, M., and Inui, T. 2004. Japanese status on the use of waste and by-products in geotechnical applications. In Aydilek & Wartman (Eds.), *Recycled Materials in Geotechnics*, 22-41: American Society of Civil Engineers.
- Kikuchi, S., Kuninishi, K., and Itaya, Y. 2012. Basic discussion on the applicability of Ca/Mg composite material in sorption layer method. *67th Annual Conference of the Japan Society of Civil Engineers*, Japan. (In Japanese).
- Kocaoba, S. 2007. Comparison of Amberlite IR 120 and dolomite's performances for removal of heavy metals. *Journal of Hazardous Materials*, 147(1-2): 488-496.
- Kuriwada, A., Sase, T., Wang, L. P., Dodbiba, G., Okaya, K., and Fujita, T. 2012. Boron removal and recovery by adsorbing effect of boron on thermally treated dolomite in the water containing boron ion. *Resources Processing*, 59(4): 149-154.
- Lange, K., Rowe, R. K., and Jamieson, H. 2010. The potential role of geosynthetic clay liners in mine water treatment systems. *Geotextiles and Geomembranes*, 28(2): 199-205.
- Li, J., Kosugi, T., Riya, S., Hashimoto, Y., Hou, H., Terada, A., and Hosomi, M. 2018. Pollution potential leaching index as a tool to assess water leaching risk of arsenic in excavated urban soils. *Ecotoxicol Environ Saf*, 147: 72-79.
- Li, J. N., Kosugi, T., Riya, S., Hashimoto, Y., Hou, H., Terada, A., and Hosomi, M. 2017a. Use of batch leaching tests to quantify arsenic release from excavated urban soils with relatively low levels of arsenic. *Journal of Soils and Sediments*, 17(8): 2136-2143.
- Li, J. S., Beiyuan, J., Tsang, D. C. W., Wang, L., Poon, C. S., Li, X. D., and Fendorf, S. 2017b. Arsenic-containing soil from geogenic source in Hong Kong: Leaching characteristics and stabilization/solidification. *Chemosphere*, 182: 31-39.
- Li, Q., Wu, Z., Chu, B., Zhang, N., Cai, S., and Fang, J. 2007. Heavy metals in coastal wetland sediments of the Pearl River Estuary, China. *Environmental Pollution*, 149(2): 158-164.
- Li, S., Wang, M., Yang, Q., Wang, H., Zhu, J., Zheng, B., and Zheng, Y. 2013. Enrichment of arsenic in surface water, stream sediments and soils in Tibet. *Journal of Geochemical Exploration*, 135: 104-

- Magnusson, S., Lundberg, K., Svedberg, B., and Knutsson, S. 2015. Sustainable management of excavated soil and rock in urban areas - A literature review. *Journal of Cleaner Production*, 93: 18-25.
- Meistro, N., Parisi, G., Scuderi, A., Pistorio, S., and Genito, S. 2019. Compliant reuse of Terzo Valico excavation material: Design and operations. In *Tunnels and Underground Cities: Engineering and Innovation meet Archaeology, Architecture and Art*, 445-454.
- Minja, R. J. A. and Ebina, T. 2002. Arsenic adsorption capabilities of soil-bentonite mixtures as buffer materials for landfill. *Clay Science*, 12(1): 41-47.
- MLIT 2010. Technical manual on the countermeasure for against soils and rocks containing naturally occurring heavy metals in construction works (Draft). Retrieved from <http://www.mlit.go.jp/sogoseisaku/region/recycle/recyclehou/manual/index.htm>. (In Japanese).
- MLIT 2014. Investigation results of construction by-products in 2012. Retrieved from <http://www.mlit.go.jp/sogoseisaku/region/recycle/fukusanbutsu/jittaichousa/index01.htm>. (In Japanese).
- Mo, J. (2019). *Soil amended with calcium-magnesium immobilizing agent against natural arsenic contamination*. Doctoral Thesis. Kyoto University, Retrieved from <https://dx.doi.org/10.14989/doctor.k21936>
- Mo, J., Inui, T., Katsumi, T., Kuninishi, K., and Shintaro, H. 2015a. Effectiveness of immobilizing agent used as a sorption layer against natural contamination. *Japanese Geotechnical Society Special Publication*, 1(4): 19-24.
- Mo, J., Inui, T., Katsumi, T., Takai, A., Kuninishi, K., and Hayashi, S. 2015b. Performance of sorption layer using Ca/Mg immobilizing agent against natural contamination. *10th Asian Regional Conference of IAEG*, Kyoto, Japan.
- Naka, A. (2014). *Hydraulic performance and chemical compatibility of mineral barriers to mitigate natural contamination from excavated rocks*. Kyoto University, Retrieved from <http://hdl.handle.net/2433/188879>
- Naka, A., Katsumi, T., Flores, G., Inui, T., Takai, A., and Ohta, T. 2012. Mineral barriers against natural contamination from excavated rocks. In Miura et al. (Eds.), *Advances in Transportation Geotechnics 2*. London: Taylor & Francis Group.
- Naruse, T., Kawashima, T., and Igarash, T. 2014. Reduction in arsenic concentration leached from excavated mudstone by half-burnt dolomite as a sorbent. *Journal of Japan Society of Civil Engineers, Ser. G (Environmental Research)*, 70(4): 78-85. (In Japanese).
- Nozaki, F., Shimizu, Y., and Ito, K. 2013. Discussion on construction method of heavy metals adsorption layer. *Proceedings of the 19th Symposium on Soil and Groundwater Contamination and Remediation*.

(In Japanese).

- Ocak, I. 2009. Environmental problems caused by Istanbul subway excavation and suggestions for remediation. *Environmental Geology*, 58(7): 1557-1566.
- Ohta, A., Imai, N., Terashima, S., and Tachibana, Y. 2011. Regional geochemical mapping in eastern Japan including the nation's capital, Tokyo. *Geochemistry: Exploration, Environment, Analysis*, 11(3): 211-223.
- Paikaray, S. 2015. Arsenic geochemistry of acid mine drainage. *Mine Water and the Environment*, 34(2): 181-196.
- Panagiotaras, D. and Nikolopoulos, D. 2015. Arsenic occurrence and fate in the environment; A geochemical perspective. *Journal of Earth Science & Climatic Change*, 6: 1-9.
- Pehlivan, E., Özkan, A. M., Dinç, S., and Parlayıcı, Ş. 2009. Adsorption of Cu^{2+} and Pb^{2+} ion on dolomite powder. *Journal of Hazardous Materials*, 167(1): 1044-1049.
- Pirajno, F. 2009. *Hydrothermal Processes and Mineral Systems*: Springer.
- Ravenscroft, P., Brammer, H., and Richards, K. 2011. *Arsenic Pollution: A Global Synthesis*: Wiley.
- Rowe, R. K. and Yu, Y. 2019. Magnitude and significance of tensile strains in geomembrane landfill liners. *Geotextiles and Geomembranes*, 47(3): 439-458.
- Salameh, Y., Al-Lagtah, N., Ahmad, M. N. M., Allen, S. J., and Walker, G. M. 2010. Kinetic and thermodynamic investigations on arsenic adsorption onto dolomitic sorbents. *Chemical Engineering Journal*, 160(2): 440-446.
- Salameh, Y., Albadarin, A. B., Allen, S., Walker, G., and Ahmad, M. N. M. 2015. Arsenic(III,V) adsorption onto charred dolomite: Charring optimization and batch studies. *Chemical Engineering Journal*, 259: 663-671.
- Sasaki, K., Yoshida, M., Ahmmad, B., Fukumoto, N., and Hirajima, T. 2013. Sorption of fluoride on partially calcined dolomite. *Colloids and Surfaces A: Physicochemical and Engineering Aspects*, 435: 56-62.
- Seo, A., Inui, T., Takai, A., Katsumi, T., Kuninishi, K., and Hayashi, S. 2015. Effects of pH and anions on arsenic sorption capacity of soil enhanced by calcium/magnesium stabilizing agent for in situ containment. *14th Global Joint Seminar on Geo-environmental Engineering*, Montreal, Canada.
- Smedley, P. L. and Kinniburgh, D. G. 2002. A review of the source, behaviour and distribution of arsenic in natural waters. *Applied Geochemistry*, 17(5): 517-568.
- Tabelin, C. B., Basri, A. H. M., Igarashi, T., and Yoneda, T. 2012a. Removal of arsenic, boron, and selenium from excavated rocks by consecutive washing. *Water, Air, & Soil Pollution*, 223(7): 4153-4167.
- Tabelin, C. B. and Igarashi, T. 2009. Mechanisms of arsenic and lead release from hydrothermally

- altered rock. *J Hazard Mater*, 169(1-3): 980-990.
- Tabelin, C. B., Igarashi, T., Arima, T., Sato, D., Tatsuhara, T., and Tamoto, S. 2014. Characterization and evaluation of arsenic and boron adsorption onto natural geologic materials, and their application in the disposal of excavated altered rock. *Geoderma*, 213: 163-172.
- Tabelin, C. B., Igarashi, T., and Takahashi, R. 2012b. Mobilization and speciation of arsenic from hydrothermally altered rock in laboratory column experiments under ambient conditions. *Applied Geochemistry*, 27(1): 326-342.
- Tabelin, C. B., Igarashi, T., Tamoto, S., and Takahashi, R. 2012c. The roles of pyrite and calcite in the mobilization of arsenic and lead from hydrothermally altered rocks excavated in Hokkaido, Japan. *Journal of Geochemical Exploration*, 119: 17-31.
- Tabelin, C. B., Igarashi, T., Villacorte-Tabelin, M., Park, I., Opiso, E. M., Ito, M., and Hiroyoshi, N. 2018. Arsenic, selenium, boron, lead, cadmium, copper, and zinc in naturally contaminated rocks: A review of their sources, modes of enrichment, mechanisms of release, and mitigation strategies. *Science of the Total Environment*, 645: 1522-1553.
- Tabelin, C. B., Igarashi, T., and Yoneda, T. 2012d. Mobilization and speciation of arsenic from hydrothermally altered rock containing calcite and pyrite under anoxic conditions. *Applied Geochemistry*, 27(12): 2300-2314.
- Tabelin, C. B., Sasaki, R., Igarashi, T., Park, I., Tamoto, S., Arima, T., Ito, M., and Hiroyoshi, N. 2017. Simultaneous leaching of arsenite, arsenate, selenite and selenate, and their migration in tunnel-excavated sedimentary rocks: I. Column experiments under intermittent and unsaturated flow. *Chemosphere*, 186: 558-569.
- Takahashi, T., Fujii, K., Igarashi, T., Kaketa, K., and Yamada, N. 2011. Distribution and leaching properties of arsenic in hydrothermally altered rock of Nakakoshi area, central Hokkaido, Japan. *Journal of the Japan Society of Engineering Geology*, 52(2): 46-54.
- Tamoto, S., Tabelin, C. B., Igarashi, T., Ito, M., and Hiroyoshi, N. 2015. Short and long term release mechanisms of arsenic, selenium and boron from a tunnel-excavated sedimentary rock under in situ conditions. *Journal of Contaminant Hydrology*, 175-176: 60-71.
- Tanaka, T. 1988. Distribution of arsenic in the natural environment with emphasis on rocks and soils. *Applied Organometallic Chemistry*, 2(4): 283-295.
- Tangvirorn, P., Hayashi, R., and Igarashi, T. 2017. Effects of additional layer(s) on the mobility of arsenic from hydrothermally altered rock in laboratory column experiments. *Water Air and Soil Pollution*, 228(5): 191.
- Tatsuhara, T., Jikihara, S., Tatsumi, T., and Igarashi, T. 2015. Effects of the layout of adsorption layer on immobilizing arsenic leached from excavated rocks. *Japanese Geotechnical Journal*, 10(4): 635-640. (In Japanese).

- Ujiie-Mikoshiba, M., Imai, N., Terashima, S., Tachibana, Y., and Okai, T. 2006. Geochemical mapping in northern Honshu, Japan. *Applied Geochemistry*, 21(3): 492-514.
- Walsh, D., McRae, I., Zirngibl, R., Chawla, S., Zhang, H., Alfieri, A., Moore, H., Bailey, C., Brooks, A., Ostock, T., Pong, S., Hard, T., Sullivan, C., and Wilding, J. 2019. Generation rate and fate of surplus soil extracted in New York City. *Sci Total Environ*, 650(Pt 2): 3093-3100.
- Yamana, M., Tomizawa, Y., Fujiwara, T., Mizuta, K., Mizuno, K., Inui, T., Katsumi, T., and Kamon, M. 2019. Management of the soils discharged from shield tunnel excavation. *Proceedings of the 8th International Congress on Environmental Geotechnics Volume 1*, Singapore.
- Yanful, E. K., Bell, A. V., and Woyshner, M. R. 1993. Design of a composite soil cover for an experimental waste rock pile near Newcastle, New Brunswick, Canada. *Canadian Geotechnical Journal*, 30(4): 578-587.
- Yokobori, N., Igarashi, T., and Yoneda, T. 2015. Leaching characteristics of heavy metals from mineralized rocks located along tunnel construction sites. *Engineering Geology for Society and Territory - Volume 6*, Cham.
- Yong, R. N. and Mulligan, C. N. 2003. *Natural Attenuation of Contaminants in Soils*: CRC Press.
- Yu, X., Yan, Y., and Wang, W.-X. 2010. The distribution and speciation of trace metals in surface sediments from the Pearl River Estuary and the Daya Bay, Southern China. 60(8): 1364-1371.
- Zhan, L.-t., Zhang, Z., Chen, Y.-m., Chen, R., Zhang, S., Liu, J., and Li, A.-g. 2018. The 2015 Shenzhen catastrophic landslide in a construction waste dump: Reconstitution of dump structure and failure mechanisms via geotechnical investigations. *Engineering Geology*, 238: 15-26.

Chapter 3 Enhanced attenuation function of a natural soil

3.1 General remarks

As a material for the attenuation layer, Ca-Mg composite has various merits due to its high attenuation capacity, suitability for several contaminants, high capability to increase pH, and so on (Kikuchi et al., 2012; Itaya et al., 2013; Mo et al., 2015). Although Mo et al. (2015) studied the effectiveness of a natural clean soil amended with the powder agent as the attenuation layer, the applicability of the composite under low pH of 2 to 4, which can naturally occur in such contaminated geological materials due to a high S/Ca mole ratio in the solid material (Inui et al., 2013; Paikaray, 2015) has not yet been verified. Also, applicability of the coarse agent which is cheaper to produce and offers better material handling has not yet been studied. In this chapter, batch-type tests were carried out to obtain basic information about the performance of a natural soil amended with different particle sizes of this agent from the viewpoints of As attenuation, and the relationship of pH and buffer capacity on As attenuation.

3.2 Materials and methods

3.2.1 Materials

Natural clean material of decomposed granite soil which is commercially available soil collected in Kyoto, was oven-dried and used after sieving with a 2-mm opening, as a base material for the tests. The sieved soil has a particle density (ρ_s) of 2.69 g/cm^3 . Particle size distribution of the soil was determined according to the Japanese testing methods, JGS 0131, and it was classified as sand with fine fraction (S-F) based on JGS 0051. Compaction property of the natural soil ($\rho_{d \max} = 2.01 \text{ g/cm}^3$ and $w_{\text{opt}} = 10.1\%$) was determined by applying the A-a method of the standard Proctor compaction test (JGS 0711). X-ray Fluorescence (XRF) analysis was carried out using a Shimadzu EDX-720 X-ray Fluorescence spectrometer equipped with a high-resolution Energy Dispersive tube (Rh X-ray tube – 50 kV – 1000 uA) to determine the composition of the soil. Figure 3.1 shows the particle size distribution and compaction curve of the natural soil, while Table 3.1 summarizes its physicochemical properties.

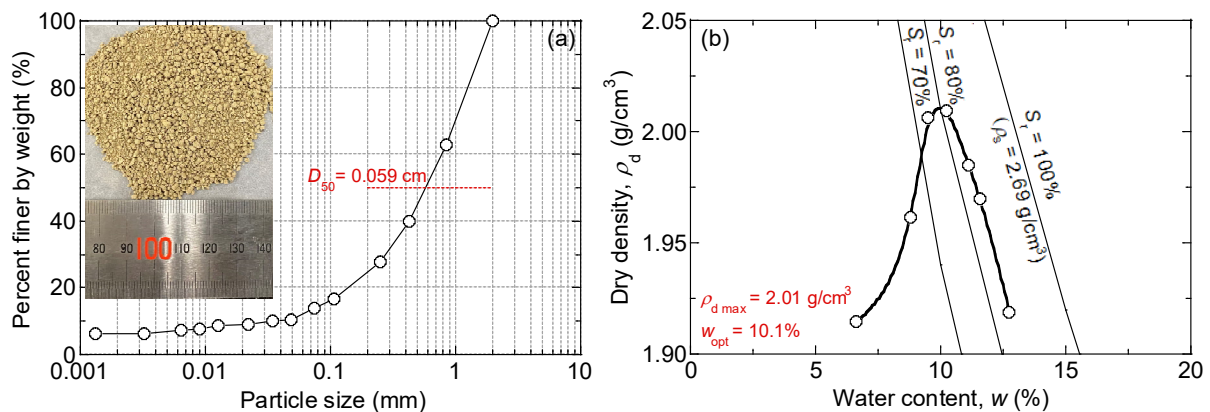



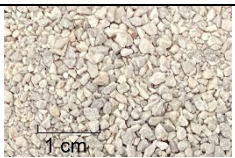

Figure 3.1: Characteristics of the sieved soil in (a) particle size distribution and (b) compaction property.

Table 3.1: Physicochemical characterization of the natural soil.

Property	Value	Method
Particle size distribution (%)		JGS 0131
Sand fraction (0.075-2 mm)	85.9	
Silt fraction (0.005-0.075 mm)	7.7	
Clay fraction (< 0.005 mm)	6.4	
Uniformity coefficient, U_c	20.2	
Coefficient of curvature, U_c'	3.32	
Particle density, ρ_s (g/cm ³)	2.69	JGS 0111
Optimum water content, w_{opt} (%)	10.1	JGS 0711
Maximum dry density, ρ_d (g/cm ³)	2.01	JGS 0711
Compacted hydraulic conductivity, k (m/s)	5.4×10^{-7}	ASTM D 5084
(optimum water content, Dc 95%)		Falling head, flexible-wall permeameter test
pH (distilled water)	9.5	JGS 0211
Loss on ignition, L_i (%)	2.09	JGS 0221
(750±50 °C, 1 h)		
Chemical composition (wt. %)	Si: 41.1; Fe: 22.9; Al: 17.4; Ca: 7.4; K: 6.9; Ti: 1.6; Zr: 0.6; Ba: 0.6; S: 0.6; Mn: 0.5; Others: 0.4	X-ray Fluorescence

Ca-Mg composite was supplied by Sumitomo Osaka Cement Co. Ltd. It is produced by blending calcinations of dolomite-like natural minerals with special additives and crushing them to different particle sizes. Calcination allows formation of CaCO₃ and MgO, which enhance metal retention (Boucif et al., 2010; Salameh et al., 2015); based on the chemical analyse for lime method (JIS R 9011), the material was determined to constitute mainly of calcium (as CaCO₃) and its content is about 35.6%. Magnesium (as MgCO₃ and MgO) content is about 19.4%. It also contains trace amounts of iron (as FeSO₄). In this study, three different particle sizes of this material ($\rho_s=2.79$ g/cm³) were used as the stabilizing agent and their appearance and physicochemical features are shown in Table 3.2. Specific surface area (SSA) of the three agent sizes was estimated via the Brunauer-Emmet-Teller nitrogen (BET N₂) adsorption method and the values of the fine agent of under 2 mm and coarse agent of 2-9.5 mm were found out to be almost same, despite their differences in particle size distribution as shown in Figure 3.2, which indicates that the micropores in the two agent types are equal. The high ignition loss of 33.5% is due to the calcium carbonate decarbonation of the dolomite component.

Table 3.2: Properties of the calcium-magnesium composite.

Agent type	Powder	Fine	Coarse	Method
Appearance				
Particle size (mm)	under 0.075	under 2	2-9.5	JGS 0131
Specific surface area (m ² /g)	9.85 ^a	3.7	3.6	BET N ₂
pH (distilled water)	10-12	10-12	9-10	JGS 0211
Chemical composition (wt. %) ^b	CaO: 35.6; MgO: 19.4; SO ₃ : 3.9; Fe ₂ O ₃ : 3.73; SiO ₂ : 1.52; Al ₂ O ₃ : 0.07; P ₂ O ₅ : 0.04; Loss on ignition: 33.5			JIS R 9011

^a Itaya et al. (2013).

^b The Society of Materials Science (2014).

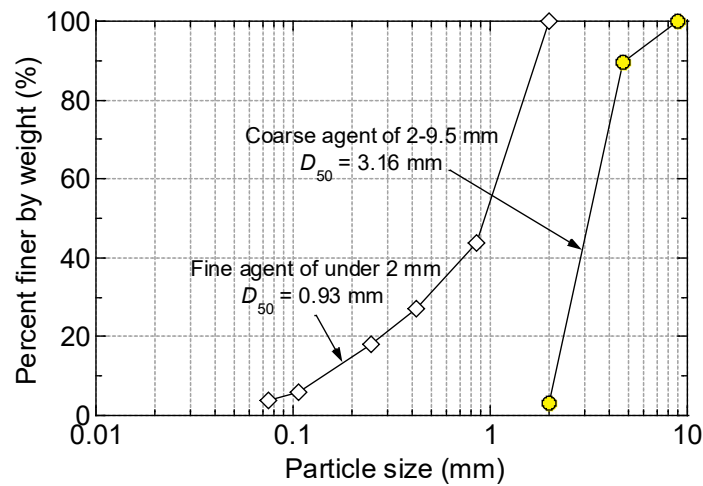


Figure 3.2: Particle size distribution of the fine and coarse Ca-Mg composite.

Several composites of the soil and different particle sizes of the agent were prepared by adding the agent to the dry soil at either 0 or 5% (50 g/kg-soil) by dry weight of the mixture and the required amount of distilled water added to achieve the optimum water content ($w_{opt}=10-11\%$). Mixing was done with a mechanical mixer, and proper care was taken to prepare a homogeneous composite. After that, a composite was either immediately subjected to the batch-type experiments (0-day cured sample) or undergo an additional step of curing it for either 7 or 28 days. To do so, a composite was compacted (w_{opt} , Dc 95%) in three equal layers (≈ 2.3 cm each) in a 6 cm-inner diameter and 7 cm-high steel mold. A compacted sample was extruded and cured for either 7 or 28 days, by wrapping it with a cling film (see Figure 3.3) and storing it in a humid, sealable plastic bag under room temperature conditions of 20 °C. To make the extrusion process easy, the inner wall of mold was smeared with silica gel (KF-96-50CS) and a parafilm was applied before the compaction step. Surplus soils after mixing and/or compaction were used for the measurement of the water content of the samples (JGS 0121).



Figure 3.3: Photo of a compacted soil sample prepared for the curing step.

3.2.2 Batch-type experiment

As summarized in Table 3.3, twenty-two cases were investigated using the batch-type test to obtain basic information about the performance of the several composites of soil and agent from the viewpoints of As attenuation and the relationship of pH and buffer capacity on As attenuation.

3.2.2.1 Arsenic attenuation

To obtain basic information about the As attenuation capacity of these composites with considerations to the curing period (Case 1-6) and low pH of 2 to 4 (Case 7-18), five different concentrations in mg/L As of 0.1, 0.5, 1, 5, and 10 were prepared. For each concentration, several solutions with three different pH of 2, 4, and 6 were prepared. The solutions were prepared by using As in the form of sodium arsenite (NaAsO_2) and the acid used was H_2SO_4 . As shown in Figure 3.4, the solid materials were added to solution in capped plastic bottles to achieve a ratio of 1:10 of solid:solution by using 50 g of soil samples and 500 mL of As solution. Note that for a cured sample, it was first gently crushed to <9 mm particle size. The soil suspension samples were horizontally shaken at 150 rpm for 24 h at a room temperature of 20 °C, using a TAITEC TS-10 mechanical shaker. This time interval is similar to that used by Mo et al. (2015). After the shaking step, samples were allowed to stand for 10-15 min, and after that centrifuged at 3,000 rpm for 10 min and filtered using a membrane filter with a particle size retention of 0.45 μm .

Table 3.3: Conditions for the batch-type experiment.

No.	Case Id	Agent type	Curing period	pH (or M)	Remarks	
1	SF-0D-PH6		0 day		Case 1-6 carried out to study the effect of curing time on arsenic attenuation. Five concentrations in ppm As of 0.1 to 10 were considered. Curing done by first compacting a composite (w_{opt} , Dc 95%), then wrapping it with a cling film before storing it in a humid, sealable plastic bag under a constant room temperature of 20 °C.	
2	SF-7D-PH6	Fine	7 days	pH 6		
3	SF-28D-PH6		28 days			
4	SC-0D-PH6		0 day			
5	SC-7D-PH6	Coarse	7 days	pH 6		
6	SC-28D-PH6		28 days			
7	S-0D-PH2			pH 2	Case 7-18 carried out to study the arsenic attenuation under low pH of 2 to 4. Five concentrations in ppm As of 0.1 to 10 were considered. For each concentration, several solutions with three different pH of 2, 4, or 6 were prepared.	
8	S-0D-PH4	No agent	0 day	pH 4		
9	S-0D-PH6			pH 6		
10	SP-0D-PH2			pH 2		
11	SP-0D-PH4	Powder	0 day	pH 4		
12	SP-0D-PH6			pH 6		
13	SF-0D-PH2			pH 2		
14	SF-0D-PH4	Fine	0 day	pH 4		
15	SF-0D-PH6			pH 6		
16	SC-0D-PH2			pH 2		
17	SC-0D-PH4	Coarse	0 day	pH 4		
18	SC-0D-PH6			pH 6		
19	S-0D-PBC	No agent				Case 19-22 carried out to study the relationship of pH and buffer capacity on arsenic attenuation. Solutions with concentration in ppm As of 0 and 0.1 were considered. Solutions with concentrations of acid of 0 to 0.588 M were prepared.
20	SP-0D-PBC	Powder	0 day	0-0.588 M		
21	SF-0D-PBC	Fine				
22	SC-0D-PBC	Coarse				



Figure 3.4: Pictorial representation of typical steps for batch-type test showing 1) preparation of arsenic solutions, 2) adding soil samples to solution, 3) shaking step, 4) centrifugation step, 5) analysis of arsenic amounts using atomic absorption spectrophotometer and 6) analysis of water-soluble ion amounts using inductively coupled spectrophotometer.

Filtrate pH, electrical conductivity (EC), and redox potential (Eh) were measured. Amounts of As remaining in filtrate were analyzed with a Shimadzu AA-6800 atomic absorption spectrometer, while amounts of other water-soluble metal ions were analyzed using an ICP-OES 700 inductively coupled spectrophotometer. The amount of As retained by the solid material, S (mg/g) was calculated as the difference in the As-applied, C_0 (mg/L) and As remaining in filtrate, C (mg/L) using equation (3.1).

$$S = \frac{V_w (C_0 - C)}{M_s} \quad (3.1)$$

where, V_w (L) is the volume of solution, and M_s (g) is the mass of soil sample.

3.2.2.2 Determination of buffer capacity using acid titration experiment

Buffer capacity of the composites (Case 19-22) was investigated by titrating each sample with increasing concentrations of acid (H_2SO_4). The acid solutions were prepared at concentrations of 0, 18, 36, 72, 144, 288, and 576 mmol/L. The acid solutions were then added to the soil at a ratio of 1:10 for soil:acid solution by using 50 g of soil sample and 500 mL of acid solution. With the ratio used, the amounts of acid contacting the soil ranged from 0 to 600 cmol H^+ /kg-soil. The pH of the soil solution was measured after the soil suspension samples were shaken for 24 h in a mechanical shaker at 20 °C and allowed to stand for 6 h, and then resuspended by shaking for 2 min. This approach is similar to that applied by Luo et al. (2015). Titration curves of the soil suspension pH vs acid input in cmol H^+ /kg-soil were plotted and the buffer capacity can be deduced from the titration curve.

3.2.2.3 Determining relationship of pH and buffer capacity on arsenic attenuation

To study the relationship of pH and buffer capacity on As attenuation (Case 19-22), several solutions with a concentration in mg/L As of 0.1 and increasing concentration of acid from 0 to 7.2 cmol/L were prepared. The solutions were prepared by using As in the form of NaAsO₂ and the acid used was H₂SO₄. The solid materials were added to the solution in capped plastic bottles to achieve a ratio of 1:10 of solid:solution by using 50 g of soil samples and 500 mL of As solution. Each As solution used also meant increasing the amounts of acid input to the soil, from 0 to 72 cmol H⁺/kg-soil. The soil suspension samples were subjected to horizontal shaking at 150 rpm for 24 h at a room temperature of 20±0.5 °C, using a TAITEC TS-10 mechanical shaker. After the shaking step, the samples were allowed to stand for 10-15 min, and then centrifuged at 3,000 rpm for 10 min and filtered using a membrane filter with a particle size retention of 0.45 µm. Filtrate pH, EC, and Eh were measured. The amounts of As remaining in filtrate were analyzed using the atomic absorption spectrometer, while the amounts of other water-soluble metal ions (e.g. Ca²⁺, Mg²⁺, K⁺) were analyzed using the inductively coupled spectrophotometer. The amount of As retained in each soil at different concentrations of As-applied was then compared and related to the amount of acid input, and the filtrate pH values.

3.3 Results and discussions

3.3.1 Effect of different particle sizes of agent

Figure 3.5 shows a non-linear relation between S and C over the concentration range of C_0 from 0.1 to 10 mg/L, which was fitted by applying the empirical Freundlich isotherm equation (3.2) with a high correlation factor ($R^2 \geq 0.9$). This non-linear relationship implies that the solid materials have a finite capacity to attenuate contaminants (Devulpalli & Reddy, 1996). Also, notice that the soil has the capacity to naturally attenuate As (indicated by a red curve in Figure 3.5), due to the reactive surfaces of the soil solids (Minja and Ebina, 2002).

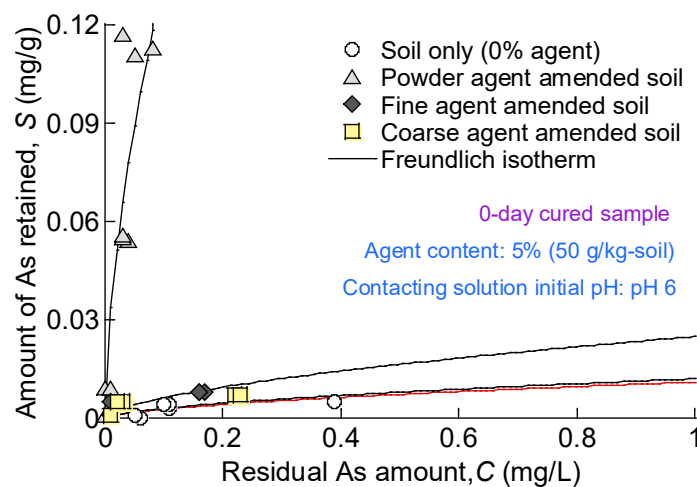


Figure 3.5: Freundlich isotherms for 0-day cured samples after contacting As solutions of pH 6 for 24 h.

This function of the natural soil plays an important role because the attenuation layer can be heterogeneous in attenuation performance and maybe cracked due to earthquakes and static deformation with time, during long-term services. Freundlich parameter, K – a good index for quantifying the contaminant attenuation property of a solid material – was estimated to be $11 \text{ cm}^3/\text{g}$.

$$S = KC^N \quad (3.2)$$

where, K (cm^3/g) which is a good index for quantifying the contaminant attenuation property of a solid material, and N which indicates the intensity of attenuation are Freundlich parameters.

By introducing the Ca-Mg composite into the soil matrix, the attenuation function of the natural soil became more effective, but in the order of decreasing particle size/ increasing surface area of this agent (i.e. coarse<fine<powder). Highest arsenic retention by the solid materials was noted in the soil-powder agent composite, where K reached $535 \text{ cm}^3/\text{g}$ which is about 50-times higher compared to that of the natural soil. Results are similar to findings by Mo et al. (2015), even though a different ratio of 1:20 of soil:solution was applied for that study. For a soil-fine agent composite, K was $25 \text{ cm}^3/\text{g}$ – nearly 1.5-times higher compared to that of the soil. For a soil-coarse agent composite, K was $12 \text{ cm}^3/\text{g}$ – almost 9% higher than that of soil.

According to Sharma and Reddy (2004), by assuming linear sorption onto the inorganic mineral (Ca-Mg composite) surfaces, a logarithmic relationship between K_d and SSA can be used to explain the increase in the amount of As-retained by the solid materials. The empirical linear isotherm equation (3.3) was applied to calculate the K_d value; it was derived from the initial slope of the Freundlich isotherm as shown in Figure 3.6. The K_d values obtained at the low concentrations are summarized in Table 3.4 and were compared and related to the SSA of the agent as shown in Figure 3.7. Powder agent has the highest SSA ($9.85 \text{ m}^2/\text{g}$) of the three agent types considered and therefore offers more surfaces for attenuation reactions.

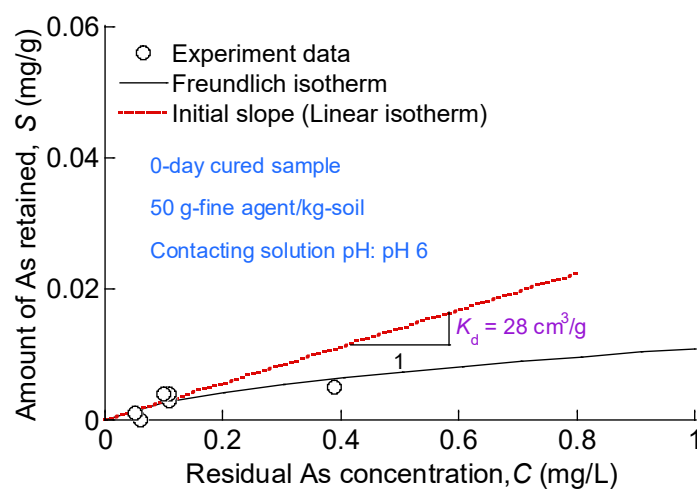


Figure 3.6: Representative linear isotherm to calculate the K_d values for 0-day cured samples at low concentration ranges under pH 6 conditions.

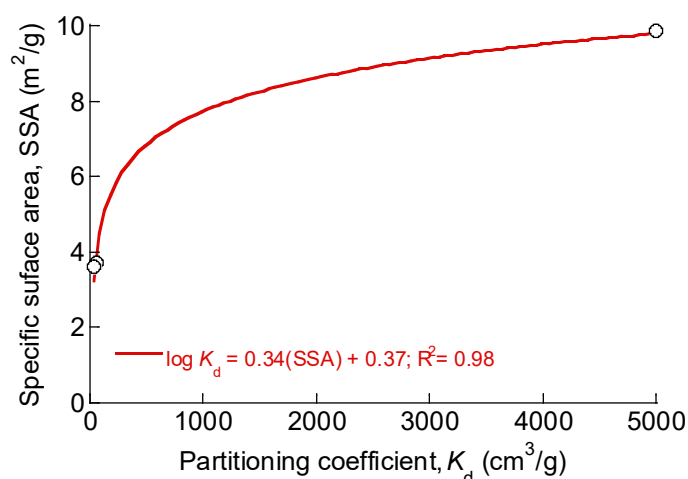


Figure 3.7: Relationship between K_d and SSA of agent.

However, reasons why the soil-fine agent composite shows better attenuation properties when compared to the soil-coarse agent composite, cannot be clearly explained from the differences in SSA value of the two agent types, determined as $3.6 \text{ m}^2/\text{g}$ for the coarse agent and $3.7 \text{ m}^2/\text{g}$ for the fine agent. The fact that the fine agent offers better performance than the coarse agent, indicates that the reactions involved are mainly controlled by the external surfaces of the agent.

$$S = K_d C \quad (3.3)$$

where K_d (cm^3/g) is the partitioning coefficient.

3.3.2 Effect of curing period

Precipitation on the surfaces of the agent is expected to be one of the main reactions involved in attenuation when the inorganic minerals (Ca-Mg composite) are introduced into the soil matrix, and will mainly include hydroxide precipitation (Blais et al., 2008) and carbonate precipitation (Salameh et al., 2015). In the hydroxide precipitation, the hydroxide sources including CaO, $\text{Ca}(\text{OH})_2$, $\text{Mg}(\text{OH})_2$ are involved in attenuating heavy metals from the leachate (Blais et al., 2008). Since such hydroxide sources can be produced from the hydration of this agent, the effect of curing time on the As attenuation by the soil-agent composites was investigated.

Figure 3.8 shows that the amounts of As retained by a soil-coarse agent composite was the same for all curing times considered ($K=12 \text{ cm}^3/\text{g}$ and $K_d=30 \text{ cm}^3/\text{g}$). According to Cao et al. (2019), the hydration process depends on the particle size, content, and crystal structure of a material. Generally, the finer the particles are, and/or the higher the content is, the more significant the acceleration effect of the hydration process will be. Results suggest that the hydration process of this coarse agent is either very slow, inherent from its particle size or does not occur.

However, as shown in Figure 3.9, the attenuation capacity of a soil-fine agent composite was improved by curing it for up to 7 days, after that the effect of curing time was not significant; For a 0-d

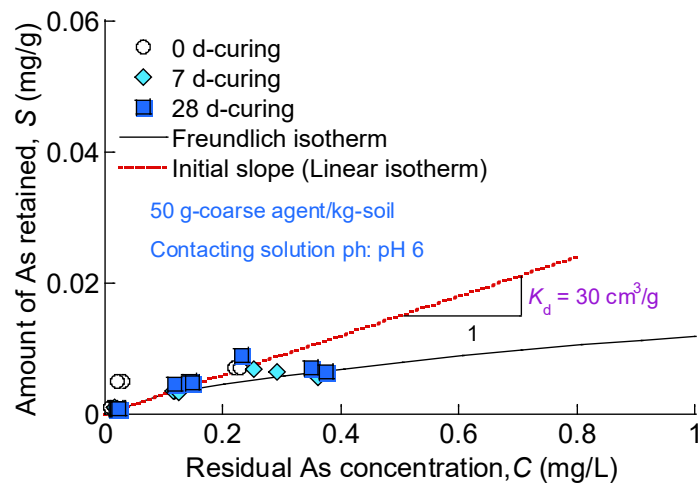


Figure 3.8: Representative linear isotherms for calculating the K_d values for the different composites.

cured composite, K_d was estimated to be $60 \text{ cm}^3/\text{g}$, but it increased by nearly 3-times when this composite was cured for 7 days, where it reached $180 \text{ cm}^3/\text{g}$. After 28-days of curing, K_d was $200 \text{ cm}^3/\text{g}$, which is about a 10 % increase. The results suggest that hydration of the fine agent had occurred at an early stage (within 7 days), and very minor hydrations occurred with prolonged curing time (after 7 days) which may have increased the availability of the hydroxide sources. There is possibility that conditions inherent in the testing method such as (1) crushing of the compacted sample to $<9 \text{ mm}$ particle sizes – before the shaking step batch tests – which might have destroyed the hydration products (CaO , $\text{Ca}(\text{OH})_2$, $\text{Mg}(\text{OH})_2$), and/or (2) soils are in suspension which limits any structural changes of the composite, might have affected the results. From Mo (2019) study using a 7-days and 28-days cured soil-powder agent composite, the column tests which unlike the batch test method did not disturb the soil-agent composite after compaction clarified that effect of curing after 7 days is not obvious.

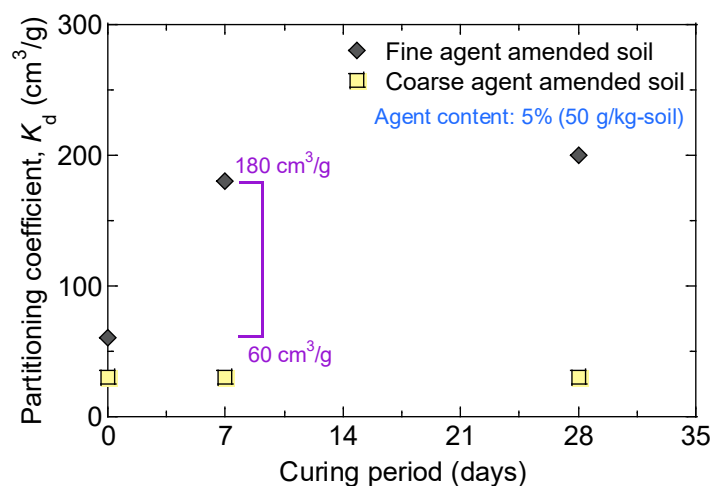


Figure 3.9: Relationship of K_d value and curing time when low concentration range is considered.

Table 3.4: Isotherm parameters for different composites cured for 0, 7, and 28 days.

Agent type	Initial pH	Linear isotherm ($S=K_dC$)	Freundlich isotherm ($S=KC^N$)		Final pH
		K_d (cm ³ /g)	K (cm ³ /g)	N	
No agent	0	28	11	0.6	8.0-8.5
Powder	0	5000	520	0.6	9.0-10.5
	7 ^a	2130	520	0.6	9.5-10.5
	28 ^a	1820	450	0.6	9.5-10.5
Fine	0	60	24	0.6	9.0-10.0
	7	180	35	0.6	10.0-10.5
	28	200	38	0.6	-
Coarse	0	30	12	0.6	9.5-10.0
	7	30	12	0.6	9.5-10.0
	28	30	12	0.6	-

^a Source: Mo (2019)

3.3.3 Effect of solution pH

Amount of As retained by the composites under pH of 2 to 6 was investigated at pH conditions of 2, 4, and 6, and the K and K_d values obtained are summarized in Table 3.5. To have a better understanding of the effect of low pH on As attenuation, the obtained K_d values were compared and related to the corresponding initial solution pH of As-applied.

Figure 3.10 shows that the attenuation capacity of soil did not change when brought into contact with solutions of pH 4 and pH 6, and K_d was estimated to be 28 cm³/g. However, solutions with low pH of 2 were found to negatively influence the amount of As-retained by the soil, where K_d dropped to 20 cm³/g. Similar results were found by Minja and Ebina (2002). The ability of this soil to attenuate As at low pH is speculated to be due to the oxidation of As(III) to As(V) by Ca²⁺; this As species has been found to be effectively attenuated under low pH (Soner Altundoğan et al., 2000; Minja and Ebina, 2002). Another possible explanation is related to the surface charge of the soil which can be involved in the retention and movement of cations and anions, and flocculation and dispersion in soils (Bolan et al., 1999). According to Bolan et al. (1999), an increase in the negative-surface charge can increase the retention of heavy metals by soil. In this study, it was observed that when the soils contacted solutions of pH 6 and 4, the final solution pH was above pH 7 (as indicated in Table 3.5). The presence of OH⁻ might have increased the negative-surface charge. However, after contacting solutions of pH 2, the final pH was below pH 3.5 (presence of more H⁺). And since this soil contains Fe, Al, and Mn oxides it is expected to carry mostly variable charge (Bolan et al., 1999), therefore more positive-surface charge is expected which reduces the amount of As-retained.

By introducing agent into the soil matrix, the high carbonate content of the material gave the soil a higher capability to increase pH to strongly alkaline conditions and retain more As either due to more negative-surface charge and/or precipitation reactions. As shown in Figure 3.11, for soil-powder agent composite, a K_d value of 5000 cm³/g could be maintained for each pH condition. For soil-fine agent composite, K_d value was found to slightly decrease in low pH, and at pH 2, K_d value for this composite was 38 cm³/g. Soil-coarse agent composite showed a slight improvement in As attenuation, and at low pH of 2, the amount of As-retained was similar to that of soil-fine agent composite ($K_d=38$ cm³/g).

Table 3.5: Isotherm parameters for different composites contacting solutions of pH of 2, 4, and 6.

Agent type	Initial pH	Linear isotherm ($S=K_dC$)	Freundlich isotherm ($S=KC^N$)		Final pH
		K_d (cm^3/g)	K (cm^3/g)	N	
No agent	2	20	12	0.6	2.5-3.5
	4	28	15	0.6	7.0-8.0
	6	28	11	0.6	7.5-8.5
Powder	2	5000	383	0.6	9.0-10.0
	4	5000	491	0.6	10.0-11.0
	6	5000	535	0.6	10.0-11.0
Fine	2	38	17	0.6	7.0-8.0
	4	58	23	0.6	9.0-10.0
	6	60	25	0.6	9.0-10.0
Coarse	2	38	17	0.6	5.0-6.5
	4	38	16	0.6	9.0-10.0
	6	30	11	0.6	9.0-10.0

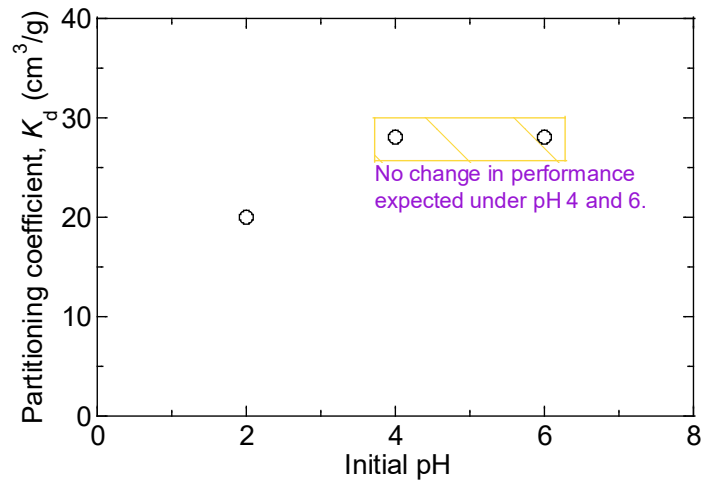


Figure 3.10: Changes in K_d of natural soil under different pH conditions.

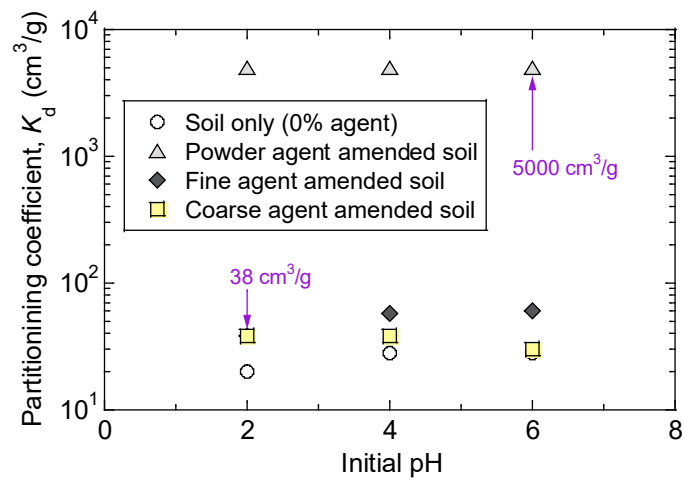


Figure 3.11: Changes in K_d of soil-agent composites under different pH conditions.

3.3.4 pH changes

Figure 3.12 shows the changes in solution pH after the composites interacted with solutions of different pH for 24 h. As shown in the figure, the base material was capable of increasing the pH of 6 and/or low pH of 4 to circumneutral conditions, which was defined by Nordstrom (2011) as a pH of 6 to 8. However, for a very low pH of 2, its ability to increase pH was very limited, and the material could only raise this pH to around pH 2.5 to 3.5.

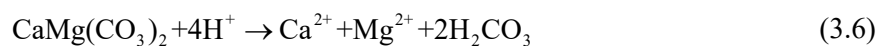
By introducing agent into the soil matrix, the ability of the natural soil to buffer pH was improved. For soil-powder agent composites, the pH was increased to strongly alkaline conditions of above pH 9, for all pH conditions considered. For soil-fine agent composite, it could raise the pH of 6 and/or low pH of 4 to strongly alkaline conditions of above pH 9. But solution with a low pH of 2 was found to reduce the pH buffering property of this composite, and it could only raise the pH to circumneutral conditions. Similar observations were found when using the soil-coarse agent composite. Results indicate that the pH buffering capacity of soil-agent composite depends on the particle size of the agent used.

Carbonate mineral buffering and/or exchangeable base cations buffering are considered to be the governing mechanisms for pH buffering. For base material, its ability to buffer pH was associated with the presence of exchangeable base cations. According to McBride (1994), base cations (e.g. Ca^{2+} , Mg^{2+} , K^+) can be exchanged for H^+ as in the following example (3.4):



where, CaX_2 represents Ca^{2+} on soil exchange sites.

On the other hand, carbonate mineral buffering is expected to be the main mechanism for the soil-agent composite due to the dissolution/precipitation of carbonate minerals (Stumm and Morgan, 2012). According to Stumm and Morgan (2012), in the presence of sufficient calcite (CaCO_3) and dolomite components ($\text{CaMg}(\text{CO}_3)_2$), the acid drainage can be neutralised as described by reactions in equation (3.5) and (3.6) respectively. The chemical reaction (3.5) shows that 2 moles of calcite are required to neutralise 4 moles of acid (H^+). The dolomite-acid buffering reaction (3.6) shows that 1 mole of dolomite is required to neutralise 4 moles of acid (H^+). Which is one of the reasons why more Ca^{2+} were leached as compared to Mg^{2+} for each pH condition, and, also, under a very low pH of 2 to 4 both their leaching values were very high compared to under pH of 6, as shown in Figure 3.12. Also, since the main chemical constituent of this Ca-Mg composite is CaCO_3 and MgCO_3 (refer to section 3.2.1), it is expected that the material will dissolve rapidly when continuously exposed to very acidic drainage over a long period, and can severely affect the structural integrity of the attenuation layer.



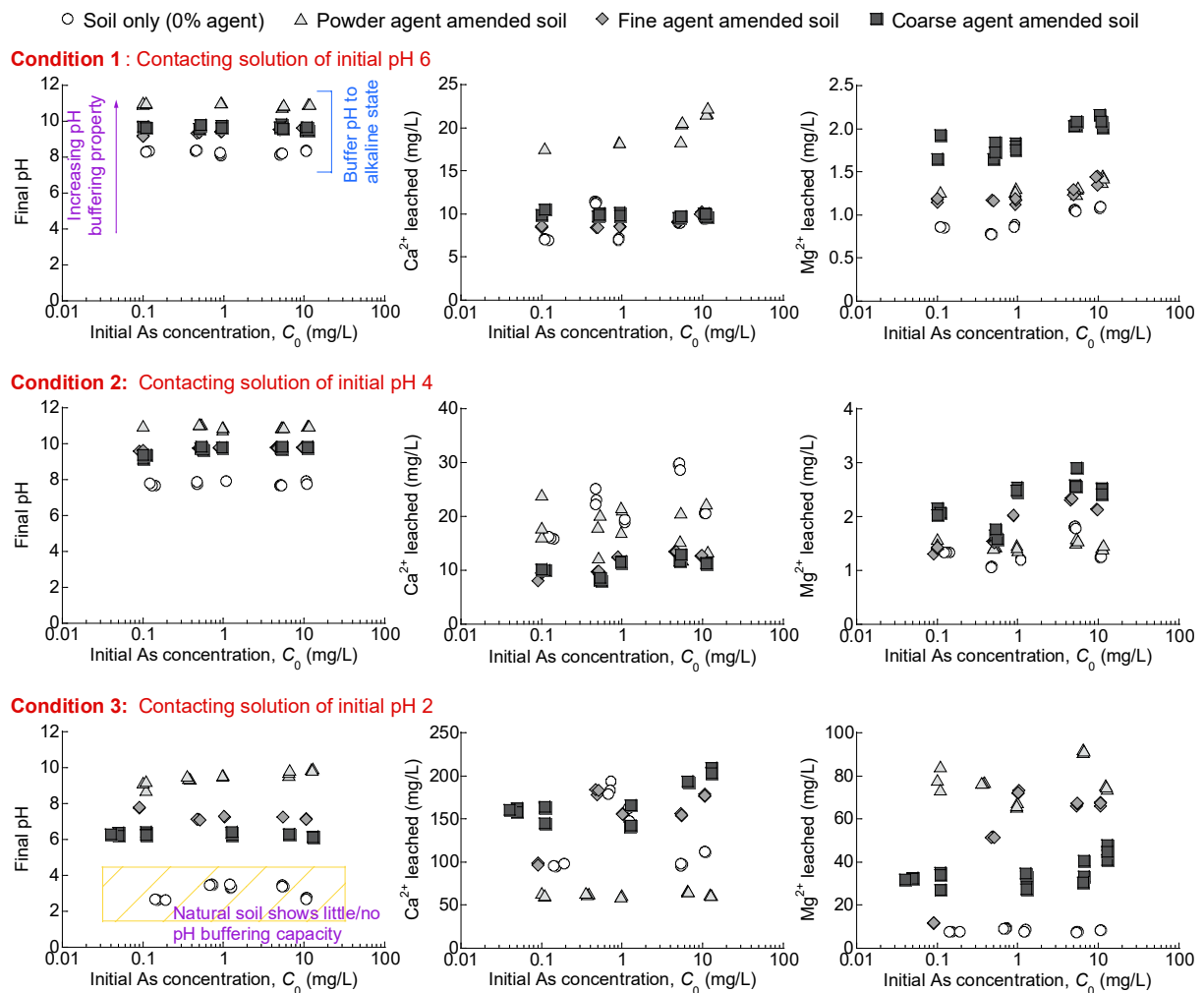


Figure 3.12: pH changes and the leaching profiles of water-soluble metal ions for four composites of sandy soil and different agent sizes.

3.3.5 Relation of pH and buffer capacity on arsenic attenuation

Titration curves of the soil suspension pH vs acid input in $\text{cmol H}^+/\text{kg-soil}$ were plotted as shown in Figure 3.13. As shown in this figure, the initial pH of the soil is about 8.5, but decreases rapidly with increase in the concentration of acid (H_2SO_4), which confirms the low buffering capacity of the natural soil. However, mixing the soil with this 5% agent, improved its buffering capabilities significantly. Very small differences were noted between soil-fine agent composite and soil-coarse agent composite.

As shown in Figure 3.14, when the pH of the soil suspension decreases below the precipitation pH (about $\text{pH}=5$), reduction in the amounts of As retained by the soil-agent composite was noted with increasing amounts of acid input. This implies that the dominant retention mechanism had changed from precipitation to other kinds of retention mechanisms – e.g. cation exchange.

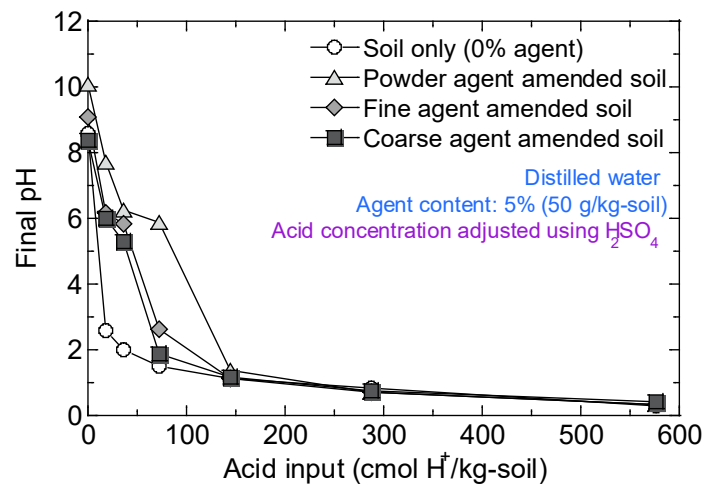


Figure 3.13: pH buffering curves of composites of soil and different agent sizes.

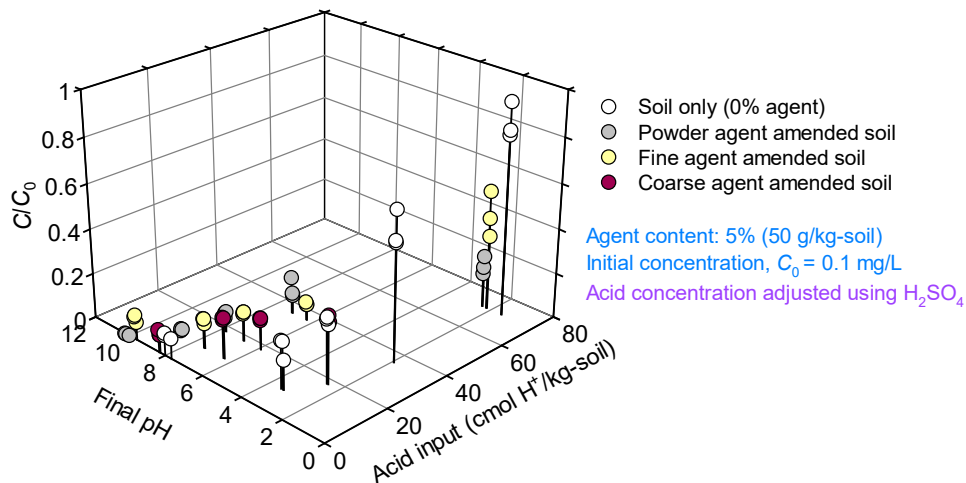


Figure 3.14: Relation of pH and buffer capacity on arsenic attenuation by composites.

3.4 Conclusions for Chapter 3

In this chapter, batch-type tests were carried out to obtain basic information regarding the performance of a natural soil amended with different particle sizes of this Ca-Mg agent from the viewpoints of As attenuation, and the relationship of pH and buffer capacity on As attenuation. It was found out that:

This natural soil has a capacity to reduce metal concentrations from solution. This function plays an important role because the attenuation layer can be heterogeneous in attenuation performance and maybe cracked due to earthquakes and static deformation with time, during long-term services. Freundlich parameter, K – a good index for quantifying the contaminant attenuation property of a solid material – was estimated to be $11 \text{ cm}^3/\text{g}$.

By introducing the Ca-Mg composite into the soil matrix, the attenuation function of the natural soil became more effective, but in the order of decreasing particle size/ increasing surface area of this agent (i.e. coarse<fine<powder). Highest arsenic retention by the solid materials was noted in the soil-powder agent composite, where K reached $535 \text{ cm}^3/\text{g}$ which is about 50-times higher compared to that of the natural soil.

Although soil-coarse agent composite had no obvious changes due to curing, the attenuation function of a soil-fine agent composite was improved by curing it for up to 7 days, after that, the effect of curing time was not significant; for a 0-day cured composite, K_d was estimated to be $60 \text{ cm}^3/\text{g}$, but it increased by nearly 3-times when this composite was cured for 7 days it, where it reached $180 \text{ cm}^3/\text{g}$, and after that very small changes were observed. This suggests that hydration of the fine agent had occurred at an early stage (within 7 days), and very minor hydration occurred with prolonged curing time, which may have increased the availability of the hydroxide sources.

By introducing agent into the soil matrix, the capabilities of the natural soil to buffer pH was also improved. Also, it was noted that the pH buffering capacity of the soil-agent composite depends on the particle size of the agent. For soil-powder agent composites, the pH was increased to strongly alkaline conditions of above pH 9, for all pH conditions considered. For soil-fine agent composite, it could raise the pH of 6 and/or low pH of 4 to strongly alkaline conditions of above pH 9. But solutions of low pH of 2 were found to reduce this property of the composite, and it could only raise the pH to circumneutral range. Similar observations were found when using soil-coarse agent composite.

By introducing agent into the soil matrix, the high carbonate content gave the soil a higher capability to increase pH to strongly alkaline conditions and retain more As with more acid input and is expected to be due to more negative-surface charge and/or precipitation reactions. However, when the pH of the soil-agent composite suspension decreases below the precipitation pH (about pH=5), reduction in the amounts of As retained by the soil-agent composite is expected with more of acid input.

References for Chapter 3

- Blais, J.-F., Djedidi, Z., Cheikh, R., Tyagi, R., and Mercier, G. 2008. Metals precipitation from effluents: Review. *Practice Periodical of Hazardous, Toxic, and Radioactive Waste Management*, 12.
- Bolan, N. S., Naidu, R., Syers, J. K., and Tillman, R. W. 1999. Surface charge and solute interactions in soils. In Sparks (Ed.), *Advances in Agronomy* 67, 87-140: Academic Press.
- Boucif, F., Marouf-Khelifa, K., Batonneau-Gener, I., Schott, J., and Khelifa, A. 2010. Preparation, characterisation of thermally treated Algerian dolomite powders and application to azo-dye adsorption. *Powder Technology*, 201(3): 277-282.
- Cao, M., Ming, X., He, K., Li, L., and Shen, S. 2019. Effect of macro-, micro- and nano-calcium carbonate on properties of cementitious composites—a review. *Materials*, 12(5): 781.
- Inui, T., Katsumi, T., Takai, A., and Kamon, M. 2013. Factors affecting heavy metal leaching in excavated rocks with natural contamination. In Manassero et al. (Eds.), *Coupled Phenomena in Environmental Geotechnics*, 587-592: CRC Press.

- Itaya, Y., Kikuchi, S., Yoshimatsu, T., and Kuninishi, K. 2013. Clarification of insolubilization mechanism of heavy metals using magnesium/calcium composite material. *Proceedings of the 19th Conference on Groundwater and Soil Contamination and its Countermeasures*, Japan. (In Japanese).
- Kikuchi, S., Kuninishi, K., and Itaya, Y. 2012. Basic discussion on the applicability of Ca/Mg composite material in sorption layer method. *67th Annual Conference of the Japan Society of Civil Engineers*, Japan. (In Japanese).
- Luo, W. T., Nelson, P. N., Li, M. H., Cai, J. P., Zhang, Y. Y., Zhang, Y. G., Yang, S., Wang, R. Z., Wang, Z. W., Wu, Y. N., Han, X. G., and Jiang, Y. 2015. Contrasting pH buffering patterns in neutral-alkaline soils along a 3600 km transect in northern China. *Biogeosciences*, 12(23): 7047-7056.
- McBride, M. B. 1994. *Environmental Chemistry of Soils*: Oxford University Press.
- Minja, R. J. A. and Ebina, T. 2002. Arsenic adsorption capabilities of soil-bentonite mixtures as buffer materials for landfill. *Clay Science*, 12(1): 41-47.
- Mo, J. (2019). *Soil amended with calcium-magnesium immobilizing agent against natural arsenic contamination*. Doctoral Thesis. Kyoto University, Retrieved from <https://dx.doi.org/10.14989/doctor.k21936>
- Mo, J., Inui, T., Katsumi, T., Takai, A., Kuninishi, K., and Hayashi, S. 2015. Performance of sorption layer using Ca/Mg immobilizing agent against natural contamination. *10th Asian Regional Conference of IAEG*, Kyoto, Japan.
- Nordstrom, D. K. 2011. Mine waters: Acidic to circumneutral. *Elements*, 7(6): 393-398.
- Paikaray, S. 2015. Arsenic geochemistry of acid mine drainage. *Mine Water and the Environment*, 34(2): 181-196.
- Salameh, Y., Albadarin, A. B., Allen, S., Walker, G., and Ahmad, M. N. M. 2015. Arsenic(III,V) adsorption onto charred dolomite: Charring optimization and batch studies. *Chemical Engineering Journal*, 259: 663-671.
- Sharma, H. D. and Reddy, K. R. 2004. *Geoenvironmental Engineering: Site Remediation, Waste Containment, and Emerging Waste Management Technologies*: Wiley.
- Soner Altundoğan, H., Altundoğan, S., Tümen, F., and Bildik, M. 2000. Arsenic removal from aqueous solutions by adsorption on red mud. *Waste Management*, 20(8): 761-767.
- Stumm, W. and Morgan, J. J. 2012. *Aquatic Chemistry: Chemical Equilibria and Rates in Natural Waters*: Wiley.
- The Society of Materials Science, J. 2014. Heavy metal insolubilization agent material 'Magic Fix'. (No.1015). *Report on Ground Improvement Technology Review and Certification*. (In Japanese).

Chapter 4 Attenuation performance with time

4.1 General remarks

It is necessary to establish the endurance of the composite of natural soil (sandy soil) and Ca-Mg composite as the attenuation layer, to gain acceptance from the public and stakeholders. Although the batch-type tests as the one carried out in Chapter 3 is a cheap, simple, and quick way to determine the attenuation capacity of solid materials, the extension of this results to practical applications can be questionable (Grathwohl and Susset, 2009), which is in part due to the conditions inherent in the testing method, such as no considerations to flow conditions (Shackelford, 1994). In this chapter, the attenuation performance with time of this composite was studied by using column tests under saturated conditions, which can more closely simulate the in-situ water in contact with the solid materials and also allow for the measurement of the time-lapse release of contaminants. Also, an analytical 1-D advection-dispersion model was applied using transport parameters obtained from the column experiments. Two key issues addressed were (1) how rapidly and for how long will this composite continue to attenuate As to acceptable levels, and (2) for how long will this composite have the capabilities to increase pH, which is important since the stability of the immobilized compounds often are pH-dependent.

4.2 Materials and methods

4.2.1 Materials

Base material of decomposed granite soil of under 2-mm and stabilizing agent of Ca-Mg composite of fine type of under 2 mm and coarse type of 2-9.5 mm were used. Properties of the materials were discussed in the previous section 3.2.1. Several composites of the natural soil and different agent sizes were prepared by adding the agent to the dry soil at either 0 or 5% (50 g/kg-soil) by dry weight of the mixture and the required amount of distilled water added to achieve the optimum water content ($w_{opt}=10-11\%$). Mixing was done using a mechanical mixer, and proper care was taken to prepare homogeneous composites. After that, each composite was compacted (w_{opt} , Dc 95%) in three equal layers (≈ 2.3 cm-thick layer) in a 6 cm-inner diameter and 7 cm-high steel mold. Properties of the composites are summarized in Table 4.1.

4.2.2 Column test under saturated flow conditions

Column tests were carried out following the ASTM D 5084 “Standard Test Methods for Measurement of Hydraulic Conductivity of Saturated Porous Materials Using a Flexible Wall Permeameter” as shown in Figure 4.1. Samples were saturated beforehand for at least 48 h in a vacuum deaerator. The upper and lower surfaces of the sample were confined with an acrylic pedestal of 6-cm diameter. A sheet of filter paper and geotextile separated the surface of the sample from the acrylic pedestals to prevent clogging of the channels by fine soil particles. To prevent air from intruding into the samples during the test, filter papers and geotextiles were deaerated in a container filled with distilled water beforehand. A

latex membrane smeared with silicone grease on the lateral face was used to confine the sides of the sample along with the top and base pedestal, to prevent side-wall leakage. Two O-rings were employed at the top and bottom pedestal to seal the sample. After assembling the apparatus and saturating all channels with distilled water, a confining pressure of 50 kPa was applied during permeation.

Solutions of 0.1 mg/L As and different pH conditions of 2 to 6, were prepared and used as permeant after deaerating them for 24 h. The solutions were prepared using As in the form of NaAsO_2 and the acid used (for adjusting pH) was H_2SO_4 . The concentration of As applied in this test is taken as an extreme case of leaching; since in many cases, geogenic contaminated soils exhibit As leaching amounts of 0.02 to 0.03 mg/L (Katsumi et al., 2019). As indicated in Table 4.1, solutions were continuously permeated through the saturated soil columns at an average flow rate (Q) of $4.5 \text{ cm}^3/\text{h}$ using a peristaltic pump. This applied flow rate (assuming steady-state flow) is equivalent to the Darcian velocity ($q=Q/A$, where A is the cross-sectional area of the sample) of $4.42 \times 10^{-5} \text{ cm/s}$. Under this flow conditions, the water residence time ($t_c=V_v/Q$, where V_v is the volume of voids in the sandy soil porous media) which refers to the duration the water is in contact with the solid materials, was estimated to be about $12 \pm 1 \text{ h}$. According to Mo et al. (2018), a high attenuation performance is expected for $t_c > 12 \text{ h}$, and therefore it was assumed that the applied flow rate will provide a better assessment regarding the attenuation performance of the composites with time. Effluents were collected at regular time intervals and filtered using a membrane with a particle size retention of $0.45 \mu\text{m}$. After that, the pH, EC, Eh, and amounts of As and other water-soluble elements in the filtrate were analysed in a similar way to the batch-type test.

Table 4.1: Experimental conditions of the column test.

Case	1	2	3	4	5	6	7
Agent type	None	None	None	Fine	Fine	Coarse	Coarse
Dry density, ρ_d (g/cm^3)	1.92	1.91	1.91	1.88	1.89	1.92	1.91
Porosity, ϕ (%)	28.5	29	27.5	29.5	29	28.1	28.1
Volume of voids, V_v (cm^3)	56.6	56.8	54.4	58.5	57.6	55.8	56
Influent pH	2	4	6	2	6	2	6
Flow condition	Saturated state						
Flow rate, Q (cm^3/h)	4.5						
Seepage velocity, v_s (cm/s)	1.55×10^{-4}	1.52×10^{-4}	1.61×10^{-4}	1.49×10^{-4}	1.52×10^{-4}	1.57×10^{-4}	1.57×10^{-4}
Residence time, t_c (h)	12.6	12.6	12.1	13	12.8	12.4	12.4

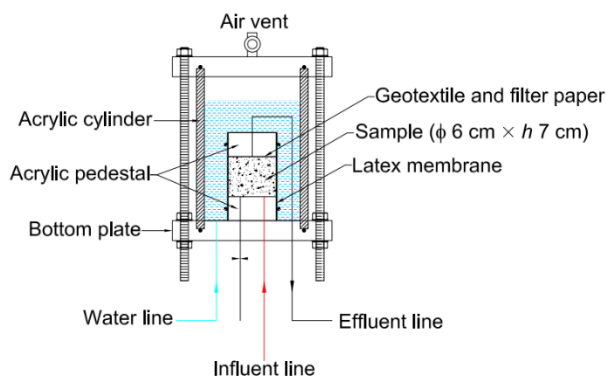


Figure 4.1: Column test in a) schematic details of the flexible wall permeameter and b) appearance of the test setup.

4.2.3 Analytical solution for a one-dimensional contaminant transport

In saturated soils, there is both diffusive flow which occurs in the micropores and advective flow which typically occurs in the macropores (Yong and Mulligan, 2003). For high-permeable soils like sands, advection will dominate over the diffusive flow, and the contaminants will be transported by the water flowing in response to the hydraulic gradient (i).

Assuming seepage is steady-state and linear sorption the governing differential equation for 1-D contaminant transport in a homogeneous soil porous media can be given by the equation (4.1). Considering the initial and the boundary conditions in equation (4.2) an analytical solution 1-D advection-dispersion equation (ADE) that accounts for sorption given by equation (4.3) is derived (Ogata and Banks, 1961).

$$R \frac{\partial C}{\partial t} = D \frac{\partial^2 C}{\partial x^2} - v_s \frac{\partial C}{\partial x} \quad (4.1)$$

$$\left. \begin{array}{l} C(x, 0) = 0 \quad x \geq 0 \quad \text{Initial conditons} \\ C(0, t) = C_0 \quad t \geq 0 \\ \frac{\partial C(\infty, t)}{\partial x} = 0 \quad t \geq 0 \end{array} \right\} \text{Boundary conditons} \quad (4.2)$$

$$C(x = L, t) = \frac{C_0}{2} \left[\operatorname{erfc} \left(\frac{Rx - v_s t}{2\sqrt{RDt}} \right) + \exp \left(\frac{v_s x}{D} \right) \operatorname{erfc} \left(\frac{Rx + v_s t}{2\sqrt{RDt}} \right) \right] \quad (4.3)$$

where, t is time, v_s is the seepage velocity (cm/s), $R = (1 + \rho_d K_d / \phi)$ is the retardation factor and is a measure of the attenuation capacity for a given soil for a given chemical species (Shackelford, 1994), and D (cm²/s) is the dispersion coefficient, which typically is a combined effect of both the longitudinal dispersivity, α_L (cm) which is roughly approximated to be $0.1L$, where L is the transport distance (Gelhar et al., 1992) and the molecular diffusion coefficient, D_m (cm²/s) which for As is estimated to be 0.727×10^{-5} cm²/s (Tanaka et al., 2013), i.e. $D = v_s \alpha_L + D_m$.

According to van Genuchten and Parker (1984), equation (4.3) can be non-dimensionalized as shown in the equation (4.4), by substituting the column Peclet number (Pe) corresponding to equation (4.5), and the effective pore volumes of flow (T) corresponding to equation (4.6).

$$C(T) = \frac{C_0}{2} \left[\operatorname{erfc} \left(\frac{R - T}{2\sqrt{\frac{RT}{Pe}}} \right) + \exp(Pe) \operatorname{erfc} \left(\frac{R + T}{2\sqrt{\frac{RT}{Pe}}} \right) \right] \quad (4.4)$$

$$Pe = \frac{v_s L}{D} \quad (4.5)$$

$$T = \frac{v_s t}{L} \quad (4.6)$$

4.3 Results and discussions

4.3.1 Attenuation performance with time based on column test

Figure 4.2 shows the concentration profiles of As in effluent with cumulative flow volumes of As solutions of different pH condition, for the natural soil. As shown in the figure, the natural soil has a certain level of attenuate performance and can reduce metal concentrations. This function of the natural soil plays an important role because the attenuation layer can be heterogeneous in attenuation performance and maybe cracked due to earthquakes and static deformation with time, during the long-term services. Similar to findings from batch-test (refer to section 3.3.3), the As-retention behaviour of soil was the same when permeated with solutions of pH 4 and pH 6. Under these conditions, the amounts of As in effluent exceeded the allowable limits after about $T > 145$.

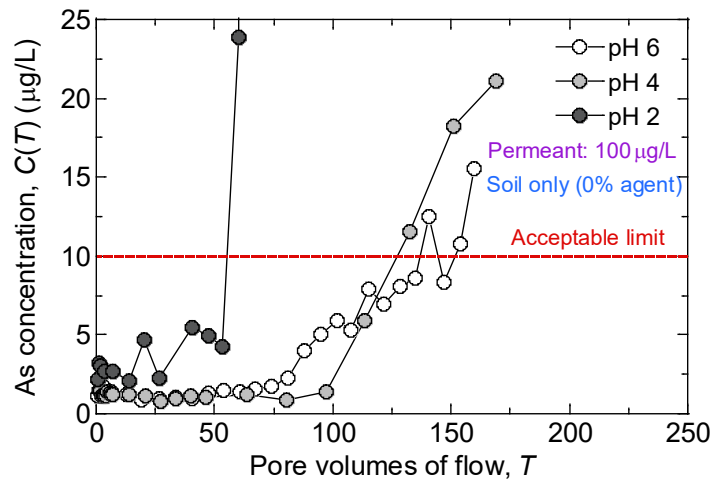


Figure 4.2: Breakthrough curves of natural soil when permeated with arsenic solutions of different pH.

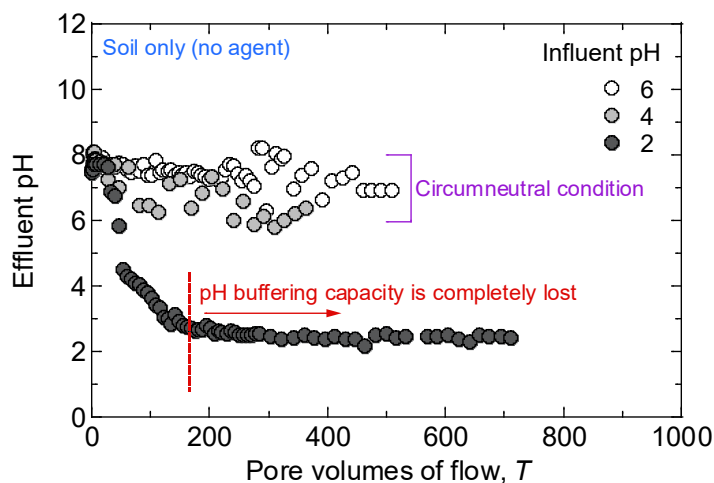


Figure 4.3: pH changes with flow volumes of solution of different pH in natural soil.

Also, similar to findings from the batch test, natural attenuation of soil was significantly affected by a solution of low pH of 2, and breakthrough occurred at a much shorter period ($T > 60$). According to Bolan et al. (1999), an increase in negative-surface charge can increase the retention of heavy metals by soil. In this study, it was noted that when the soils are permeated with solutions of pH 6 and 4, the final pH of the solution was generally maintained at above pH 6, as shown in Figure 4.3, which promotes the increase in the negative-surface charge. However, when permeated with solutions of pH 2, the final pH drastically dropped with more flow volumes. As the pH became more acidic, more positive-surface charge of soil solids occurs and reduces the amount of As-retained by the solid materials.

As was explained in section 3.3.4, cation exchange is expected to be one of the main buffering mechanisms by the natural soil, therefore lower amounts of Ca^{2+} leached caused a decrease in pH, as shown in Figure 4.4. Also, as shown in Figure 4.5, some relation was observed between the amounts of Ca^{2+} leached and As-retained. Generally, as the amounts of the base cation decreased, the lower the amount of As was retained. However, effect of Mg^{2+} leached on pH and/or As-retained was not obvious.

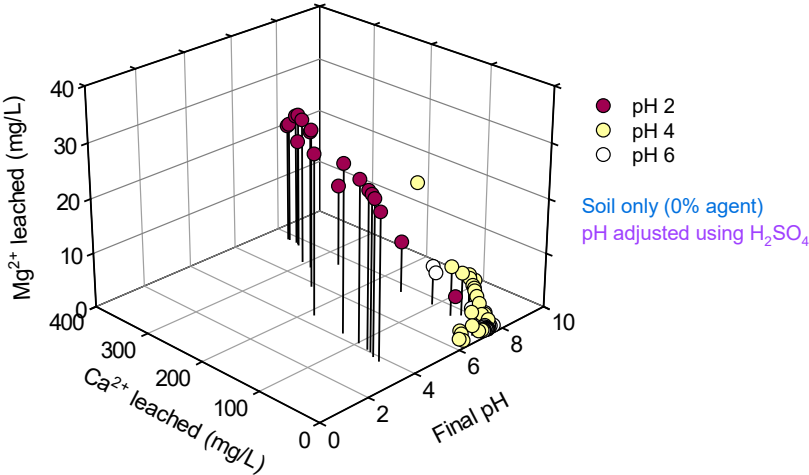


Figure 4.4: Relationship between Ca^{2+} , Mg^{2+} and pH changes by natural soil.

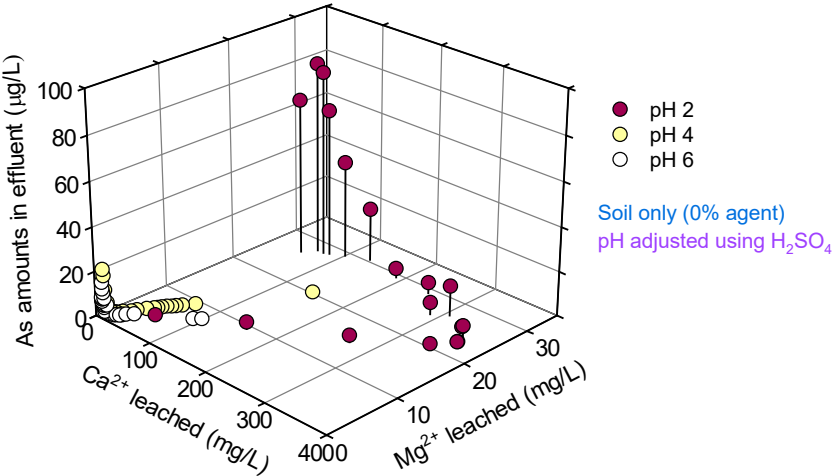


Figure 4.5: Relationship between Ca^{2+} , Mg^{2+} and arsenic attenuated by natural soil.

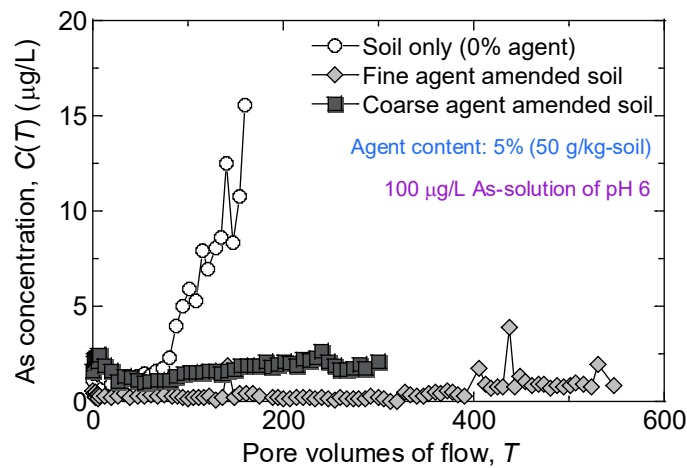


Figure 4.6: Arsenic breakthrough curves for composites permeated with arsenic solutions of pH 6.

Figure 4.6 shows the concentration profiles of As in the effluent with flow volumes for soil-agent composites when permeated with solutions of pH 2. As shown in the figure, the amount of As-retained by the solid materials was similar in the short-term of $0 < T < 100$, during which the removal efficiency ($Rr = (C - C_0) / C_0$) $> 95\%$. However, notice that after this point ($T > 100$), although Rr of natural soil decreased with more flow volumes, the soil-agent composites were still able to effectively remove $> 95\%$ of As-applied, and their concentrations were under the allowable limit of 0.01 mg/L . Also, although batch test showed that the coarse agent offers very little improvement to the attenuation property of natural soil, through the column test, it was made clear that the coarse agent will enhance this property.

Figure 4.7 shows that even when the soil-agent composites were permeated with acidic solutions, Rr was generally $> 95\%$, and their concentrations were under the allowable limit. However, some fluctuations in As concentrations were noticed in the beginning stages of permeation of a soil-coarse agent composite, which might be due to preferential flow. This suggests that by lining possible acid-generating materials on top of the attenuation layer constructed using sandy soil mixed with this agent, we still can expect a competent attenuation function for a long period.

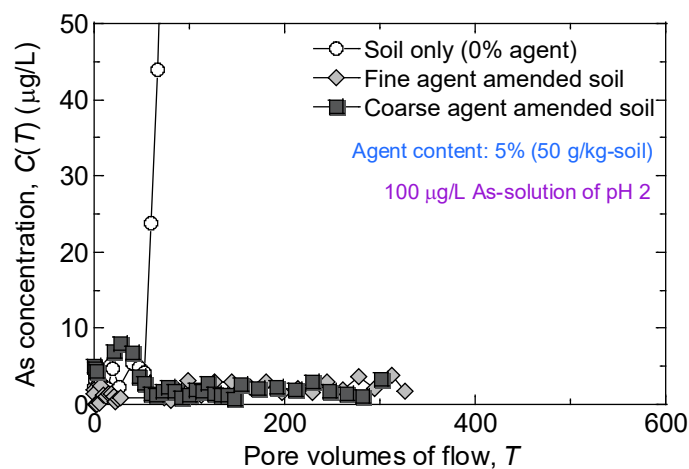


Figure 4.7: Arsenic breakthrough curves for composites permeated with arsenic solutions of low pH of 2.

Figure 4.8 shows that the capacity of the soil to buffer pH became more effective due to the adding of agents in the soil matrix. The pH of effluent was found to be alkaline conditions when the composite was permeated with solutions of pH 6 or low pH of 2. Under permeation with solutions of pH 6 conditions, fine agent offered very high capabilities to increase pH; in the initial stages, pH was raised from the pH-applied of 6 to strongly alkaline conditions of pH 10, but with more volumes of flow this property decreased. Under similar conditions, soil-coarse agent in the initial stages could increase pH to about pH 8 to 9. Under permeation with solutions of pH 2, the fine agent offered slightly better improvement, but the differences of the agents were considered not significant. Although the agents offered a higher pH buffering property, this feature decreased over time with continuous permeation, as indicated by the gradual drop in the outflow water pH value with cumulative volumes of flow. Leaching of carbonates from the agent will slowly deplete the carbonate buffer capacity, and ultimately the soil pH is lowered. It is expected that as the pH becomes lower than the precipitation pH (about pH=5), the amount of As-retained will reduce with more volumes of flow of pH 2 solution.

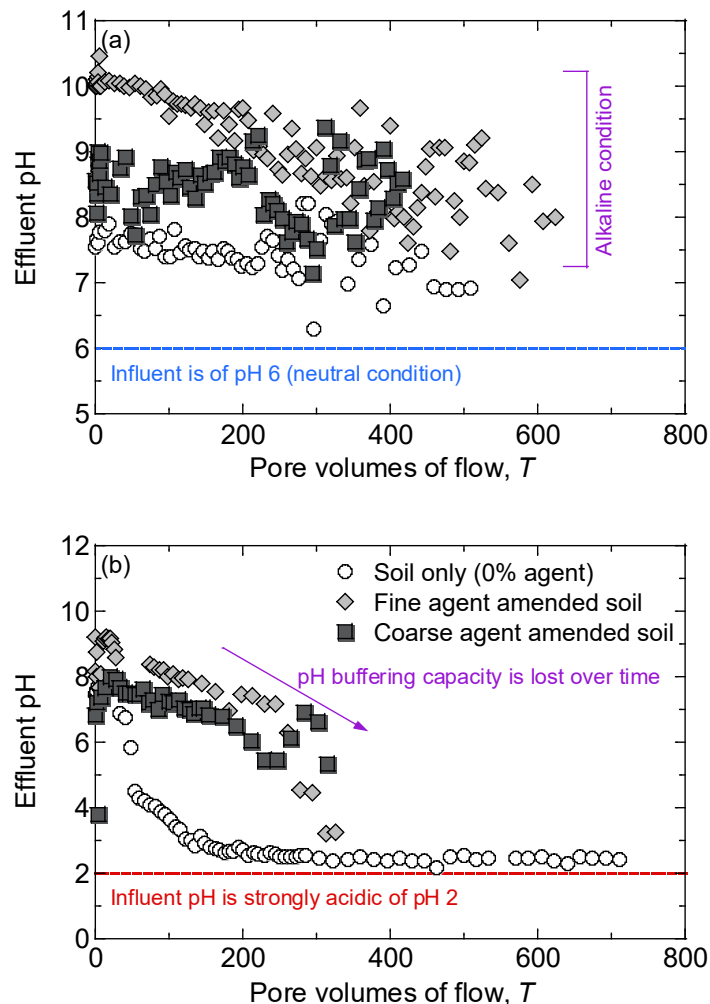


Figure 4.8: pH changes with flow volumes of contaminated solution of (a) pH 6 and (b) low pH of 2 in columns of different composites.

Figure 4.9 shows that the materials, under permeation with solutions of pH 6, released similar amounts of Ca^{2+} but showed distinctive differences in pH, which is due to the differences in pH buffering mechanisms between the soil (cation exchange) and soil-agent composite (dissolution/precipitation of carbonate minerals from agent), and differences in particle sizes in the case of comparing soil-agent composites.

Figure 4.10 shows that as the amounts of Ca^{2+} decreased the amounts of As retained also decreased for the natural soil. Below concentration of 10 mg/L Ca^{2+} , the amount of As-retained in solution decreased with more volumes of flow. This confirms that this base cation has an important role to play in As retention through either (1) oxidizing As(III) to As(V) and/or directly involved in heavy metal retention.

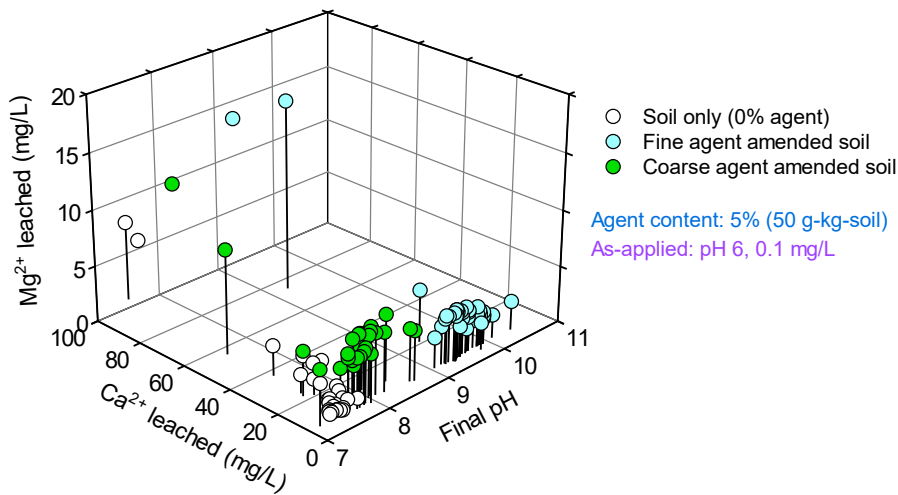


Figure 4.9: Relationship between Ca^{2+} , Mg^{2+} and pH changes for composites permeated with solutions of pH 6.

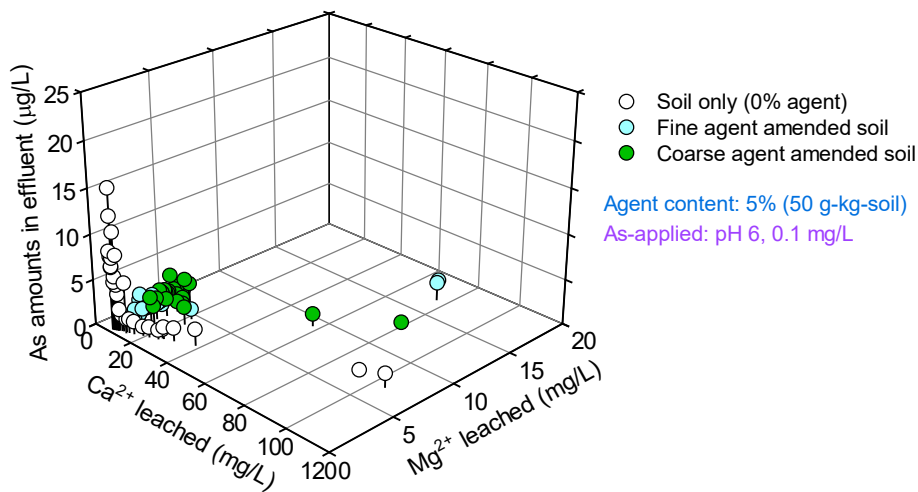


Figure 4.10: Relationship between Ca^{2+} , Mg^{2+} and As attenuated by composites permeated with solutions of pH 6.

4.3.2 Analytical solution for arsenic transport in the soil columns

Concentration profiles of As measured during the column tests were used to estimate the retardation factor (R) of the three composites of sandy soil and different agent sizes permeated with pH 6 solutions of 0.1 mg/L As. Considering steady-state flow conditions applied in the column tests, seepage velocity ($v_s=q/\phi$, where ϕ is the porosity of the sandy soil medium) was estimated to be 1.6×10^{-4} cm/s. Having determined the soil parameters (v_s , α_L , and D_m), D was estimated to be around 1.15×10^{-4} cm²/s and from which Pe was estimated to be 9.37 ± 0.02 and confirms that the advection process plays a dominant role in contaminant transport in the sandy soil medium.

A trial and error approach was applied to determine the R of the composites, whereby the unknown R was adjusted to obtain different concentration profiles, and from the various trials, the most representative R was that which produced a reasonable match between the theoretical concentration profile and the observed profile from experimental data. The partitioning coefficient (K_d) was calculated from the assumed R , considering the empirical linear isotherm equation.

Table 4.2 summarizes the contaminant transport parameters of the three composites. As shown in the table, the K_d value of natural soil (sandy soil) was enhanced significantly by about 3-times when the coarse agent was used, where it reached 120.5 cm³/g. And by nearly 6-times when the fine agent was used, where it was highest and K_d reached 256.9 cm³/g.

Figure 4.11 shows the concentration profiles of As at the column exit obtained using the analytical solution and from the column test, assuming a constant source concentration in mg/L As of 0.1 at the column inlet. As shown in this figure, the fitted curves were analogous to the measured data, which suggests that the equation (4.4) can be applied to simulate the transport of As under the conditions of this study. Amount of As at the column exit was found to exceed the regulatory limits after about $T>145$ for natural soil, $T>430$ for soil-agent composite, and $T>860$ for soil-fine agent composite.

Figure 4.11 also confirmed reproducibility of the testing method. Considering three replications for the soil-coarse agent composite, and replications for the soil-fine agent composite, the data were found not to vary significantly for a given material, although slight differences were noted for the soil-coarse agent composites.

Table 4.2: Contaminant transport parameters applied in the analytical model.

Case	1	2	3
Agent type	No agent	Fine	Coarse
Dry density, ρ_d (g/cm ³)	1.91	1.89	1.91
Porosity, ϕ (%)	27.5	29	28.1
Flow condition	Saturated state		
Darcian velocity, q (cm/s)	4.42×10^{-5}		
Seepage velocity, v_s (cm/s)	1.61×10^{-4}	1.51×10^{-4}	1.57×10^{-4}
Dispersion coefficient, D (cm ² /s)	1.20×10^{-4}	1.13×10^{-4}	1.17×10^{-4}
Peclet number, Pe	9.39	9.36	9.38
Retardation factor, R	285	1675	840
Partitioning coefficient, K_d (cm ³ /g) (ADE solution)	40.8	256.9	120.5
Partitioning coefficient, K_d (cm ³ /g) (Batch test)	28	60	30

Note: Continuous contaminant source at inlet, $C_0=100$ μ g/L; $Q=4.5$ cm³/h; Permeant pH=pH 6.

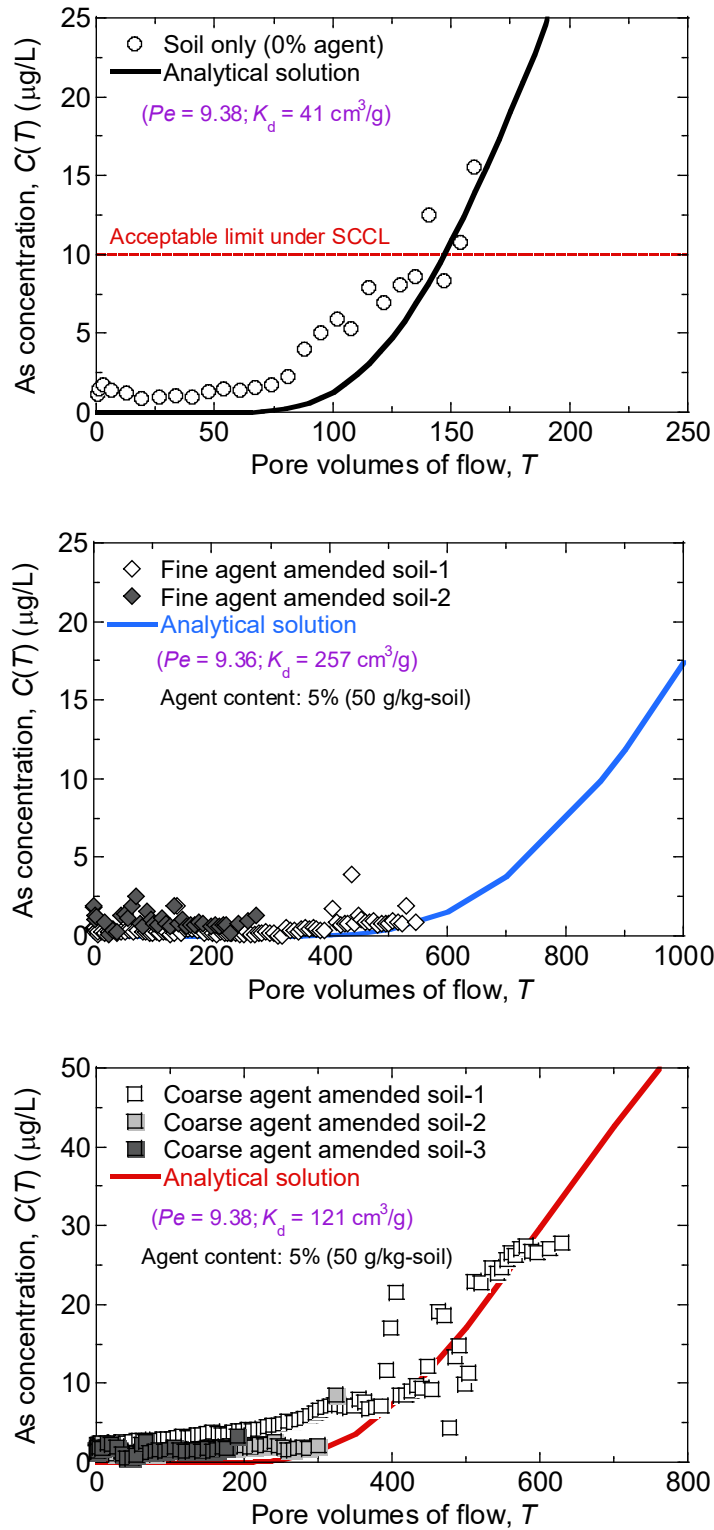


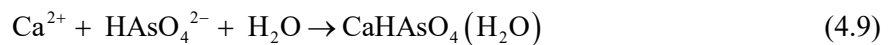
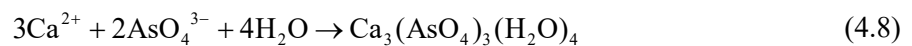
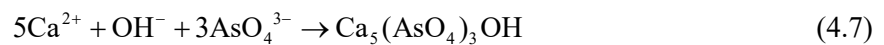
Figure 4.11: Profile of arsenic concentration at column exit for a natural soil (top), soil-fine agent composite (middle), and soil-coarse agent composite (bottom).

Comparing K_d values determined from batch sorption experiment and those from column test, it was found out that the difference was very big, with batch tests providing very low K_d values for example $11 \text{ cm}^3/\text{g}$ for a sandy soil mixed with agent of coarse type. Although in some situations the use of distribution coefficients from the sorption isotherm information tends to produce higher transport performance predictions (Yong and Mulligan, 2003), in this study much lower predictions are expected. Although not verified, this might be because a shaking time of 24 h might not be sufficient to achieve equilibrium concentrations.

4.3.3 Expected arsenic attenuation mechanism

Attenuation refers to the overall mechanism which results in the reduction of toxicity and concentration during the transport of contaminants in a sandy soil porous medium (Yong and Mulligan, 2003). These reactions can be cation exchange, precipitation, and in general any binding between solutes and the solid matrix (Yong et al., 1992). In this study, there seem to be two possible mechanisms to be considered. In the case of natural, it is expected that sorption reactions would be the governing mechanism for contaminant attenuation. In this case, the amount of cations and surface charge will influence the concentration of As in the effluent (McBride, 1994). By adding the agents, the presence of Ca and Mg carbonates increases the extent of precipitation mechanism. Precipitates in the form of oxides, hydroxides and/or carbonates are likely to be formed (McNeill and Edwards, 1997; Moon et al., 2004; Salameh et al., 2010; Salameh et al., 2015).

In an effort to clarify the As sorption mechanism of this Ca-Mg composite, Itaya et al. (2013) carried out X-ray diffraction (XRD), X-ray fluorescence (XRF), scanning electron microscopy and energy dispersive spectroscopy (SEM-EDS) analysis on the residue after the batch-type test. According to the authors, due to the addition of this material, pH will increase and H_3AsO_3 will start to transfer into H_2AsO_3^- . As (III) will be oxidized to As (V). Precipitation of calcium arsenate will be generated according to the following chemical reactions:



In this study, pH-Eh characteristics of the flow volumes were plotted against As amounts in those solutions. It was found that the As-applied as NaAsO_2 [or As(III)] was oxidized to As(IV). This As species and its associated compounds are less mobile and toxic, and stable over a wide pH range (Bothe and Brown, 1999). However, it is not clear whether the oxidation was due to the agent and/or because the testing conditions did not consider anaerobic conditions, therefore further study is necessary to clarify this concern.

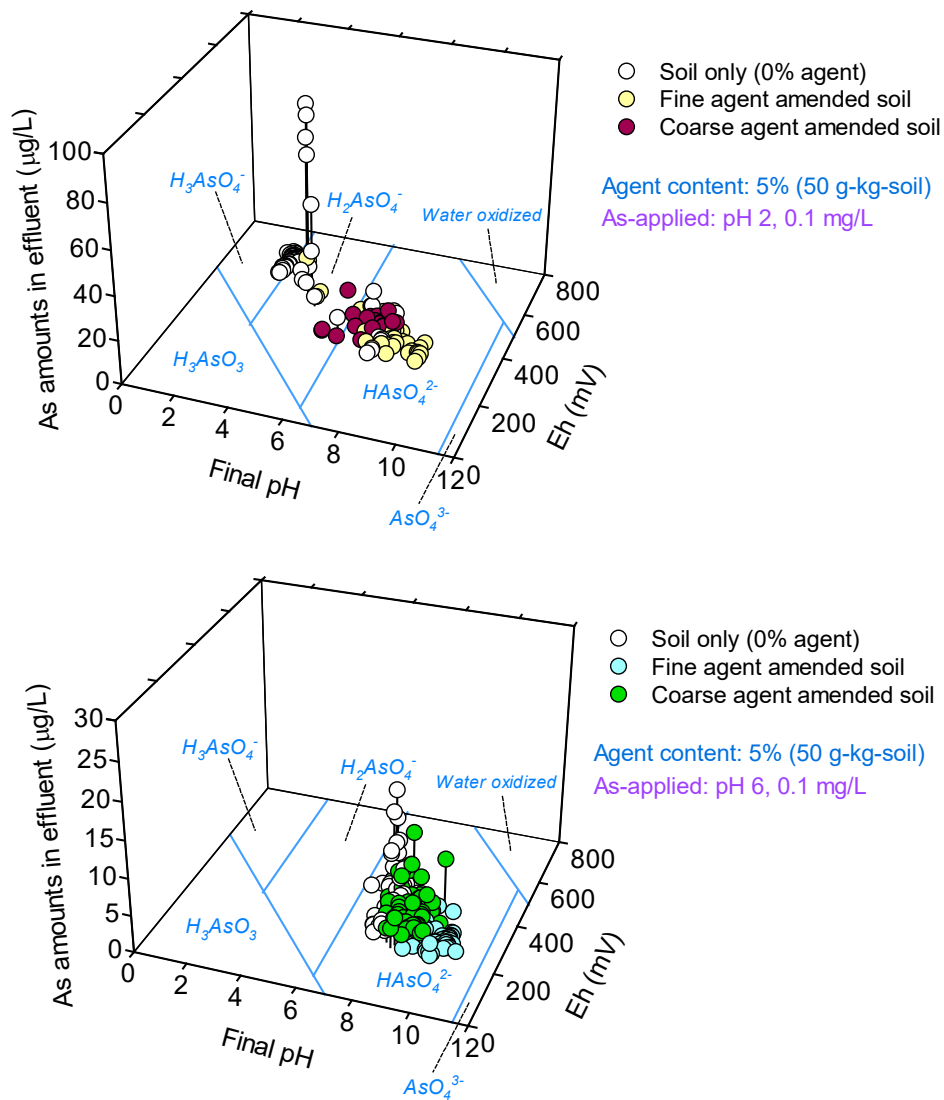


Figure 4.12: Eh-pH-As characteristics of composites of soil and different sizes of agent when permeated with solution of low pH of 2 (above) and pH 6 (bottom).

4.4 Conclusions for Chapter 4

Attenuation performance with time of soil-agent composites was studied by applying column tests under saturated conditions, which can more closely simulate the in-situ water in contact with the solid materials and also allow for the measurement of the time-lapse release of contaminants. Also, an analytical 1-D advection-dispersion model was applied using transport parameters obtained from the column tests. It was found out that:

By mixing natural soil with 5% (50 g/kg-soil) agent, its capacity to decrease concentrations of As-applied became more effective. The soil-agent composite could lower concentrations of As-applied to values below the acceptable limit; for many flow volumes and different pH conditions. Removal ratio (R_r) was generally $>95\%$, and As concentrations were under the allowable limit 0.01 mg/L As. This

suggests that by lining possible acid-generating materials on top of the attenuation layer constructed using sandy soil mixed with this agent, we still can expect to reduce As in leachate to negligible amounts for a long period/ volumes of flow. Although coarse agent is less effective compared to the other agent sizes, it can still ensure that As concentrations are below the allowable limit for many flow volumes/long-term services.

Comparing K_d values determined from batch-type experiment in Chapter 3, and those from the column test, it was found out that the difference was extremely large, with batch-type tests providing extremely low values, for example, $K_d=11 \text{ cm}^3/\text{g}$ for a sandy soil mixed with agent of coarse type. This shows that results from batch test may not be a reliable tool/index for evaluating the performance of the materials.

The capacity of the soil to buffer pH became more effective due to the adding of agents in the soil matrix. The pH of effluent was found to be alkaline conditions when the composite was permeated with solutions of pH 6 or low pH of 2. Under permeation with solutions of pH 6 conditions, the fine agent offered very high capabilities to increase pH; in the initial stages, pH was raised from the pH-applied of 6 to strongly alkaline conditions of pH 10, but with more volumes of flow this property decreased. Under similar conditions, soil-coarse agent in the initial stages could increase pH to about pH 8 to 9. Under permeation with solutions of pH 2, the fine agent offered slightly better improvement, but the differences of the agents were considered not significant. Although the agents offered a higher pH buffering property, this feature decreased over time with continuous permeation due to the leaching of carbonates from the agent with more volumes of flow.

Presence of Ca and Mg carbonates (from the agent) in the soil increases the extent of precipitation mechanism. Precipitation of calcium arsenate is expected. This precipitate is less mobile and toxic, and stable over a wide pH range.

References for Chapter 4

- Bolan, N. S., Naidu, R., Syers, J. K., and Tillman, R. W. 1999. Surface charge and solute interactions in soils. In Sparks (Ed.), *Advances in Agronomy* 67, 87-140: Academic Press.
- Bothe, J. V. and Brown, P. W. 1999. The stabilities of calcium arsenates at 23 +/- 1 degrees C. *Journal of Hazardous Materials*, 69(2): 197-207.
- Gelhar, L. W., Welty, C., and Rehfeldt, K. R. 1992. A critical review of data on field-scale dispersion in aquifers. *Water Resources Research*, 28(7): 1955-1974.
- Grathwohl, P. and Susset, B. 2009. Comparison of percolation to batch and sequential leaching tests: Theory and data. *Waste Management*, 29(10): 2681-2688.
- Itaya, Y., Kikuchi, S., Yoshimatsu, T., and Kuninishi, K. 2013. Clarification of insolubilization mechanism of heavy metals using magnesium/calcium composite material. *Proceedings of the 19th Conference on Groundwater and Soil Contamination and its Countermeasures*, Japan. (In Japanese).
- Katsumi, T., Inui, T., Yasutaka, T., and Takai, A. 2019. Towards sustainable soil management — reuse

- of excavated soils with natural contamination —. *Proceedings of the 8th International Congress on Environmental Geotechnics Volume 1*, Hangzhou, China.
- McBride, M. B. 1994. *Environmental Chemistry of Soils*: Oxford University Press.
- McNeill, L. S. and Edwards, M. 1997. Arsenic Removal during Precipitative Softening. *Journal of Environmental Engineering*, 123(5): 453-460.
- Mo, J., Inui, T., Katsumi, T., Takai, A., Kuninishi, K., and Hayashi, S. 2018. Time-dependent arsenic sorption of soil amended with calcium-magnesium composite powder as a sorption layer. *Proceedings of the 7th China-Japan Geotechnical Symposium*, Sanya China.
- Moon, D. H., Dermatas, D., and Menounou, N. 2004. Arsenic immobilization by calcium–arsenic precipitates in lime treated soils. *Science of The Total Environment*, 330(1): 171-185.
- Ogata, A. and Banks, R. B. 1961. *A solution of the differential equation of longitudinal dispersion in porous media* (411A). Retrieved from <http://pubs.er.usgs.gov/publication/pp411A>
- Salameh, Y., Al-Lagtah, N., Ahmad, M. N. M., Allen, S. J., and Walker, G. M. 2010. Kinetic and thermodynamic investigations on arsenic adsorption onto dolomitic sorbents. *Chemical Engineering Journal*, 160(2): 440-446.
- Salameh, Y., Albadarin, A. B., Allen, S., Walker, G., and Ahmad, M. N. M. 2015. Arsenic(III,V) adsorption onto charred dolomite: Charring optimization and batch studies. *Chemical Engineering Journal*, 259: 663-671.
- Shackelford, C. D. 1994. Critical concepts for column testing. *Journal of Geotechnical Engineering*, 120(10): 1804-1828.
- Tanaka, M., Takahashi, Y., Yamaguchi, N., Kim, K.-W., Zheng, G., and Sakamitsu, M. 2013. The difference of diffusion coefficients in water for arsenic compounds at various pH and its dominant factors implied by molecular simulations. *Geochimica et Cosmochimica Acta*, 105: 360-371.
- van Genuchten, M. T. and Parker, J. C. 1984. Boundary conditions for displacement experiments through short laboratory soil columns. *Soil Science Society of America Journal*, 48(4): 703-708.
- Yong, R. N., Mohamed, A. M. O., and Warkentin, B. P. 1992. *Principles of contaminant transport in soils*: Elsevier.
- Yong, R. N. and Mulligan, C. N. 2003. *Natural Attenuation of Contaminants in Soils*: CRC Press.

Chapter 5 Water retention properties

5.1 General remarks

In many cases, stakeholders put emphasis on the hydraulic conductivity (Nozaki et al., 2013; Mo et al., 2015a) and attenuation capacity (Tabelin et al., 2013; Tabelin et al., 2014; Mo et al., 2015b) when selecting suitable materials as the attenuation layer. However, seepage conditions in this layer are not well understood/considered and can significantly influence its functions (Ghasemzadeh, 2008; Francisca et al., 2012). Soil water retention characteristics, is one of the important soil hydraulic properties in the simulation of seepage conditions, as it is used to define the relationship between the coefficient of permeability and soil suction (Fredlund et al., 1994). In this chapter, the water retention characteristics of six composites with different agent sizes and base materials were investigated, to acquire detailed quantitative information pertaining to the effect of using different base material and particle sizes of Ca-Mg composite.

5.2 Materials and methods

5.2.1 Materials

Two base materials namely decomposed granite soil of under 2 mm and silica sand, were used for the tests. Particle size distribution of the soils is shown in Figure 5.1 and was determined according to JGS 0131. Decomposed granite soil was classified as well-graded sand with fine fraction (S-F) and silica sand as poorly-graded sand (S), according to JGS 0051. Basic properties of the soils are summarized in Table 5.1. Ca-Mg composite of powder type of under 0.075 mm and coarse type of 2-9.5 mm was used as the stabilizing agent. Properties of the material were introduced in section 3.2.1.

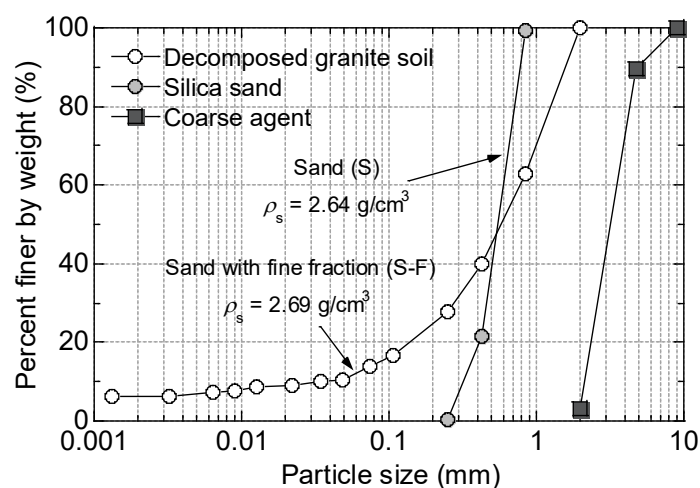


Figure 5.1: Particle-size distribution curves of base materials and coarse Ca-Mg composite.

Table 5.1: Basic properties of soils.

Property	Value		Method
	Decomposed granite soil	Silica sand	
Particle size distribution (%)			JGS 0131
Sand fraction (0.075-2 mm)	85.9	100	
Silt fraction (0.005-0.075 mm)	7.7	0	
Clay fraction (< 0.005 mm)	6.4	0	
Uniformity coefficient, U_c	20.2	2.7	
Coefficient of curvature, U_c'	3.32	1.53	
Particle density, ρ_s (g/cm ³)	2.69	2.64	JGS 0111
Optimum water content, w_{opt} (%)	10.1	11.6	JGS 0711
Maximum dry density, ρ_d (g/cm ³)	2.01	1.55	JGS 0711

5.2.2 Water retention tests

As summarised in Table 5.2, the water retention characteristics of six composites with different agent sizes and base materials were investigated by the Tempe cell method or soil column experiment. The composites were prepared by adding agent to the dry soil, at 0 or 5% (50 g/kg-soil) by dry weight and distilled water that depends on their optimum water content ($w_{opt}=10-12\%$). All mixing was done with a mechanical mixer, and proper care taken to prepare a homogeneous composite at each stage of mixing.

Tempe cell, shown in Figure 5.2 was applied to obtain the water retention curves of composites with base material of decomposed granite soil (Case 1-3). The mixture (in wet state) was compacted in three equal layers (=1 cm-high layer) in a 5.4-cm inner diameter and 3-cm high brass cylinder and then confined by a base plate and top cap. After this, the specimen was saturated for 24 hours in a vacuum deaerator. The amount of mass for each layer was standardised based on the results of the standard Proctor compaction test (JGS 0711) and considering a D_c 95%. Drainage tests were carried out at several air-entry pressures (u_a) for the 3 cases.

Table 5.2: Summary of experimental approach.

Case	1	2	3	4	5	6
Base material	Decomposed granite soil			Silica sand		
Agent type	No agent	Powder	Coarse	No agent	Powder	Coarse
Content of agent (%)	0	5	5	0	5	5
Method	Tempe cell			Soil column		

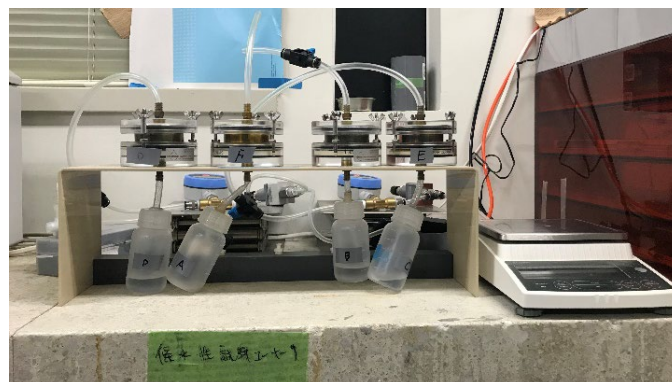


Figure 5.2: Schematic setup of the low suction device (Tempe cell) for measuring the water retention property.



Figure 5.3: Schematic setup of the soil column method.

Air pressure was supplied through the inlet tube at the top cap and water allowed to drain out from the bottom outlet, which was open to the atmosphere (0 kPa). Change in weight of the system with time was recorded for the corresponding air-entry pressure. Air pressure was incrementally adjusted after equilibrium was achieved. In sandy soil, the residual saturation tends to remain constant for $u_a > 10$ kPa (Fredlund and Xing, 1994), so we applied u_a ranging from 0-10 kPa. Suction (ψ) was calculated by taking the difference of air pressure (u_a) and water pressure (u_w), i.e. $\psi = u_a - u_w$.

Because it was difficult to properly control the air entry pressure in low ranges ($u_a < 2$ kPa), due to the low water retention capacity inherent by poorly-graded soils like silica sand, the soil column method shown in Figure 5.3 was used instead to obtain the water retention curves of composites with base material of silica sand (Case 4-6). For the soil column method, a polyvinyl-chloride pipe of 2.5 cm in inner diameter was first cut into 12 fractions (each 5-cm high), and then attached together by curing tape and supported by a pole. Column was then partially submerged in water, by placing it inside a tank containing distilled water. Mixture (in wet state) was poured in the column and compacted in several equal layers, under submerged conditions, so as to prepare a fully saturated soil column. By determining the dry mass of the soil (m_s) after the test, Dc 92-95% was verified. More water was poured to the soil column from the top until the water level was above the soil layer, so as to ensure that the soil was fully saturated before the drainage test. With the top part of the column open to the atmosphere, water was allowed to drain from the soil for 24 hours. After the drainage test, the soil column was divided into 5-cm fractions and soil in each fraction carefully extracted for water content and dry mass measurements. Considering the air pressure in the tube is atmospheric ($u_a = 0$) and water pressure ($u_w = -\rho_w g H$, where ρ_w is the density of (1 Mg/m³), g is the gravitational acceleration (9.81 m/s²), and H (m) is the height of soil sample), suction (ψ) was calculated by taking the difference between air pressure and water pressure i.e. $\psi = u_a - u_w$.

Saturation (S_r) was determined using the equation (5.1), by considering the particle density (ρ_s), void ratio (e), and water content (w) of the soil which was determined by oven-drying the soil.

$$S_r = \frac{w}{100} e^{-\frac{\rho_s}{\rho_w}} \quad (5.1)$$

5.2.3 Fitting water retention parameters with van Genuchten model

The equation (5.2) proposed by van Genuchten (1980) was applied to obtain the best fit curve to the experimental results for the drainage process. Under the conditions of available measured data of the soil water content and suction, the parameters of van Genuchten (VG) model were estimated by the least square method, and the corresponding water retention curves acquired.

$$S_r(\psi) = S_{rf} + \frac{1 - S_{rf}}{[1 + (\alpha\psi)^n]^{1-\frac{1}{n}}} \quad (5.2)$$

where, S_{rf} is the residual saturation, α and n are VG model parameters, whereby, α is related to the point of curvature and n is related to the pore size distribution.

Soil-water characteristic curve (SWCC), is one of the important soil hydraulic properties in the simulation of seepage conditions. As shown in Figure 5.4, SWCC can be defined with some parameters such as the saturated volumetric water content (θ_s), residual volumetric water content (θ_r), and air-entry value, AEV (or ψ_a), which is defined as the matric suction at which air first enters the largest pores of the soil from which the saturated soil commences to desaturate (Fredlund et al., 1994). Since SWCC are sigmoidal in character, they do not provide a reasonable description of water storage below the AEV and above residual conditions (Fredlund et al., 2012).

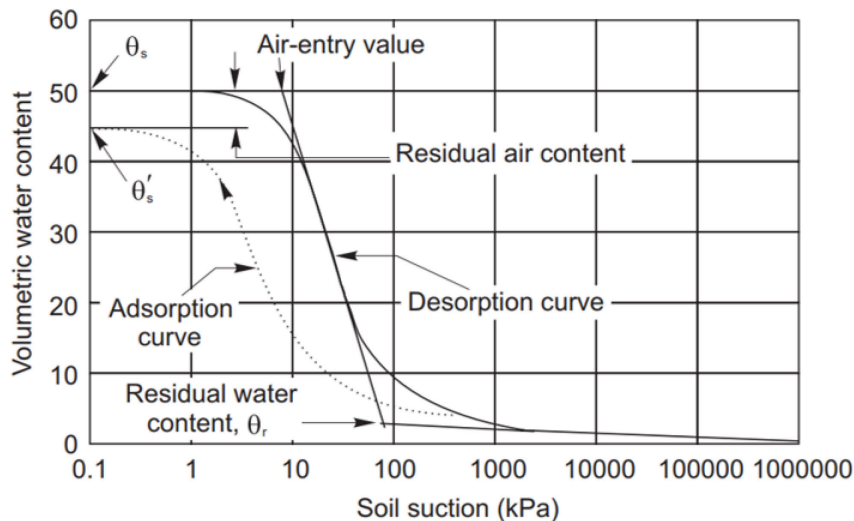


Figure 5.4: Typical soil-water characteristic curve (Fredlund et al., 1994).

5.3 Results and discussions

5.3.1 Water retention property

Figure 5.5 shows the SWCC for the composites of decomposed granite soil (Case 1-3) and Figure 5.6 for composites of silica sand (Case 4-6). The symbols represent measured data and the fitting curves, obtained using the soil hydraulic parameters given in Table 5.3, are shown by solid lines. Inspection of the curves shows a good agreement between measured and predicted degree of saturation using the S-shape curve fitting equation proposed by van Genuchten (1980).

Notice that in both figures the sandy soil as compared to soil-agent composites loses its water relatively quickly. By adding powder agent to the soils, ψ_a , and S_{rf} were increased, and the highest S_{rf} is expected for the granite soil-powder agent composite; but not verified due to the applied air pressures. Increase in ψ_a , for example for silica sand ($\psi_a=0.9$ kPa), adding 5% powder agent increase the AEV ($\psi_a=1.5$ kPa) suggests that the occupies the voids and/or increases the fines content in the soil. Also, noted was that, although the coarse agent reduced ψ_a of the soil, due to its particle size, the soil-coarse agent composite still exhibited a higher S_{rf} . For example, for granite soil-coarse agent composite, $\psi_a=0.7$ kPa, which is much lower than the natural soil. However, S_{rf} of this composite was 63%, which is much higher than the natural soil. This shows that Ca-Mg composite does not only enhance the attenuation function of soil, as was found in both Chapter 3 and Chapter 4, as well as by other researchers (Mo et al., 2015b), but it can also improve the water retention properties of sands, especially well-graded soil.

While the majority of pores in the composites with silica sand drain at relatively small negative pressures, the majority of pores in the composites with decomposed granite soil do not drain until very relatively large negative pressures were applied, This is because the decomposed granite soil had a high $\psi_a=3.5$ kPa, as compared to silica sand, $\psi_a=0.9$ kPa, as is expected for well-graded soils. As shown in Figure 5.7, when granite soil-coarse agent composite is used in the site, S_{rf} of about 63% is expected for high negative pressures, which is much higher than for composites with silica sand, where $S_{rf}=4\%$.

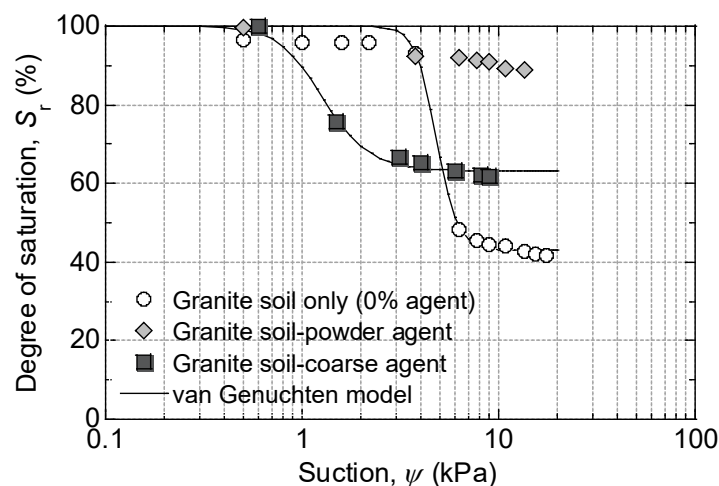


Figure 5.5: Effect of different Ca-Mg composite sizes on the water retention property of a well-graded sandy soil.

Table 5.3: Soil hydraulic parameters.

Case	1	2	3	4	5	6
Saturated hydraulic conductivity, k_{sat} (m/s)	1×10^{-6}	1×10^{-6}	1×10^{-6}	1×10^{-4}	1×10^{-4}	1×10^{-4}
Air-entry value, ψ_a (kPa)	3.5	-	0.7	0.9	1.5	0.5
Porosity, ϕ	0.32	0.29	0.30	0.45	0.45	0.46
Residual degree of saturation, S_{rf} (%)	43	-	63	4.5	17	3.8
VG constant, α (1/cm)	0.21	-	0.86	0.79	0.55	1.1
VG constant, n	8.4	-	4.1	4.8	7.2	3.0
Residual volumetric water content, θ_r	0.13	-	0.18	0.020	0.076	0.017
Saturated volumetric water content, θ_s	0.32	0.29	0.30	0.45	0.45	0.46

Note: Values of k_{sat} are generic and were based on previous literature.

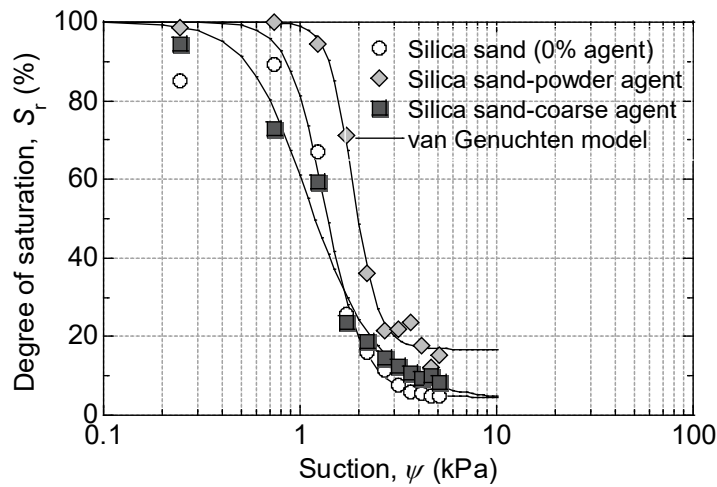


Figure 5.6: Effect of different agent sizes on the water retention property of a poorly-graded sandy soil.

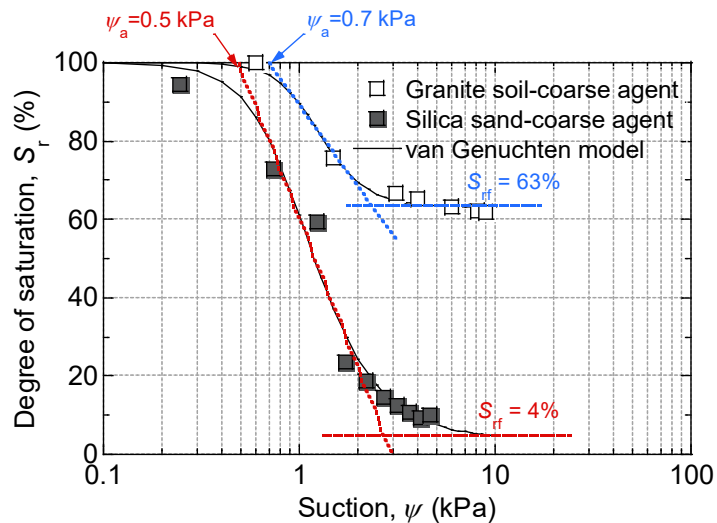


Figure 5.7: Water retention properties of sands mixed with Ca-Mg composite of coarse type (Case 3 and 6).

5.3.2 Permeability function of sands mixed with different agent sizes

Unsaturated hydraulic conductivity (k) was calculated using the van Genuchten-Mualem equation (5.3).

$$k(\theta) = k_{sat} \times S_e^\gamma \left[\left\{ 1 - \left(1 - S_e^{\frac{1}{m}} \right)^m \right\} \right]^2$$

$$\begin{cases} S_e = \frac{\theta - \theta_r}{\theta_s - \theta_r} \\ m = 1 - \frac{1}{n} \end{cases} \quad (5.3)$$

where S_e is effective degree of saturation, θ is the volumetric water content, θ_r is residual volumetric water content, θ_s is saturated volumetric water content, k_r is relative hydraulic conductivity, γ is constant and usually used as 0.5, n and m are VG model parameters, k is unsaturated hydraulic conductivity, and k_{sat} is saturated hydraulic conductivity.

As shown in Figure 5.8, k decreases with an increase in negative pressures (which forces pore water out) and tends to remain constant at relatively high pressures. Although silica sand mixed coarse agent was permeable ($k=1 \times 10^{-4}$ m/s) at relatively small negative pressures, which is ascribed to the initial k_{sat} value, its permeability function drastically dropped by several orders until the soil became impermeable ($k=1 \times 10^{-14}$ m/s), because at the boundary of the soil layer, even if the water content becomes discontinues, pore water pressure keeps the continuity, which is much noticeable for a poorly graded soil. Residual k for the composite with silica sand (Case 6) was relatively lower compared to that of decomposed granite soil mixed with the coarse agent, which tends to remain constant at $k=1 \times 10^{-11}$ m/s. Also noted, adding the agent to decomposed granite soil, sharp decrements of k are suppressed with increased negative pressures, and relatively small changes in k were observed when the agent was employed.

As shown in Figure 5.9, k decreased exponentially with reducing saturation as pore water was forced out, which was drastic for composites with silica sand. Poorly graded soils have large voids, therefore when small negative pressure is applied, pore water is forced out easily, for it cannot stay in the large voids. In unsaturated conditions, infiltrate water flows in the consecutive fluid phase and it circumvents the relatively large gaps. From this view, as the soil becomes unsaturated, the permeability function decrease, since water flow is deterred.

When permeability is too low, infiltrate water cannot pass through the layer, and S_r in the embankment will increase, which risks the stability of the embankment. Therefore, poorly graded sands (such as silica sand) are not a suitable base material, for they drastically become impermeable ($k=1 \times 10^{-14}$ m/s) for small changes in negative pressures. This is valuable in terms of recognising the limitations of suitable base materials.

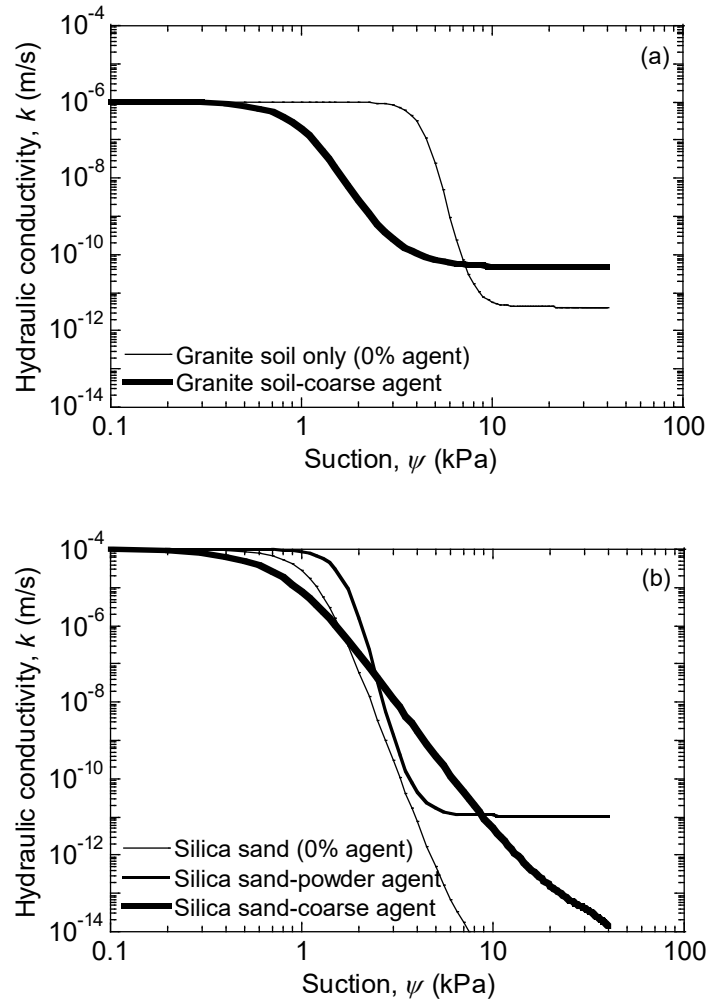


Figure 5.8: Permeability functions of (a) decomposed granite soil and (b) silica sand mixed with different agent sizes.

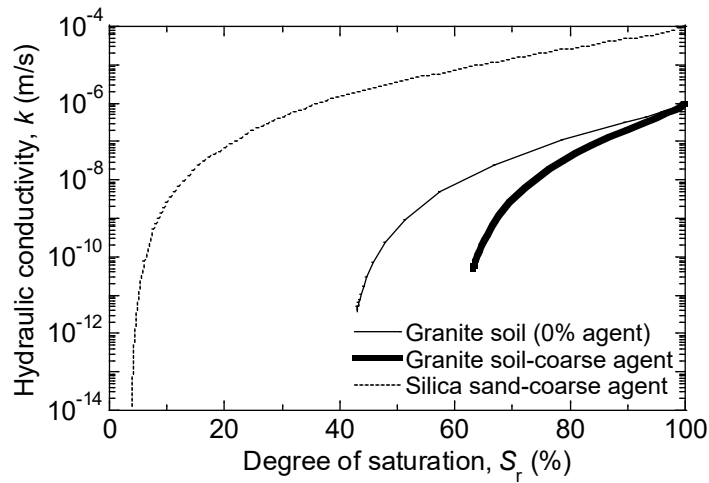


Figure 5.9: Water permeability characteristics of composites with changes in the degree of saturation.

If the water permeability characteristics of the composite Case 3 and Case 6 is expressed by the leachate residence time ($t_c=L\phi/ki$, where L is the thickness of the attenuation layer, ϕ is the porosity of the layer, and i is hydraulic gradient), for a typical 30 cm-thick layer, and assuming $\phi=0.3$, t_c is expected to be 24 h for Case 3, which is much higher than Case 6 and is preferred because it provide better attenuation performance (Mo, 2019). When the permeability characteristics of the layer decrease, the time will increase, and will improve the attenuation function of the bottom layer.

5.4 Conclusions for Chapter 5

This chapter focused on the characterization of water retention properties of several composites of different base materials and particle sizes of Ca-Mg composite, with the aim of better understanding and recognising the limitations of base material of sandy soil for construction of attenuation layer. From the investigation carried out, we concluded that:

By adding powder agent to the soils, ψ_a , and S_{rf} were increased, and the highest S_{rf} is expected for the granite soil-powder agent composite; but not verified due to the applied air pressures. Increase in ψ_a , for example for silica sand ($\psi_a=0.9$ kPa), adding 5% powder agent increase the AEV ($\psi_a=1.5$ kPa) suggests that the occupies the voids and/or increases the fines content in the soil. Also, noted was that, although the coarse agent reduced ψ_a of the soil due to its particle size, the soil-coarse agent composite still exhibited a higher S_{rf} . Taking granite soil-coarse agent composite (of $\psi_a=0.7$ kPa) as an example, S_{rf} reached 63%, which is much higher than that of the natural soil. This shows that Ca-Mg composite does not only enhance the attenuation function of soil but also can improve the water retention properties of sands, especially for a well-graded soil.

Poorly graded sandy soils like silica sand may not be suitable base material, for they drastically become impermeable ($k=1\times 10^{-14}$ m/s) from small changes in negative pressures. When permeability is too low, infiltrate water cannot pass through the layer, and S_r in the embankment will increase, which risks the stability of the embankment.

If the water permeability characteristics of the decomposed granite soil-coarse agent is expressed by the leachate residence time ($t_c=L\phi/ki$, where L is the thickness of the attenuation layer, ϕ is the porosity of the layer, and i is hydraulic gradient), for a typical 30 cm-thick layer, and assuming $\phi=0.3$, t_c is expected to be 24 h which is preferred for better attenuation performance.

References for Chapter 5

- Francisca, F., Carro Pérez, M., Glatstein, D., and Montoro, M. 2012. Contaminant transport and fluid flow in soils. In Szigethy (Ed.), *Horizons in Earth Science Research*, 97-131: Nova Science Publishers, Inc.
- Fredlund, D. G., Rahardjo, H., and Fredlund, M. D. 2012. *Unsaturated Soil Mechanics in Engineering Practice*: Wiley.
- Fredlund, D. G. and Xing, A. 1994. Equations for the soil-water characteristic curve. *Canadian Geotechnical Journal*, 31(4): 521-532.

- Fredlund, D. G., Xing, A. Q., and Huang, S. Y. 1994. Predicting the permeability function for unsaturated soils using the soil-water characteristic curve. *Canadian Geotechnical Journal*, 31(4): 533-546.
- Ghasemzadeh, H. 2008. Heat and contaminant transport in unsaturated soil. *International Journal of Civil Engineering*, 6(2): 90-107.
- Mo, J. (2019). *Soil amended with calcium-magnesium immobilizing agent against natural arsenic contamination*. Doctoral Thesis. Kyoto University, Retrieved from <https://dx.doi.org/10.14989/doctor.k21936>
- Mo, J., Inui, T., Katsumi, T., Kuninishi, K., and Shintaro, H. 2015a. Effectiveness of immobilizing agent used as a sorption layer against natural contamination. *Japanese Geotechnical Society Special Publication*, 1(4): 19-24.
- Mo, J., Inui, T., Katsumi, T., Takai, A., Kuninishi, K., and Hayashi, S. 2015b. Performance of sorption layer using Ca/Mg immobilizing agent against natural contamination. *10th Asian Regional Conference of IAEG*, Kyoto, Japan.
- Nozaki, T., Matsuyama, Y., Sugiyama, A., Moriya, M., Komukai, Y., and Nagase, T. 2013. Fundamental study of soil materials for absorbent construction method using MgO material. *Proceedings of the 19th Symposium on Soil and Groundwater Contamination and Remediation*. (In Japanese).
- Tabelin, C. B., Igarashi, T., Arima, T., Sato, D., Tatsuhara, T., and Tamoto, S. 2014. Characterization and evaluation of arsenic and boron adsorption onto natural geologic materials, and their application in the disposal of excavated altered rock. *Geoderma*, 213: 163-172.
- Tabelin, C. B., Igarashi, T., Yoneda, T., and Tamamura, S. 2013. Utilization of natural and artificial adsorbents in the mitigation of arsenic leached from hydrothermally altered rock. *Engineering Geology*, 156: 58-67.
- van Genuchten, M. T. 1980. A closed-form equation for predicting the hydraulic conductivity of unsaturated Soils. *Soil Science Society of America Journal*, 44(5): 892-898.

Chapter 6 Practical implications

6.1 General remarks

To better understand the performance of this method and the relative performance of an attenuation layer constructed using a composite of sandy soil and different agent sizes, considering compliance with regulations, an analytical solution of the 1-D advection-dispersion equation was applied.

6.2 Analytical solution of arsenic transport in attenuation layer

A simplified condition, as shown in Figure 6.1, of a saturated 30-cm thick attenuation layer with a porosity (ϕ) of 0.28 to 0.29, hydraulic conductivity (k) of 1×10^{-6} m/s, and seepage is steady-state and under a hydraulic gradient ($i = h_w/L$, where h_w is the leachate head) which in the field is generally close to 1 (Sharma and Lewis, 1994). Assuming the soil properties (e.g. ϕ , K_d , and D) are homogeneous and do not change with time, and suction is ignored, the concentration profiles of As exiting the layer, $C(x=L, t)$, with time (t) were determined considering the initial and boundary conditions listed in Table 6.1.

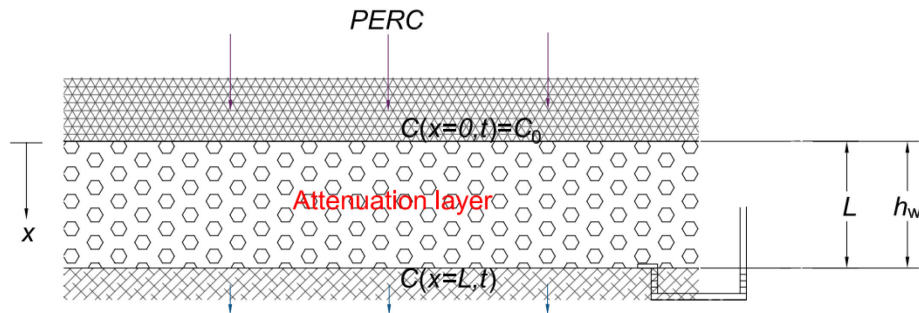


Figure 6.1: Conceptual model for the simplified field condition.

Table 6.1: Contaminant transport parameters of different composites.

Case	1	2	3
Agent type	No agent	Fine	Coarse
Dry density, ρ_d (g/cm ³)	1.91	1.89	1.91
Porosity, ϕ (%)	27.5	29	28.1
Attenuation layer thickness, L (cm)	30	30	30
Hydraulic conductivity, k (cm/s)	1×10^{-4}	1×10^{-4}	1×10^{-4}
Seepage velocity, v_s (cm/s)	3.64×10^{-4}	3.45×10^{-4}	3.64×10^{-4}
Dispersion coefficient, D (cm ² /s)	1.1×10^{-3}	1.1×10^{-3}	1.1×10^{-3}
Peclet number, Pe	9.93	9.93	9.93
Retardation factor, R	285	1675	840
Partitioning coefficient, K_d (cm ³ /g) (ADE solution)	40.8	256.9	120.5
Boundary conditions			
Entrance boundary conditions, $C(x=0, t)$		100 $\mu\text{g/L}$	
Exit boundary conditions, $C(x=L, t)$		0	
Initial conditions, $C(x, t=0)$		0	

As shown in the table, D increases following an increase in distance of transport, which is because the longitudinal dispersivity (α_L) is proportional to the transport distance L , i.e. $\alpha_L=0.1L$ (Gelhar et al., 1992). Considering a seepage velocity ($v_s=ki/\phi$) of 3.6×10^{-4} cm/s, D was estimated to be 1.1×10^{-3} cm²/s, from which Pe was estimated to be 9.93, indicating that advection played a dominant role in the contaminant transport process.

Figure 6.2 shows that breakthrough will occur much faster when relying solely on the natural attenuation capacity of soil. Adding 5% agent contributes significantly to the prolonged breakthrough time. For a better understanding, we calculated the breakthrough time (t) in years, taking into account an assumed percolation ($PERC$) of 500 mm/year and cumulative infiltration (CI) given by the term ($T\times L\times \phi$), using the equation (6.1).

$$t = \frac{T \times L \times \phi}{PERC} \quad (6.1)$$

Figure 6.3 shows the profiles of arsenic concentration at exit of a 30-cm thick attenuation layer constructed with a composite of sandy soil and different agent sizes. As shown in the figure, for an attenuation layer constructed with only sandy soil, it will take about 25 years for As concentration to exceed the regulatory limit under SCCL. While for a layer constructed with sandy soil and 5% agent of either coarse type or fine type, it will take about 73 and 142 years respectively for the concentrations to exceed the acceptable levels. The analysis confirms the reliability of a sandy soil mixed with the agent as an attenuation layer. The addition of agent content, minimizing percolation of rainwater into the embankment, and increase in layer thickness, and so on, all can contribute to the prolonged service time of the composite before breakthrough.

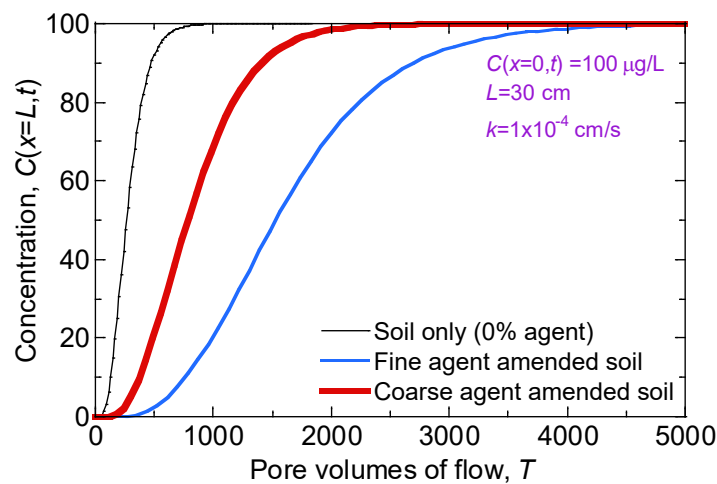


Figure 6.2: Profiles of arsenic concentration exiting the attenuation layer with volumes of flow.

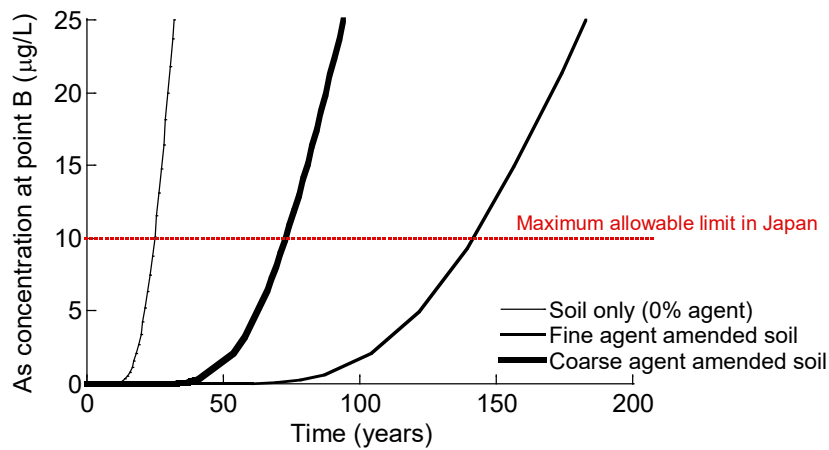


Figure 6.3: Breakthrough curve for an initial arsenic concentration of 100 µg/L in a 30 cm-thick attenuation layer.

In evaluating the attenuation layer, one of the primary factors required is the estimation of the layer thickness under a given set of performance requirements. By applying the design criterion proposed by Acar and Haider (1990) for earthen barriers, the influence of the thickness of the attenuation layer on the breakthrough time required to exceed the acceptable levels was evaluated. Figure 6.4 presents an estimate of breakthrough time for various thicknesses of the attenuation layer, given by the relationship of concentration at exit of layer $C(x=L, t)$ to concentration at inlet $C(x=0, t)$ ratios i.e. C/C_0 . As shown in the figure, breakthrough time increased when a thicker layer was used. Considering a 30-cm thick layer, it will take 73 years for the arsenic concentration to exceed the acceptable levels under SCCL.

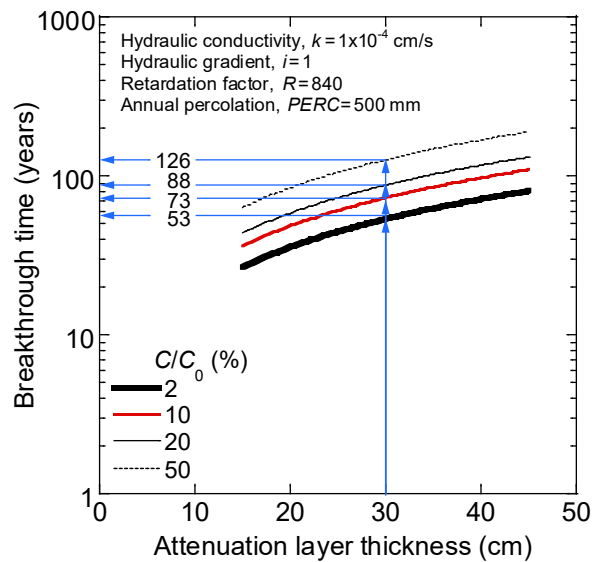


Figure 6.4: Breakthrough time for solute under one set of performance criteria for a composite of a sandy soil and agent of coarse type.

References for Chapter 6

- Acar, Y. B. and Haider, L. 1990. Transport of low-concentration contaminants in saturated earthen barriers. *Journal of Geotechnical Engineering*, 116(7): 1031-1052.
- Gelhar, L. W., Welty, C., and Rehfeldt, K. R. 1992. A critical review of data on field-scale dispersion in aquifers. *Water Resources Research*, 28(7): 1955-1974.
- Sharma, H. D. and Lewis, S. P. 1994. *Waste Containment Systems, Waste Stabilization, and Landfills: Design and Evaluation*: Wiley.

Chapter 7 Conclusions and future research

7.1 Conclusions

One strategy currently being explored in the development of a cost-effective countermeasure when reusing geogenic contaminated soils as fill materials in an embankment involves the installation of a compacted attenuation layer underlain the contaminated geomaterials. A key issue related to its design is the selection of a suitable base material and stabilizing agent to achieve the desired permeability and attenuation function, considering the availability, ease of use, suitability for several contaminants, compliance with regulations, and so on.

Main objective of this study was to evaluate the geoenvironmental reliability of natural soil (sandy soil) mixed with the coarse agent of 2-9.5 mm. To achieve this goal, (1) batch-type tests were carried to obtain basic information regarding the performance of composites of the soil and different particle sizes of this agent from the viewpoints of As attenuation, and the relationship of pH and buffer capacity on As attenuation. (2) Performance of the composite over time was investigated using column test under saturated conditions, which can more closely simulate the in-situ water in contact with the solid materials and allows for the measurement of the time-lapse release of contaminants. (3) Water retention characteristics were investigated using the Tempe cell and soil column method, to acquire detailed quantitative information pertaining to the effect of using different base materials and particle sizes of this agent.

From Chapter 3 it was found out that this natural soil has a capacity to reduce metal concentrations from solution. This function plays an important role because the attenuation layer can be heterogeneous in attenuation performance and maybe cracked due to earthquakes and static deformation with time, during long-term services. Freundlich parameter, K – a good index for quantifying the contaminant attenuation property of a solid material – was estimated to be 11 cm³/g. By introducing the Ca-Mg composite into the soil matrix, the attenuation function of the soil became more effective, but in the order of decreasing particle size (i.e. coarse < fine < powder). Highest As retention by the solid materials was noted in the soil-powder agent composite, where K reached 535 cm³/g which is about 50-times higher compared to that of the natural soil.

Although soil-coarse agent composite had no obvious changes due to curing, the attenuation function of a soil-fine agent composite was improved by curing it for up to 7 days, after that, the effect of curing time was not significant; for a 0-day cured composite, partitioning coefficient, K_d , for low concentrations, was estimated to be 60 cm³/g, but it increased by nearly 3-times when this composite was cured for 7 days it, where it reached 180 cm³/g, and after that very small changes were observed. This suggests that hydration of the fine agent had occurred at an early stage (within 7 days), and very minor hydration occurred with prolonged curing time, which may have increased the availability of the hydroxide sources.

By introducing agent into the soil matrix, the high carbonate content gave the soil a higher capability to increase pH to strongly alkaline conditions and retain more As with more acid input, and this was either due to more negative-surface charge and/or precipitation reactions. However, when the

pH of the soil suspension decreases below the precipitation pH (about pH=5), reduction in the amounts of As retained by the soil-agent composite is expected with increasing amounts of acid input.

From Chapter 4 it was found out that the soil-agent composite could lower concentrations of As-applied to values below the acceptable limit; for many flow volumes and different pH conditions. Removal ratio (R_r) was generally >95%, and As concentrations were under the allowable limit 0.01 mg/L As. This suggests that by lining possible acid-generating materials on top of the attenuation layer constructed using sandy soil mixed with this agent, we still can expect to reduce As in leachate to negligible amounts for a long period/ volumes of flow. Although the coarse agent is less effective compared to the other agent sizes, it can still ensure that As concentrations are below the allowable limit for many flow volumes/ longer time. Comparing K_d values determined from batch-type experiments in Chapter 3, and those from the column tests, it was found out that the difference was extremely large, with batch-type tests providing extremely low values, for example, $K_d=11 \text{ cm}^3/\text{g}$ for a sandy soil mixed with agent of coarse type. This shows that results from batch test may not be a reliable tool/index for evaluating the performance of the materials.

The capacity of the soil to buffer pH became more effective due to the adding of agents in the soil matrix. The pH of effluent was found to be alkaline conditions when the composite was permeated with solutions of pH 6 or low pH of 2. Under permeation with solutions of pH 6 conditions, fine agent offered very high capabilities to increase pH; in the initial stages, pH was raised from the pH-applied of 6 to strongly alkaline conditions of pH 10, but with more volumes of flow this property decreased. Under similar conditions, soil-coarse agent in the initial stages could increase pH to about pH 8 to 9. Under permeation with solutions of pH 2, the fine agent offered slightly better improvement, but the differences of the agents was considered not significant. Although the agents offered a higher pH buffering property, this feature decreased over time with continuous permeation due to the leaching of carbonates from the agent with more volumes of flow.

Presence of Ca and Mg carbonates (from the agent) in the soil increases the extent of precipitation mechanism. Precipitation of calcium arsenate is expected. This precipitate is less mobile and toxic, and stable over a wide pH range.

From Chapter 5 it was found out that adding powder agent to the soils, ψ_a , and S_{rf} were increased, and the highest S_{rf} is expected for the granite soil-powder agent composite; however, for this composite, it can not be verified with the applied air pressures. Increase in ψ_a , for example for silica sand ($\psi_a=0.9 \text{ kPa}$), adding 5% powder agent increase the AEV ($\psi_a=1.5 \text{ kPa}$) suggests that the occupies the voids and/or increases the fines content in the soil. Also, noted was that, although the coarse agent reduced ψ_a of the soil due to its particle size, the soil-coarse agent composite still exhibited a higher S_{rf} . Taking granite soil-coarse agent composite (of $\psi_a=0.7 \text{ kPa}$) as an example, it was determined that S_{rf} of this composite was 63%, which is much higher than that of the natural soil. This shows that Ca-Mg composite does not only enhance the attenuation function of soil, as was demonstrated in both Chapter 3 and Chapter 4, as well as by other researchers, but it can also improve the water retention properties of sands, especially well-graded soil.

Poorly graded sandy soils like silica sand may not be suitable base material, for they drastically become impermeable ($k=1 \times 10^{-14} \text{ m/s}$) from small changes in negative pressures. When permeability is

too low, infiltrate water cannot pass through the layer, and S_r in the embankment will increase, which risks the stability of the embankment.

If the water permeability characteristics of the decomposed granite soil-coarse agent is expressed by the leachate residence time ($t_c=L\phi/ki$, where L is the thickness of the attenuation layer, ϕ is the porosity of the layer, and i is hydraulic gradient), for a typical 30 cm-thick layer, and assuming $\phi=0.3$, t_c is expected to be 24 h which is preferred for better attenuation.

In Chapter 6, a simplified condition of a saturated 30-cm thick attenuation layer of a sandy soil mixed with this agent, having a porosity (ϕ) of 0.28, hydraulic conductivity (k) of 1×10^{-6} m/s, and seepage under a hydraulic gradient (i) of 1, was considered. Assuming constant continuous source (C_0) of As applied at the top of the layer, seepage is steady-state, suction existing at the bottom of the layer is ignored, and the soil properties (ϕ , k , K_d) are homogenous and do not change with time, the concentration (C) of As at the bottom of the layer at time (t) were obtained using 1-D form of advection-dispersion equation. It was estimated that it will take nearly 25 years for natural soil, 73 years for soil-coarse agent composite and 150 years for soil-fine agent composite, for the heavy metal concentrations to exceed the acceptable levels regulated under the Soil Contamination Countermeasures Law (SCCL) when using soil-coarse agent composite as the attenuation layer.

In conclusion, although the powder agent offers a better improvement to the attenuation, pH buffering, and water retention properties of natural soil, coarse agent which is cheaper to produce and offers better material handling, can be applied as a material for the attenuation layer. Less, but long-term reactivity expected when using this particle size of agent.

7.2 Future research

In this study, batch experiments and column tests under saturated conditions were carried to evaluate the attenuation function of a sandy soil mixed with a stabilizing agent of calcium-magnesium composite. But, these approaches do not fully represent the actual field conditions, for example (1) the flow condition in the attenuation layer is downwards and often under unsaturated conditions, and (2) anaerobic condition which is the more likely state in the embankment is ignored. Therefore, it is important to consider such aspects in future studies.

In the context of mechanisms involved in the attenuation of As, this study did not provide any comprehensive information about the contaminant speciation nor the precipitates formed. It is of importance to evaluate the concentrations and speciation of both cations and anions present in the effluent, in addition to conducting X-ray diffraction analysis on the solid material to evaluate its chemical and structural composition before and after the tests. This information will be useful in enhancing the understanding of the mechanism of As attenuation by a sandy soil mixed with the agent.

Because of the heterogeneous nature of excavated soils and rocks, large differential settlement can occur, which might cause the development of large cracks in the attenuation layer and other problems. The permeability function of the attenuation layer may be severely affected, thereby affecting its attenuation function. This is an important issue that needs to be clarified.